Bioenergetic Regulation of Neuronal Vacuolar-type H^+- ATPase

By

Lucy He

Submitted to the graduate degree program in Pharmacology and Toxicology and the Graduate Faculty of the University of Kansas in partial fulfillment of the requirements for the degree of Master of Science.

Chair: Liqin Zhao, Ph.D.

Jackob Moskovitz, Ph.D.

Eduardo Rosa-Molinar, Ph.D.

Date Defended: June 5th, 2019

The Thesis Committee for Lucy He certifies that this is the approved version of the following thesis:

Bioenergetic Regulation of Neuronal Vacuolar-type H^+ ATPase

_____

Chair, Liqin Zhao, Ph.D.

Date Approved: August 30th, 2019

Abstract

Neuronal vacuolar-type H^+-ATPase (V-ATPase) is an ATP-dependent proton pump that functions to acidify intracellular organelles such as lysosomes and synaptic vesicles, creating a proton gradient by which neurotransmitters can enter the vesicle through proton-coupled neurotransmitter transporters, a crucial step in neurotransmission (Moriyama, Maeda, & Futai, 1992). It is composed of two reversible domains, the integral V_0 that allows proton translocation and catalytic peripheral V_1 that is responsible for ATP hydrolysis. The V-ATPase regulates its activity through a process called reversible disassembly. When the V_0 and V_1 domains assemble, V-ATPase is activated and allows the influx of protons. When the domains disassemble, V-ATPase is inactivated, and proton transport does not occur (Beltran & Nelson, 1992).

V-ATPase assembly was previously demonstrated to be regulated by glucose in yeast (Kane, 1995) and some mammalian cells (Toei, Saum, & Forgac, 2010), but whether and how glucose regulates neuronal V-ATPase is unclear. This study investigates the effect of bioenergetic substrates on neuronal V-ATPase assembly. Neuro2a (N2a) cells were differentiated for 96 hours, glucose-deprived overnight, and then treated with substrates such as glucose, beta-hydroxybutyrate, sodium pyruvate, creatine phosphate, and creatine monohydrate for 20 minutes prior to cell lysate preparation. To study V-ATPase assembly, assembled V-ATPase were captured through co-immunoprecipitation. Equal amounts of cell lysate were incubated with V_1 antibody-coupled resin. Immunoblotting was then performed on the eluate to detect the V_1 and V_0 domains. The density of the bands was quantified and the ratio of V_0 and V_1 domains was used to determine V_0/ V_1 assembly.

The results demonstrate changes in glucose availability (deprivation/stimulation) did not impact V-ATPase assembly in differentiated N2a cells. Furthermore, the results show other

bioenergetic substrates (pyruvate, beta-hydroxybutyrate, and creatine molecules) did not induce changes in neuronal V-ATPase assembly. Our results did not support the well-documented role of glucose regulation of V-ATPase assembly demonstrated in previous studies conducted in yeast and mammalian cells.

Several pitfalls of this study may have contributed to the negative results. The glucose concentration for stimulation and incubation time for glucose-deprivation may not have been optimal for differentiated N2a cells; further investigation will be needed to optimize these conditions. The glucose concentration used for stimulation after overnight glucose-deprivation did not exceed the physiological glucose concentration; higher concentrations of glucose should be tested. Previous studies had various incubation times for glucose-deprivation that could be experimentally optimized. Furthermore, the experiments could be replicated in other neuronal cells or in primary neurons to validate the results.

Acknowledgements

First, I would like to express my deepest gratitude to my mentor Dr. Liqin Zhao for her unconditional support, unfaltering patience, constant encouragement, and scholastic guidance during my time in the master's program. Her positive attitude and insightful ideas were a constant source of encouragement in my work. I came into the program wanting to learn more about the process of molecular science research from a background of behavioral science. My shift into thinking and understanding molecular science research was slow but her patience and gentle nudge helped guide me through. Additionally, Dr. Zhao's commitment to teaching and ambition in advancing research was a great inspiration. I am extremely thankful for the opportunity to learn from such a great mentor.

I would also like to express my gratitude to my committee members Dr. Eduardo Rosa-Molinar and Dr. Jackob Moskovitz for their support and invaluable guidance. I am extremely thankful to Dr. Rosa-Molinar for his positive and encouraging words, knowledge, technical guidance, PANC-1 cells, unwavering support, and contagious laughs. I am also thankful to Dr. Jackob Moskovitz for his invaluable insights and for taking the time to patiently explain concepts for my journal club paper.

I am also thankful for the support and guidance I received from others in the department. I would like to sincerely thank the members of the Microscopy and Analytical Imaging Research Resource Core Laboratory for all the encouragement, patience, kindness, and guidance in helping me build expertise on various microscopes and for helping me brainstorm ideas. Specifically, I would like to thank Heather Shinogle, Dr. Noraida Martinez-Rivera, Irma Torres-Vazquez, Aidyn Medina-Lopez, Dr. Prem Singh Thapa-Chetri for all the help and encouragement. I am also thankful for Kenneth McFarlin for being my mentor and for

encouraging me to pursue graduate school. Finally, I am thankful to all the faculty in the department of Pharmacology and Toxicology for their invigorating coursework, guidance, and desire to advance scientific knowledge.

My lab members have been a constant source of laughter, encouragement, and source of knowledge. I am especially grateful for Dr. Sarah Woody Herring for teaching me everything step by step, from western blotting and cell culturing, to technology hacks on PowerPoint. I am also thankful for Dr. Heejung Moon and Xin Zhang for helping me troubleshoot and providing support. Also, I'm thankful for Punam Rawal for her kind encouragement and wisdom.

Finally, I am happy and grateful for the friends I have made in the department. I am grateful for all the support, help, and fun from the students in the department. I would also like to thank my parents and family for their unconditional support throughout my journey. This would not be possible without them. Thank you for a wonderful, challenging, and stimulating two years.

Contents

List of Figures

List of Abbreviations

N2a	Neuro2a (Neuroblastoma) cells
dN2a	differentiated N2a cells
V-ATPase	Vacuolar-type H^+-ATPase
CrP	Creatine-Phosphate, Phosphocreatine
CrMH	Creatine-Monohydrate
RA	all-*trans*-Retinoic Acid
Pyr	Pyruvate
βhb	Beta-hydroxybutyrate
ANOVA	Analysis of Variance
CK	Creatine Kinase
AMPK	AMP-activated protein kinase
PI3K	Phosphoinositide 3-kinase
mTORC	Mammalian target of rapamycin
SV	Synaptic Vesicle
VMAT	Vesicular monoamine transporter
GABA	Gamma-aminobutyric acid
RAVE	Regulator of the H^+-ATPase of Vacuolar and Endosomal Membranes
PFK-1	Phosphofructokinase 1
PKA	Protein kinase A
LKB1	Liver Kinase B1
LSD	Lysosomal Storage Disorder
AD	Alzheimer's Disease

PD	Parkinson’s Disease
ATP	Adenosine Tri-Phosphate
AGAT	Arginine Glycine Amindinotransferase
GAMT	Guanidinoacetate N-methyltransferase
LDH	Lactate dehydrogenase
CRT	Creatine Transporter

Chapter 1: Introduction

1.1. Vacuolar-type H^+ ATPases

1.1.1. Structure and Function

V-ATPase Structure

The Vacuolar-type H^+ ATPase, or V-ATPase, is a multifaceted ATP-dependent proton pump (Gluck & Caldwell, 1987; Sun-Wada & Wada, 2015). It has two reversible domains, the membrane bound V_0 and cytosolic V_1 (Parra & Kane, 1998) (Nishi & Forgac, 2002). The membrane bound V_0 domain is made up of 5 subunits denoted by the lowercase letters a, c, c'', d, and e (Sagermann, Stevens, & Matthews, 2001). Subunit a has four isoforms, a1 to a4 (Kawasaki-Nishi, Nishi, & Forgac, 2001b). Subunit a1-a3 are expressed ubiquitously whereas a4 is expressed in renal cells, heart, lung, skeletal muscle, and testis. Subunit a1 is expressed mainly in neurons, a2 in the liver and kidneys, and a3 in osteoclasts. The V_0 domain in yeast includes an additional subunit c' and mammals have an additional Ac45 (Jansen et al., 2010). The catalytic V_1 domain contains 8 subunits denoted by the uppercase letters A-H. Subunits B, C, E, and G each have specific isoforms.

Similar to other members of the ATPase, the V-ATPase functions by a rotary mechanism (Murata, Yamato, Kakinuma, Leslie, & Walker, 2005) and many structural aspects are conserved. According to Beyenbach, the accepted functional model of the V-ATPase states that it is composed of two parts, a stator and rotor (Boekema, Ubbink-Kok, Lolkema, Brisson, & Konings, 1997) (Imamura et al., 2003). The rotor is made of subunit D, F, and c-ring, whereas the rest of the subunits make up the stator (Yokoyama & Imamura, 2005).

Figure 1. V-ATPase Structure

(Sun-Wada & Wada, 2015)

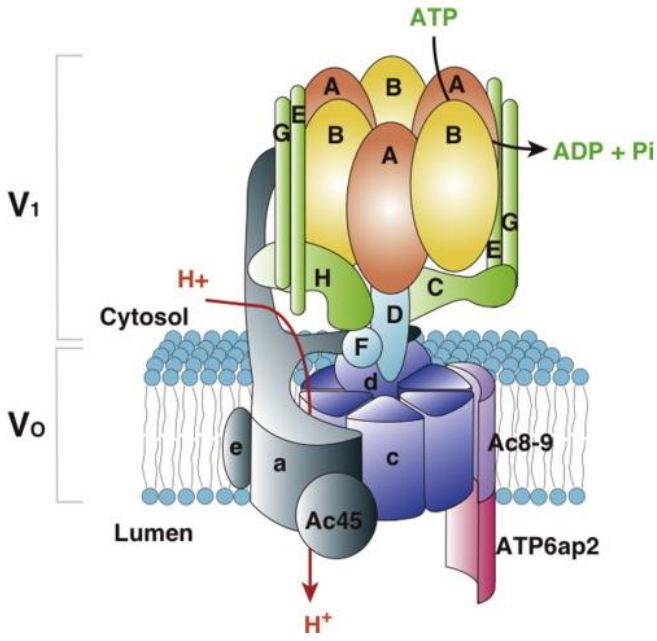

V_1 domain of V-ATPase

The cytosolic V_1 domain consists of three subdomains – the A3B3 head, central rotational stalk, and peripheral stalk (MacLeod, Vasilyeva, Baleja, & Forgac, 1998; Maher et al., 2009). The A3B3 head is composed of three alternating subunits of A and B in a ring structure (Forgac, 2007).The central rotational stalk is made of subunit D, F, and d (Muench et al., 2009) (Benlekbir, Bueler, & Rubinstein, 2012; Z. Zhang et al., 2008). Finally, the peripheral stalk consists of subunit C, E, G, and H. In the A3B3 head, the A and B subunits contain ATP hydrolytic sites. Together, the central rotational stalk and fixed peripheral stalk serve to connect the V_0 and V_1 domains. The stator peripheral stalk stabilizes and prevents the rotation of the A3B3 head, especially through the actin-binding function of subunit C (Forgac, 2007). Subunit H, in the peripheral stalk, was found to be vital in the inhibition of free V_1 by its' interaction with subunit F to inhibit ATP hydrolysis (Jefferies & Forgac, 2008). Although Free V_1 with subunit H

was found to hydrolyze Ca-ATP, only free V_1 without subunit H could hydrolyze Mg-ATP (Parra, Keenan, & Kane, 2000).

V_0 Domain of V-ATPase

The membrane bound V_0 domain is involved in proton transport and is composed of subunits a, d, e, and c-ring, which is made of hydrophobic c subunits in the structure of a ring. Subunit a creates two hemichannels for proton entry and has a buried arginine residue that is crucial in proton translocation (Wilkens & Forgac, 2001). The d subunit is a component of the central rotational stalk and serves to connect the V_0 and V_1 domains. The role of subunit e is unknown. The rotation of the c-ring allows proton translocation into the intracellular compartment.

Table 1. V-ATPase subunits and their function

Complex	Subunit	Gene Name	Classification	Subunit Function	Binding Partners	Expression
V_1 Complex	A	Atp6v1A	Catalytic Stator	Catalytic site for ATP Hydrolysis		
	B	Atp6v1B	Stator	Interacts with subunit A	Actin aldolase	B2: Ubiquitous brain isoform
ATP Hydrolysis	C	Atp6v1C	Peripheral Stalk Stator	Supplies attachment site for the EG stator Involved in assembly/disassembly of V_1/V_0 complexes	Actin RAVE	
	D	Atp6v1D	Rotor Central Stalk	Structural support for rotor		
	E	Atp6v1E	Stator Peripheral Stalk	Heterodimerizes with the G subunit to form the three stators	RAVE Aldolase	
	F	Atp6v1F	Central Stalk Rotor	Connects V_1 and V_0 domains Required for successful assembly of V-ATPase		
	G	Atp6v1G	Peripheral Stalk Stator	Heterodimerizes with the E subunit to form the three stators	RAVE	G1: ubiquitous G2: Synaptic vesicles
	H	Atp6v1H	Peripheral Stalk Stator	Activates ATP-powered proton pumping in fully assembled V-ATPase Blocks activity in partially assembled and disassembled V-ATPase		
V_0 Complex Primary Function: Proton Transport	a	Atp6v0a	Stator	Involved in fusion of synaptic vesicles in presynaptic neurons Consists of Arg residue required for proton transport Controls dissociation Involved in vesicular trafficking Involved in microfilament binding	aldolase	a1: neurons a2: liver and kidney a3: osteoclast a4: renal, heart, lung, skeletal muscle, testis
	b	Atp6v0b	Stator	Directly involved with proton transport – provides one component of the proteolipid spinning transmembrane ring		
	c	Atp6v0c	Rotor	Directly involved in proton transport – provides multiple components of the proteolipid spinning transmembrane ring Contains Glu residue that undergoes reversible protonation Interacts with GTPases to direct membrane trafficking		
	c'		Rotor	Contains Glu residue that undergoes reversible protonation		
	c''		Rotor	Contains Glu residue that undergoes reversible protonation		
	d	Atp6v0d	Central Stalk Stator	Connects the central stalk of V_1 and proteolipid ring of V_0 Controls reversible dissociation or coupling		
	e	Atp6v0e	unknown	Function unknown		

Function of V-ATPase

The main function of the V-ATPase is to acidify intracellular membrane-enclosed compartments (Parra & Kane, 1998), such as lysosomes, endosomes, vacuoles, secretory vesicles, through ATP hydrolysis and to create a proton gradient to facilitate proton-coupled transport of solutes across the membrane (Moriyama et al., 1992; Parsons, 2000) (Stevens & Forgac, 1997). The membrane bound V_0 domain functions to translocate protons whereas the cytosolic V_1 domain plays a role in ATP hydrolysis. The V-ATPase is involved in a multitude of physiological processes such as endocytosis, membrane trafficking, and the coupled uptake of neurotransmitters (Lafourcade, Sobo, Kieffer-Jaquinod, Garin, & van der Goot, 2008; O. Muller, Neumann, Bayer, & Mayer, 2003). Abnormal activity in the V-ATPase has been associated with viral infections, diabetes, cancer, osteoporosis, and neurodegenerative diseases (Liu et al., 2017; K. H. Muller et al., 2011; Nixon, 2013; Sennoune et al., 2004). Due to this, the V-ATPase is a potential drug target for many diseases. Neuronal V-ATPase accounts for approximately 8% of the total protein resided on the membrane of synaptic vesicles, making it vital for neurotransmitter release and synaptic transmission (Takamori et al., 2006).

Mechanism of V-ATPase

The fundamental model of the rotary mechanism is constructed of two proton hemichannels, a proton binding site on each subunit on the c-ring, and ATP hydrolysis driven c-ring rotation (Sambongi et al., 1999) (Forgac, 2007). The coupling ratio for V-ATPase activity is 2 - 4 protons transported per ATP consumed (Kawasaki-Nishi et al., 2001b) (Tomashek & Brusilow, 2000). When the V_0 and V_1 domains are assembled, the V-ATPase is activated, and proton translocation is allowed. First, cytoplasmic protons enter through the inner H^+

hemichannel formed by subunit a and each protonate one c subunit on the c-ring, specifically by binding a glutamic acid residue. Then ATP hydrolysis, at the catalytic A3B3 head, causes a conformation change that drives rotation of the central rotational stalk, leading to a 360° c-ring rotation (Meier, Polzer, Diederichs, Welte, & Dimroth, 2005). Rotation of the c-ring allows protonated glutamic acid residues to interact with an arginine residue in the outer hemi-channel and become stabilized (Kawasaki-Nishi, Nishi, & Forgac, 2001a). After stabilization, protons then unbind from the c-ring and exit through the outer hemi-channel of subunit a. The proton then enters the intracellular membrane and acidifies the lumen (Nishi & Forgac, 2002). Concanamycin a, a specific inhibitor of V-ATPase, binds to subunit c of the V_0 domain to prevent c-ring rotation and subsequently ATP hydrolysis. Interestingly, concanamycin a binding prevents V-ATPase from disassembling but has no effect on its' reassembly (Parra & Kane, 1998).

1.1.1.1. Lysosomal Activity

The function of lysosomal V-ATPase has been studied extensively in yeast and mammalian cells to a lesser extent. Lysosomes are organelles that contain degradative enzymes known as hydrolases and function in intracellular digestion (de Duve, 2005; De Duve & Wattiaux, 1966). Therefore, V-ATPase plays a crucial role in the proper functioning of lysosomes by acidifying the lysosomal lumen to an optimal pH of 4.5-5 (Pillay, Elliott, & Dennison, 2002). The acidification of lysosomes is a necessity for degradative enzyme activity and the export of degradation products by coupled transporters (Rahman, Ramos-Espiritu, Milner, Buck, & Levin, 2016) (Mellman, Fuchs, & Helenius, 1986) (Sagne et al., 2001). Lysosomal V-ATPase participate in bone resorption, transportation of acid hydrolases, and

tumor growth. The dysfunction of lysosomal acidification leads to the pathogenesis of lysosomal storage disorders (LSDs), Osteoporosis, and neurodegenerative diseases such as Alzheimer's and Parkinson's disease (Bagh et al., 2017) (Futerman & van Meer, 2004) (Nixon, 2013; Saftig & Klumperman, 2009). However, the mechanisms surrounding dysfunctional lysosomal acidification for neurodegenerative diseases are unclear.

Osteoclasts are multinucleated cells involved in bone reabsorption by secreting digestive enzymes to dissolve bone tissue (Teitelbaum, 2007). A mature osteoclast can form a lacunae between the ruffled border membrane and bone surface (Ochotny et al., 2011). Subunit a3 of the V-ATPase is expressed in osteoclasts and provides an acidic pH of the lacunae that leads to mineral solubilization and the hydrolysis of bone matrix (Toyomura et al., 2003). The degraded matrix is then transported into luminal acidic vesicles to the secretory domain (Boyle, Simonet, & Lacey, 2003). Mutations in subunit a3 can cause impaired proton translocation, bone resorption, and an increase in bone density that can lead to hyper or hypoactivity of osteoclasts (Ochotny et al., 2011). Hyperactivity of osteoclasts is associated with osteoporosis and periodontal disease (Teitelbaum, 2000). Osteoporosis develops as the result of genetic defects in osteoclast V-ATPase, 50% of patients with autosomal recessive osteoporosis have a mutation in subunit a3 (Frattini et al., 2000). Conversely, hypoactivity of osteoclasts leads to an increase of bone mass and osteopetrosis.

1.1.1.2 Synaptic Transmission

The V-ATPase is vital in the storage of neurotransmitters in synaptic vesicles (SV) and subsequently in neuronal transmission. Neuronal V-ATPase allows the transport of protons into synaptic vesicles through ATP hydrolysis, creating a proton gradient and membrane potential.

The accumulation of protons creates an electrochemical gradient that drives the uptake of neurotransmitters into synaptic vesicles by a neurotransmitter transporter (Moriyama et al., 1992). The inhibition by concanamycin a, specific V-ATPase inhibitor, decreased the uptake of neurotransmitters, providing evidence for the uptake of neurotransmitters for V-ATPase. V-ATPase makes up 8% of the total protein in synaptic vesicles (Takamori et al., 2006). SV are equipped with monoamine, acetylcholine, anionic glutamate, GABA, and zwitterionic glycine transporters.

Prior to neurotransmission, synaptotagmin responds to a calcium influx by docking the filled synaptic vesicle to an active site on the presynaptic membrane before fusion to release its neurotransmitters into the synaptic cleft (Morel, Dunant, & Israel, 2001). This process called priming, utilizes the SNARE (soluble N-ethylmaleimide sensitive factor attachment protein receptors) protein complex. The SNARE complex is composed of two parts, the vesicle-SNARE (v-SNARE) and target-SNARE (t-SNARE). The v-SNARE is present in synaptic vesicles and expressed by synaptobrevin and VAMP2. The t-SNARE is expressed by syntaxin1 and SNAP-25 on the presynaptic membrane and functions to stabilize and guide v-SNARE's to bind and form the SNARE complex for membrane fusion. The c subunit of V_0 (referred to as V0c) of the V-ATPase interacts with v-SNARE to form a fusion pore that opens and expands to diffuse neurotransmitters into the synaptic cleft (Di Giovanni et al., 2010; El Far & Seagar, 2011). In a "kiss and run" scenario, the fusion pore may close after a brief opening. Additionally, subunit a1 of the V0 domain (V0a1) was discovered in synaptic terminals and found to interact with v-SNARE (Morel, Dedieu, & Philippe, 2003). V0a1 is a vital regulator of synaptic vesicle fusion that acts downstream of SNARE-complex priming (Hiesinger et al., 2005). These studies implicate that the V-ATPase not only plays a role in acidifying synaptic vesicles for the uptake

of neurotransmitters, but they also have a vital role in synaptic vesicle fusion in the release of neurotransmitters into the synaptic cleft.

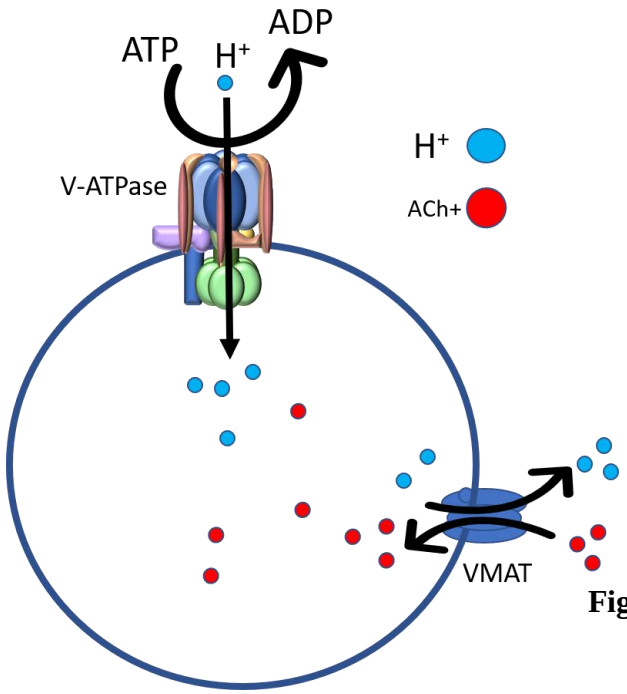

Figure 2. Synaptic Vesicular V-ATPase

1.1.1.3 Tumor cell invasion

Plasma membrane V-ATPase have been actively studied for its role in the metastasis of tumor cells (Sennoune et al., 2004) (Hinton et al., 2009). In this context, plasma membrane V-ATPases provide alkaline intracellular environment and an acidic extracellular environment. The alkaline intracellular environment is predicted to allow tumor growth, whereas the acidic extracellular environment supports invasion (Sennoune & Martinez-Zaguilan, 2007). Subunit a2 isoform of V-ATPase is expressed in cancer cells. A defective a2 in tumor cells leads to an alteration in macrophage numbers and affects the growth of tumors (Katara et al., 2016). A strong indicator for cancer is the increased use of glycolysis and dependence on V-ATPase to create the alkaline

intracellular pH and acidic extracellular pH for tumor cell proliferation (Torigoe et al., 2002). The increased use of glycolysis for cellular bioenergetics is activated by the alkaline intracellular pH and inhibits oxidative phosphorylation (Alfarouk et al., 2014). Conversely, an acidic intracellular pH drives oxidative phosphorylation. The transformation from preference for oxidative phosphorylation to glycolysis is known as the Warburg effect (Liberti & Locasale, 2016).

1.1.2 Regulatory mechanisms

The V-ATPase responds to a multitude of factors, the most well studied is reversible disassembly. Disassembly of the V-ATPase leads to the V_1 domain and subunit C to disassociate from the membrane bound V_0 domain (Kane, 1995). Free V_1 domains cannot hydrolyze the ATP (Graf, Harvey, & Wieczorek, 1996) and free V_0 domains cannot allow the passage of protons (Beltran & Nelson, 1992), which renders the V-ATPase inactive. For disassembly to occur, the V-ATPase must be catalytically active, as there are V-ATPase that are inactive and do not disassemble (Parra & Kane, 1998). Microtubules are also involved in the disassembly of V-ATPase (Xu & Forgac, 2001). The disassembly of domains was first confirmed in yeast, glucose deprivation for 5 min was able to trigger the disassembly of 70% of the complexes (Kane, 1995). The readdition of glucose reversed disassembly and allowed the complexes to reassemble. V-ATPase reassembly factors are species specific but typically include the RAVE (Regulator of ATPases of Vacuoles and Endosomes), rabconnectin, glycolytic enzymes, and several signaling pathways. V-ATPase reversible disassembly is a regulatory mechanism crucial to the conservation of ATP, pH homeostasis, salt stress, and amino acid availability (Stransky & Forgac, 2015).

The regulatory mechanisms of V-ATPase reversible disassembly are not completely understood. For a long time, V-ATPase reversible disassembly was thought to be universally regulated by glucose (Sautin, Lu, Gaugler, Zhang, & Gluck, 2005). Conversely, the results of a yeast cell study (Diakov & Kane, 2010) showed V-ATPase activity actually increased in glucose deprived and high external pH conditions. The authors concluded that the increase in external pH somehow stabilized V-ATPase complexes by suppressing disassembly in glucose deprived conditions and allowed the V-ATPase to be more active and less likely to disassembly. The increased external pH and glucose-deprived conditions were thought to increase V-ATPase activity as a mechanism to protect intracellular compartments from being acidified from the export of cytosolic protons outside the cell by Pma1 (Diakov & Kane, 2010). Additionally, V-ATPase activity was also found to increase in glucose-deprived mammalian cells (McGuire & Forgac, 2018). These studies emphasize how much there is still to learn about the regulation of V-ATPase.

1.1.2.1 Glycolytic regulation

V-ATPase regulation by glucose is the most widely studied regulatory mechanism. Glycolysis is important in the production of ATP and in promoting V-ATPase assembly. The generated ATP stimulate proton-pumping for the acidification of intracellular compartments. V-ATPase assembly with glucose stimulation was observed in yeast and mammalian cells (Kane, 1995; Sautin et al., 2005). Glucose addition leads to the assembly of V-ATPase and its activation. Disassembly by glucose deprivation inactivates the V-ATPase. Furthermore, V-ATPase disassembly functions to maintain pH and conserve ATP during glucose starvation. V-

ATPase assembly functions to acidify the intracellular lumen as well as ameliorate cytosolic acidification from glycolysis (Parra, Chan, & Chen, 2014).

Assembly Factors

In yeast cells, V-ATPase is thought to assemble with the help of RAVE and glycolytic enzymes such as aldolase and phosphofructokinase-1 (PFK-1). RAVE is a chaperone protein with three components, Skp1p protein and subunits Rav1p and Rav2p. RAVE binds free V_1 and subunit C to stabilize the free V_1 for reassembly (Seol, Shevchenko, Shevchenko, & Deshaies, 2001). Interestingly, RAVE only binds Vph1p, a vacuolar subunit 'a' isoform, from vacuoles and not stv1p, a Golgi and endosomal subunit 'a' isoform. Also, RAVE aids in assembly independently from glucose (Smardon, Tarsio, & Kane, 2002). PFK-1 is a rate-limiting enzyme in glycolysis that functions as a glucose sensor. PFK-1 functions to regulate V-ATPase proton transport with the fluctuation of glycolysis (Parra et al., 2014). PFK-1 signals RAVE in the presence of glucose which triggers RAVE to assemble the V-ATPase. Aldolase binds subunits E, B, and a to stabilize the V-ATPase (Lu, Sautin, Holliday, & Gluck, 2004).

Signaling pathways

Signaling pathways also play a role in the assembly of V-ATPase. In yeast cells, the most studied pathway is the Ras/cAMP/PKA (protein kinase A) pathway (Bond & Forgac, 2008). In the presence of glucose, Ras activation leads to the activation of adenylated cyclase followed by the production of cAMP. The increase in cAMP initiates PKA activity and intensifies V-ATPase assembly. Cytosolic acidification was shown to alter PKA and subsequently V-ATPase assembly (Dechant et al., 2010).

In mammalian cells, the phosphoinositol-3 kinase (PI3K) pathway, AMP-activated protein kinase (AMPK), and mTORC pathway have been shown to play a role. The PI3K pathway aids in the reassembly of V-ATPase by the readdition of an active PI3K subunit (Sautin et al., 2005). AMPK and mTORC are crucial nutrient sensors that require the activation of the V-ATPase Ragulator complex (C. S. Zhang et al., 2014). The V-ATPase Ragulator complex allows LKB1 (liver kinase B1) to dock and become phosphorylated, this leads to AMPK activation under glucose deprivation (C. S. Zhang et al., 2014). mTORC1 regulates cell growth by modulating growth factor signals and amino acid availability, it is activated in nutrient rich conditions. AMPK regulates energy homeostasis and is activated in nutrient poor conditions. Furthermore, the V-ATPase Ragulator serves to switch energy metabolism from catabolic to anabolic and vice versa. In a recent study, the traditional mechanism of glucose deprivation leading to V-ATPase disassembly was challenged by a study that reported the increase in V-ATPase assembly after glucose-deprivation (McGuire & Forgac, 2018). This study focused on lysosomal renal cells and determined glucose-deprived V-ATPase disassembly activated AMPK. The authors concluded the increase in lysosomal V-ATPase assembly and activity under glucose-deprived conditions was likely due to the need to change methods of energy production to non-glycolytic processes and activate autophagy. Glucose deprivation activates autophagy, which necessitates the need for functional V-ATPase for the acidic requirements needed for autophagy. Autophagy breaks down proteins and lipids to provide energy products that can be further metabolized to generate ATP.

Figure 3. The Glycolytic Regulation of V-ATPase

(Hayek, Rane, & Parra, 2019)

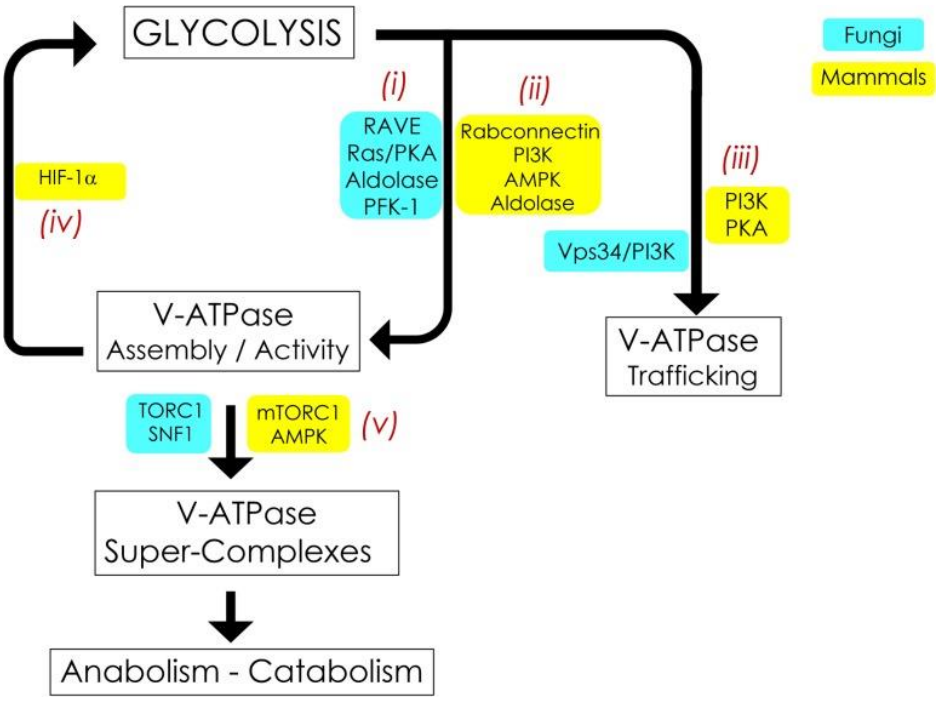

Figure 4. Nutrient signaling pathway for Glucose Stimulation

(Deprez, Eskes, Wilms, Ludovico, & Winderickx, 2018)

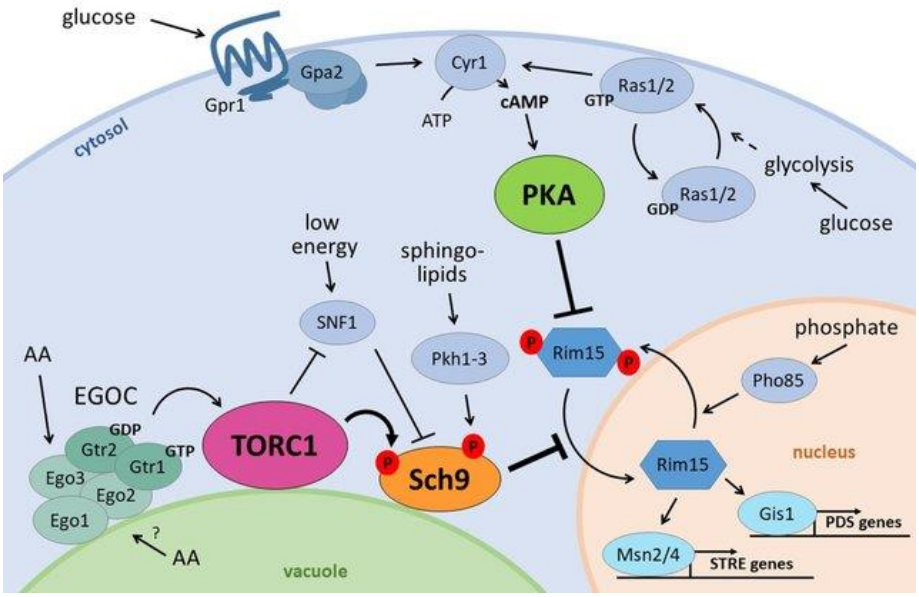

1.1.3 V-ATPase dysregulation in neurodegenerative diseases

Synaptic-vesicular V-ATPase function to acidify synaptic vesicles for neurotransmitter uptake and create a fusion pore for the exocytosis of neurotransmitters into the synaptic cleft (Morel et al., 2003). These functions are vital in neurotransmission and the proper functioning of the brain. Although current research focuses on the function of lysosomal V-ATPase in the brain, further research is required to understand the impact of synaptic-vesicular V-ATPase and its implication in neurodegenerative diseases.

Lysosomal V-ATPase play a crucial role in neurodegenerative diseases (Bagh et al., 2017). Lysosomes function in intracellular digestion and function to clear debris in neurons. Dysfunctional neuronal lysosomes may result in either the inhibition of hydrolases by an aberrant increase in pH or cytotoxicity and partially digested intermediates by a more neutral pH (Colacurcio & Nixon, 2016). Lysosomal storage disorder (LSD) is an inheritable family of disorders caused by gene mutations that has been implicated in many neurodegenerative diseases including neurodegenerative disease in childhood and more age-related diseases such as Alzheimer's and Parkinson's disease (Fuller, Meikle, & Hopwood, 2006). LSD is characterized by an accumulation of macromolecules or monomeric compounds inside endosomes or lysosomes involved in the autophagic system. The cause of the disease can be traced to defective hydrolases and lysosomal membrane proteins such as the V-ATPase (Saftig & Klumperman, 2009).

1.2 Bioenergetic substrates

In this thesis, various bioenergetic substrates targeting different points in cellular respiration were used to treat differentiated N2a cells. The following bioenergetic substrates were used to treat 96 h differentiated N2a cells. D-glucose is the naturally occurring form of glucose, the first step in glycolysis (Mergenthaler, Lindauer, Dienel, & Meisel, 2013). Pyruvate is the end product of glycolysis, formed by the breakdown of glucose (Rogatzki, Ferguson, Goodwin, & Gladden, 2015). Beta-hydroxybutyrate, known as ketone bodies, are a secondary source of energy formed through the breakdown of fatty acids and can enter the citric acid cycle (TCA) in less steps than glucose. Beta-hydroxybutyrate enters the mitochondria where it is converted into acetyl-coA and enters the TCA cycle (Newman & Verdin, 2014). Creatine is synthesized endogenously in the liver and is distributed throughout the body by blood. When phosphorylated, creatine-phosphate can donate high energy phosphate groups rapidly to generate ATP (Cooper, Naclerio, Allgrove, & Jimenez, 2012).

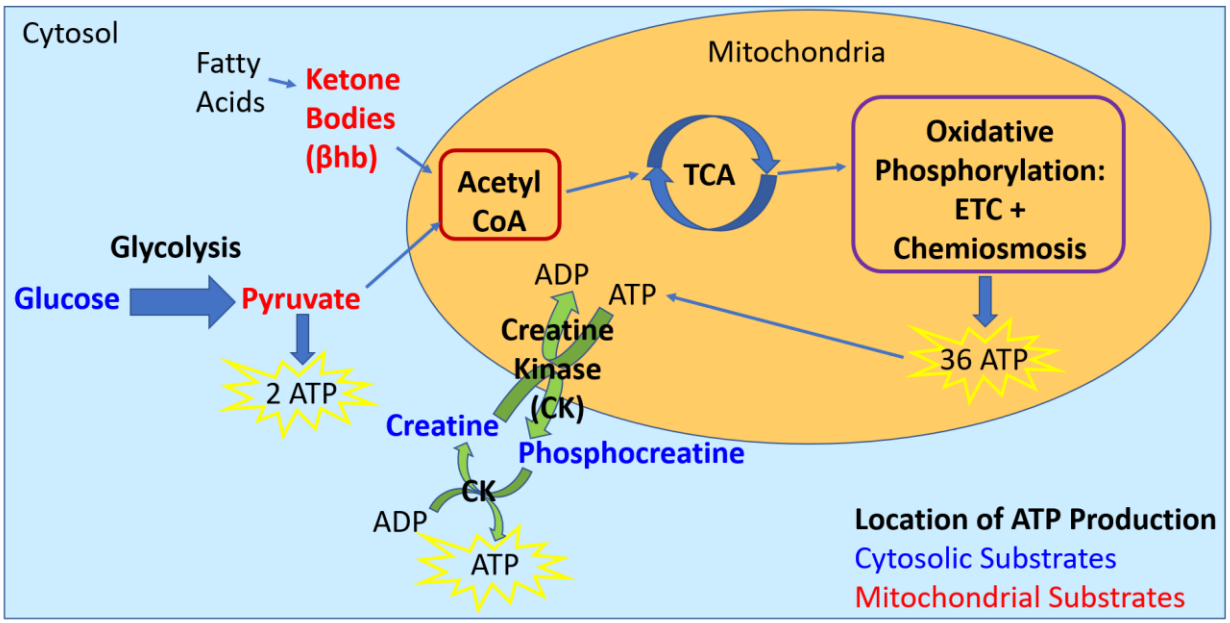

Figure 5. Location of ATP Production for Bioenergetic Substrates

1.2.1 Glucose

Glycolysis is the primary source of energy for many animals and leads to extracellular acidification, cytosolic alkalization, and the net production of 2 cytosolic ATP's (Mookerjee, Gerencser, Nicholls, & Brand, 2017). Glycolysis is the main form of energy production in yeast cells, cancer cells, and astrocytes. In organisms with mitochondrial respiratory chain dysfunction, a shift from oxidative metabolism to glycolytic metabolism is predicted to occur as an adaptive mechanism to limit ROS (reactive oxygen species) production and abnormal signaling (Jain et al., 2016). Glucose is broken down into pyruvate in glycolysis (Rogatzki et al., 2015). In this study, glucose was used for preliminary studies because it was the most direct source of energy and the first substrate in cellular respiration. We wanted to investigate whether glucose could regulate neuronal V-ATPase before testing other bioenergetic substrates.

1.2.2. Pyruvate

Pyruvate, the product of glycolysis, is the last product formed in the cytosol in cellular respiration. Pyruvate enters the mitochondria where it becomes acetyl-CoA and enters the TCA cycle and then electron transport chain for oxidative phosphorylation (Rogatzki et al., 2015). Lactate dehydrogenase (LDH) can catalyze the conversion of lactate to pyruvate and vice versa. This creates the opportunity for lactate to participate in the TCA cycle.

1.2.3. Ketone bodies

Beta hydroxybutyrate (βhb), one of three ketone bodies, are a secondary source of energy utilized by the body under low glucose conditions to maintain its' bioenergetic needs. The brain utilizes the largest supply of energy, up to 20% of the body's energy (Erbsloh, Bernsmeier, &

Hillesheim, 1958) (Newman & Verdin, 2014). Beta hydroxybutyrate (βhb) are synthesized in the liver and broken-down from fatty acids in the cytosol. D- βhb can then enter the mitochondria where it becomes acetoacetate and then acetyl-CoA, a crucial metabolic intermediate that enters the TCA cycle and then undergoes oxidative phosphorylation (Dedkova & Blatter, 2014). βhb is found predominately in blood, allowing it to easily circulate throughout the body.

1.2.4. Creatine/Phosphocreatine system

Creatine is a popular amino acid energy supplement for athletes who need a burst of short-term energy (Cooper et al., 2012). Creatine can be obtained through consuming red meat or naturally synthesized in the liver, pancreas, and kidney. There is also evidence to point to the brain endogenously synthesizing creatine due to the low permeability of creatine through the blood brain barrier (Hanna-El-Daher & Braissant, 2016). Creatine is synthesized in the liver from glycine and L-arginine catalyzed by AGAT (arginine-glycine amidinotransferase) into Guanidinoacetate (Nouioua et al., 2013). A methionine is added and GAMT catalyzes Guanidinoacetate to form Creatine, where it can travel through the blood to enter the heart, muscle, brain, and other organs.

Creatine-phosphate is the active energy donating form of creatine that can be formed through creatine kinase (CK) in the creatine-phosphate shuttle. There are two main forms of CK, cytosolic CK and mitochondrial CK. Mitochondrial CK lies in the intermembrane of the mitochondria and it phosphorylates creatine by using ATP to donate a free inorganic phosphate to creatine. The phosphorylated creatine, now creatine-phosphate, can then diffuse out of the CRT (creatine transporter) transporter back into the cytosol and donate a phosphate catalyzed by cytosolic CK for energy needs (Li et al., 2010). The creatine can then be shuttled back into the

mitochondria to become phosphorylated again. This cycle continues if there are available ATP/free inorganic phosphate, creatine-phosphate can even work under anaerobic conditions, making it an excellent source of ATP.

Creatine has been implicated to be regulated by AMPK activation (Ramirez Rios et al., 2014). The creatine transporter (CRT), involved in the uptake of creatine into cells, was found to be stimulated by mTOR (Shojaiefard, Christie, & Lang, 2006). Additionally, AMPK is upstream of mTOR (Shaw et al., 2004) and can function to regulate mTOR. Previously, there was a study that demonstrated the inhibition of CRT by the activation of AMPK (Li et al., 2010). Taken together, this suggests that mTOR stimulated CRT could be inhibited by AMPK activation, resulting in decreased creatine uptake into cells.

1.3. Statement of Purpose

The Vacuolar H^+ ATPase (V-ATPase) is an ATP-dependent proton pump that functions to acidify intracellular compartments (Parra & Kane, 1998). They are present in lysosomes, endosomes, plasma membranes, Golgi, vacuoles, and synaptic vesicles. The V-ATPase can respond to factors such as pH fluctuations, amino acid (AA) availability, intracellular ATP levels, and glucose availability by reversible disassembly. There are two domains that make up the V-ATPase, the membrane bound V_0 and the cytosolic V_1. During glucose deprivation in yeast cells, the V_1 domain of the V-ATPase responds by dissociating or disassembling from the integral V_0 to conserve intracellular ATP levels.

The V-ATPase have been extensively studied in yeast cells as well as recent advances in mammalian cells, with lysosomal V-ATPase as the focus of the studies. The mechanism and underlying signaling pathways for V-ATPase regulation by reversible disassembly are still not completely clear. This thesis seeks to elucidate the regulation of neuronal V-ATPase, an area that is poorly understood. Neuronal V-ATPase are concentrated in lysosomes and synaptic vesicles. Lysosomes are responsible for the intracellular digestion of macromolecules and in the brain, they function to clear debris. Functional V-ATPase are critical to acidifying lysosomes to an optimal pH to activate hydrolases for the subsequent digestion of debris (De Duve & Wattiaux, 1966). Lysosomal Storage Disease (LSD), that alter the function of lysosomes, have been implicated in diseases such as osteoporosis, periodontal disease, osteopetrosis, and neurodegenerative diseases such as AD and PD (Bagh et al., 2017). Furthermore, synaptic vesicular V-ATPase create a proton gradient that couples the uptake of neurotransmitters, making it critical for synaptic vesicle filling (Moriyama et al., 1992). This process is a vital step preceding neurotransmission.

In the first specific aim of this thesis, we sought to determine whether neuronal V-ATPase could be regulated by glucose stimulation. The N2a cells were differentiated for 96 h before overnight glucose deprivation. The next day, the differentiated N2a (dN2a) cells were treated for 20 min with 10 mM of glucose before cell lysis. Co-immunoprecipitation was utilized to capture the V-ATPase complex and the eluted protein was immunoblotted. Antibodies to recognize the V_0 and V_1 domain were utilized to detect the bands. Finally, the density of the bands for each antibody were quantified with Image Studio Version 4.0 imaging digitizing software and the V_0/V_1 ratio was calculated and served as an index of V-ATPase assembly.

In the second specific aim, we sought to determine if neuronal V-ATPase could be regulated by other bioenergetic substrates that participated at different steps in cellular respiration. The bioenergetic substrates used were beta-hydroxybutyrate, sodium pyruvate, creatine-phosphate, and creatine-monohydrate. The same procedure described above was used to measure V-ATPase assembly.

Chapter 2: Materials and Methods

Materials

The mouse neuroblastoma cell line, known as Neuro2a cells (ATCC CCL-131), and human pancreatic epithelioid carcinoma (PANC-1) (ATCC CRL-1469) cells gifted by the Rosa-Molinar laboratory were from American Type Culture Collection (ATCC, Manassas, VA). The antibodies V-ATPase B2 (D-11) (cat# sc-166045) and V-ATPase D (E-12) (cat# sc-390384) were from Santa Cruz Biotechnology. The anti-ATP6V0D1 (ab202899) was purchased from Abcam. The horseradish peroxidase secondary antibodies, Pierce Co-immunoprecipitation kit (26149), Dulbecco's Modified Eagles Medium high glucose (DMEM) (cat# 11965092), glucose-free DMEM (cat# 11966025), and Fetal Bovine Serum (FBS) (cat# 10437028) were from Thermo Fisher Scientific. Concanamycin A (Cat# sc-202111) was purchased from Santa Cruz Biotechnology. The ATPase Activity Assay kit (MAK113-1KT) and all-*trans*-Retinoic acid ≥ 98% (HPLC) (Cat# R2625) were from Sigma – Aldrich. The Mouse on Mouse Basic Kit (M.O.M) (BMK-2202), VECTASHIELD Antifade Mounting Medium with DAPI (H-1200), and Normal Goat Serum (S-1000) were purchased from Vector Laboratories. The Normal Mouse, Rabbit, and Donkey serums were purchased from Jackson ImmunoResearch Laboratories.

Cell Culture

The Neuro2a (N2a) and PANC-1 cells were cultured in complete growth medium containing Dulbecco's Modified Eagles Medium (DMEM, high glucose) supplemented with 10% Fetal bovine Serum (FBS) and 1% penicillin/streptomycin. The cells were maintained in a humidified incubator with 5% $C0_2$ at 37°C. The cells were sub-cultured every 3 days as needed or when the confluency reached 90%. PANC-1 cells were gifted at passage 2. New N2a stocks

of frozen cells were recovered at Passage 5, 7, or 8 and sub-cultured until they reached passage 13. Thawed N2a cells were sub-cultured twice before use to ensure optimal health. Preliminary studies were performed in passage 7 or 8 cells, and later studies were performed in passage 5 cells. The N2a cells were authenticated by IDEXX BioAnalytics by STR markers to generate the genetic profile (Supplementary).

RA-Induced Neuronal Differentiation

The N2a cells were differentiated into a neuron-like phenotype with retinoic acid (RA). To investigate this neuronal model, N2a cells were seeded at a density of $1x10^5$ to $1.5x10^5$/mL in growth medium for 24 hours. The next day when cells reached 40 to 50% confluency, the medium was changed to differentiation medium containing 2% FBS, 20 uM all-*trans*-RA, and DMEM. The RA was prepared fresh before use from aliquoted stocks in the dark. The differentiation medium was replaced every 48 hours. After 96 hours, the morphological phenotype was validated with phase contrast imaging and western blotting with neuronal biomarkers such as synaptophysin, NeuN, and PSD95. The differentiated neurons were then treated for further studies.

Antibody Validation

Neuronal and V-ATPase antibodies, such as synaptophysin, PSD95, NeuN, V-ATPase V_1, and V-ATPase V_0, were validated in 96-hour differentiated N2a (dN2a) cells to ensure the specificity and sensitivity of the antibodies. Positive controls included both tissue and cell line; muscle tissue was used for the negative control.

Mouse brain tissue and PANC-1 cells were used as positive controls. PANC-1 cells are a human pancreatic carcinoma cell line with neuroendocrine differentiation (Gradiz, Silva, Carvalho, Botelho, & Mota-Pinto, 2016). The neuroendocrine differentiation in PANC-1 cells was validated by the expression of chromogranin A and CD56. Chromogranin A is a granin protein present in the secretory granules of neuroendocrine cells and is widely used as a marker for neuroendocrine tumors (Theurl et al., 2010). CD56, or neural-cell adhesion molecule (NCAM), is a glycoprotein that regulates neuron to neuron interactions and promotes neurite outgrowth (Doherty & Walsh, 1996; Kolkova, Novitskaya, Pedersen, Berezin, & Bock, 2000). Due to these properties, PANC-1 cells were chosen as a positive control.

The selection of the appropriate negative control for both neuronal and V-ATPase antibodies was challenging since V-ATPase is known to be ubiquitous and present in intracellular organelles such as lysosomes. Previous studies have reported the controversial presence of lysosomes in skeletal muscle, it was found to have a low activity of acid hydrolases, promoting the idea that skeletal muscle used lysosomes from macrophages and connective tissue cells. A study investigating the contribution of lysosomes from various sources in skeletal muscle tissues concluded muscle fibers do not have secretory or excretory functions; therefore there was no need for an advanced lysosomal vacuolar system to be in place (Canonico & Bird, 1970). Due to this, mouse skeletal muscle, specifically the latissimus dorsi, was used as a negative control for neuronal antibodies and tested for V-ATPase antibodies.

Differentiated N2a cells were grown, differentiated, and harvested according to previously stated methods. Passage 4 PANC-1 cells were grown until a confluency of 80% was reached and incubated in RIPA buffer with protein phosphatase inhibitor for 5 min before harvesting. The cells were centrifuged at 12,000 x g for 10 min and the supernatant was

collected. Mouse Brain tissue and skeletal muscle in RIPA buffer supplemented with protease and phosphatase inhibitor was homogenized with a homogenizer and placed on ice for 30 minutes. The tissue extracts were then centrifuged at 10,000 x g for 10 min and the supernatant was collected. A bicinchoninic acid assay was performed to determine the protein concentration. Western blotting steps follow the procedures stated below and was performed with 20 µL of brain tissue loaded at a concentration of 0.7µg/µL and 1 µg/µL of skeletal muscle and cell lysate.

Table 2. Antibodies for Immunoblots and Co-immunoprecipitation

Antibodies	**Source**	**Dilution**	**Purpose in study**
Synaptophysin (D35E4) Rabbit mAB	Cell Signaling, cat#5461S	1:1000	Neuronal Marker for validating model
NeuN (D4G4O) Rabbit mAB	Cell Signaling, cat#24307S	1:1000	Neuronal Marker for validating model
PSD95 (D27E11) Rabbit mAB	Cell Signaling, cat#3450S	1:5000	Neuronal Marker for validating model
V-ATPase B2 (D-11) – V_1 Mouse Ab	Santa Cruz, cat# sc-166045	IP: 1:20 WB: 1:1000	Antibody used for capturing V-ATPase complex
V-ATPase D (E-12) – V_1 Mouse Ab	Santa Cruz, cat# sc-390384	1:1000	Detected the V_1 domain by WB
V-ATPase d1 – V_0 Rabbit Ab	Abcam, ab202899	1:5000	Detected the V_0 domain by WB
Goat anti Mouse	Thermo Fisher, cat#A16078	IP: 1:1250	Secondary antibody
Goat anti Rabbit	Thermo Fisher, cat#31462	IP: 1:1000	Secondary antibody

Treatments

The 96-hour differentiated N2a (dN2a) cells was treated with glucose-deprived medium (2% FBS, glucose-free DMEM) overnight. The non-glucose-deprived (NGD) condition was treated with 2% FBS and high glucose DMEM. After overnight glucose-deprivation, dN2A cells were treated with vehicle treatment of sterile ddH_2O or ethanol and substrates such as 10 mM glucose (D-(+)-Glucose, Sigma G8720), 3-Hydroxybutyric acid (Sigma, 166898), sodium pyruvate (Sigma, P2256), creatine phosphate (Sigma, CRPHO-Ro Roche), or creatine monohydrate (Sigma, C3630) for 20 minutes prior to collection. Cells were washed with ice-cold Phosphate Buffered Saline (1x PBS, pH 7.4) and collected on ice with IP Lysis and protein phosphatase inhibitor for 5 minutes. Then the cells were centrifuged 12,000 x g for 10 minutes to remove insoluble material and the supernatant was collected. Further experiments were conducted on the cell lysates or stored in -80°C for later use.

Immunoblotting

Differentiated N2a cells were washed three times with ice-cold phosphate-buffered saline (PBS) (pH 7.4, Thermo Fisher Scientific) before lysing with IP Lysis (Pierce Co-immunoprecipitation kit, Thermo Fisher Scientific) containing protease and phosphatase inhibitors (Thermo Fisher Scientific) for 5-10 minutes on ice. Whole cell lysate was centrifuged at 12,000 x g for 10 min. The supernatant was collected and Bicinchoninic acid assay (BCA)(Thermo Fisher Scientific) was performed to determine the levels of protein concentration. Equal amounts of protein concentration were calculated and diluted in Laemmli 4x sample buffer (Bio-RAD) with 2-mercaptoethanal (Bio-RAD) before being boiled at 95°C for 5 minutes. Equal amounts of protein were loaded into each lane on the 10% sodium dodecyl

sulfate-polyacrylamide gel electrophoresis (SDS-PAGE). After SDS-PAGE, the gel was transferred onto a methanol-activated 0.2 µm pore-sized PVDF membrane (Bio-Rad). Then the membrane was blocked with 2% of non-fat milk in 1x TBS for at least 40 minutes at room temperature on a rocker. The primary antibody was incubated overnight at 4°C. The next day the membranes were washed three times with 1x TBST for 8 minutes each before detection with horseradish peroxidase (HRP) conjugated secondary antibody for 1-2 hours. The membrane was washed again before adding the enhanced chemiluminescence (ECL) reagent (Bio-Rad) for the appropriate amount of time between 5-20 minutes. The membrane was then scanned, and the bands were quantified with Image Studio Version 4.0 imaging digitizing software.
The band density was quantified with the same size of rectangle in each membrane.

V-ATPase Assembly – Co-immunoprecipitation

The N2a cells were differentiated and treated according to the methods described previously. The cells were collected with IP-Lysis buffer, provided by the Pierce co-immunoprecipitation kit, and protein phosphatase inhibitor. The supernatant was collected after centrifugation and a bicinchoninic acid (BCA) protein assay (Pierce) was used to determine the protein concentration in the cell lysate. The V-ATPase B2(V_1)-specific Mab was used for the immunoprecipitation of the V-ATPase complex. Equal amounts of pre-cleared cell lysate were loaded into each antibody immobilized spin column (V-ATPase B2(V_1) monoclonal antibody and control Ms IgG antibody) and incubated overnight on a rotator at 4°C. The next day, the free V_1 domains and assembled V-ATPase complex were eluted from the antibody-coupled spin columns. The eluted samples collected were diluted in 4x Laemmli sample buffer (Bio-Rad, CA) with 2-mercaptoethanol (Bio-Rad, CA) and heated at 95°C for 5 minutes. Equal amounts of

protein were separated by SDS-PAGE (10% acrylamide gels) and transferred onto 0.2 µm pore-sized PVDF membranes (Bio-Rad, CA). The membrane was blocked with 2% non-fat milk in TBST for at least 40 minutes at room temperature and incubated with anti-V-ATPase V_0 1:5000 overnight at 4°C and then horseradish peroxidase secondary antibody for 1 hour the following day. After scanning, the membrane was stripped for 5 minutes and washed before re-blocking the membrane. The same procedure as previously described was repeated with the incubation of anti-V-ATPase V_1 1:1000 overnight at 4°C. The membrane was scanned using C-Digit Blot Scanner (LI-COR, Lincoln, NE) and the intensity of protein bands were quantified with Image Studio Version 4.0 imaging digitizing software. The ratio of the protein band densities for the anti-V-ATPase V_0/V_1 antibodies were used to calculate V-ATPase assembly. The conditions were normalized to the V_0/V_1 ratio of the control condition for comparison.

Statistical Analysis

GraphPad Prism 6 (GraphPad Software, La Jolla, CA, USA) was used to conduct statistical analyses. The data was analyzed with a one-way analysis of variance (ANOVA) and Tukey's post hoc multiple comparisons of mean±sd. Pyruvate and Beta-hydroxybutyrate treated conditions were analyzed with a Students T-test. Statistically significant values were $p < 0.05$.

Chapter 3: Results

1. Biochemical Validation of Neuronal and V-ATPase Antibodies in Differentiated Neuro2a cells

Neuronal and V-ATPase antibodies were validated to ensure their specificity and sensitivity in differentiated N2a (dN2a) cells. Two positive controls and a negative control were tested with the dN2a cells. Mouse brain tissue was homogenized and served as a positive control. PANC-1 is a human pancreatic carcinoma cell line with neuroendocrine differentiation (Gradiz et al., 2016) and served as a positive control. Since V-ATPase is known to be present in intracellular organelles and is ubiquitous, mouse skeletal muscle, specifically the latissimus dorsi, was thought to be an appropriate negative control for neuronal and V-ATPase antibodies due to its' controversial presence of lysosomes (Canonico & Bird, 1970). The results demonstrate the antibodies were positively characterized in brain tissue, dN2a, and in PANC-1 cells, except for synaptophysin, which is congruent with a previous study (Gradiz et al., 2016). As expected, skeletal muscle tissue did not detect neuronal markers but detected V-ATPase antibodies. However, the V-ATPase antibodies were detected with lower levels of specificity. This indicates skeletal muscle was an appropriate negative control for neuronal antibodies but not for V-ATPase antibodies.

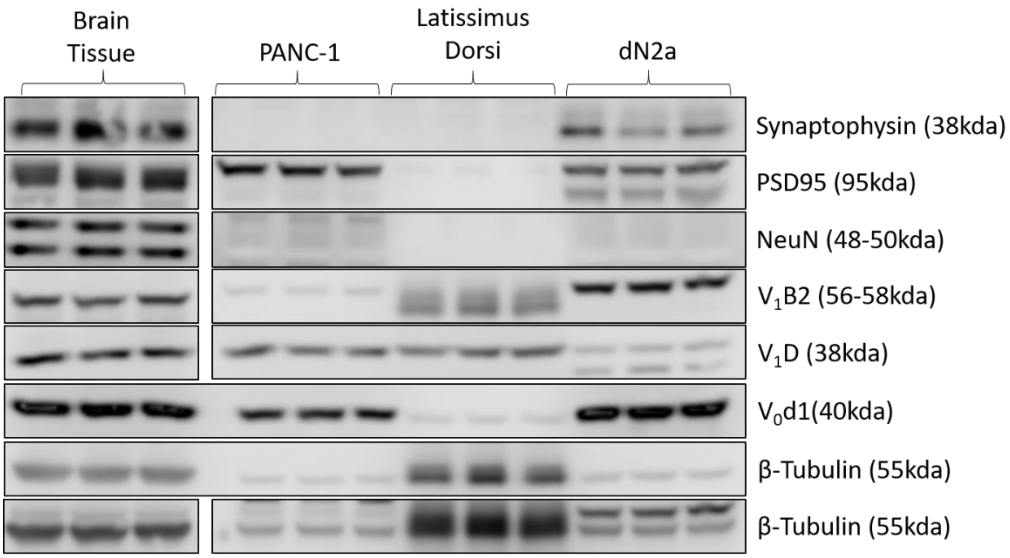

Figure 6. Antibody Validation for Differentiated Neuro2a cells.
Neuronal and V-ATPase antibodies were validated in dN2a cells with brain tissue and in PANC-1 cells used as positive controls and mouse latissimus dorsi muscle used as a negative control. Antibodies were successfully detected in brain tissue and PANC-1 cells, except for synaptophysin in PANC-1 cells. Latissimus dorsi muscle was a successful negative control for neuronal antibodies but not for V-ATPase antibodies. V-ATPase antibodies were detected in latissimus dorsi muscle, albeit with lower sensitivity, which suggests latissimus dorsi muscle was not the appropriate negative control.

2. Morphological and Biochemical Characterization of Neuronal Phenotype of RA-differentiated N2a cells

To investigate the effects of various substrates on neuronal V-ATPase, N2a cells were differentiated into a neuronal phenotype by a combination of all-*trans*-retinoic acid (RA) and serum deprivation according to previous studies (Mao et al., 2000; Tremblay et al., 2010; Namsi et al., 2018). The N2a cells were seeded at a density of $1.5x10^5$/mL and allowed to proliferate for 24 hours in growth medium containing 10% FBS, 1% antibiotics, and DMEM. The N2a cells were then differentiated for 96 hours in 20 uM RA in 2% FBS and DMEM. The differentiated N2a (dN2a) phenotype was examined morphologically and biochemically in a time-dependent manner at 0 hours, 48 hours, and 96 hours. Validated neuronal markers such as Synaptophysin, NeuN, and PSD95 were utilized to validate the neuronal phenotype biochemically through

immunoblotting. Synaptophysin is a ubiquitous synaptic vesicle membrane protein involved in the formation of synapse, regulation of neurotransmitter release, and the production of synaptic vesicles (Wheeler et al., 2002; Eshkind et al., 1995; J Alder et al., 1995; Janz R et al., 1999). NeuN protein is expressed in nervous system tissues, specifically cell nuclei, and has been used as a neuron-specific marker for studying stem cell differentiation (Hess et al., 2002; Verdiev Bl et al., 2009). PSD95, post-synaptic density protein, is a scaffolding protein present in mature synapses (Yoshii A et al., 2011). V-ATPase B2 (V_1), an isoform expressed in the brain, was also used as a marker for the V_1 domain of neuronal V-ATPase (C. Pietrement et al., 2006; S. T. Boesch et al., 2003). A time-dependent increase in optical density was observed in immunoblots probed with synaptophysin, NeuN, PSD95, and V-ATPase B2 (V_1) shown in (**Fig 7b**), indicating a progressive increase in neuronal phenotype. Western blots for NeuN and V-ATPase B2 (V_1) demonstrated significant protein expression levels as early as 48 hours. Synaptophysin and PSD95 did not show significant protein expression levels until 96 hours of differentiation. The morphological phenotype was validated through inverted microscope imaging. Progressive neuron-like processes were observed in a time-dependent manner with RA stimulation (**Fig 7a).** In summary, the morphological and biochemical results confirm the neuronal phenotype of the 96 h – differentiated N2a cells and validate dN2a cells as a suitable in-vitro neuronal model for subsequent studies of V-ATPase activity and assembly.

a)

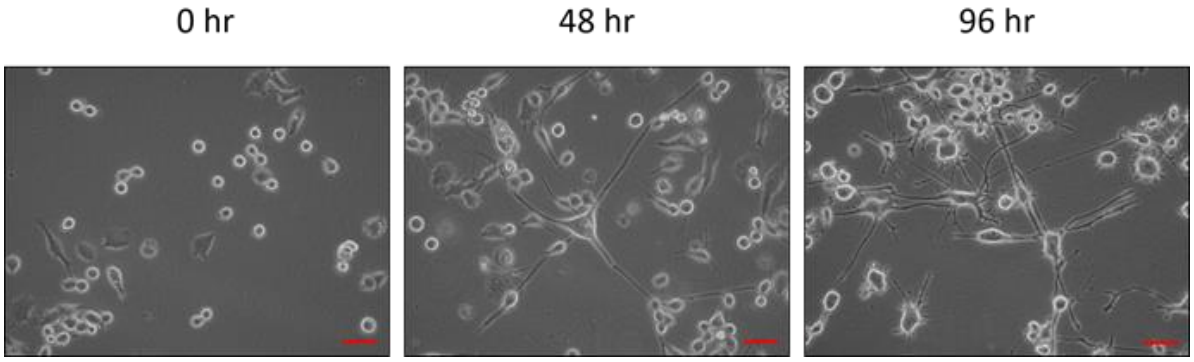
0 hr
48 hr
96 hr

b)

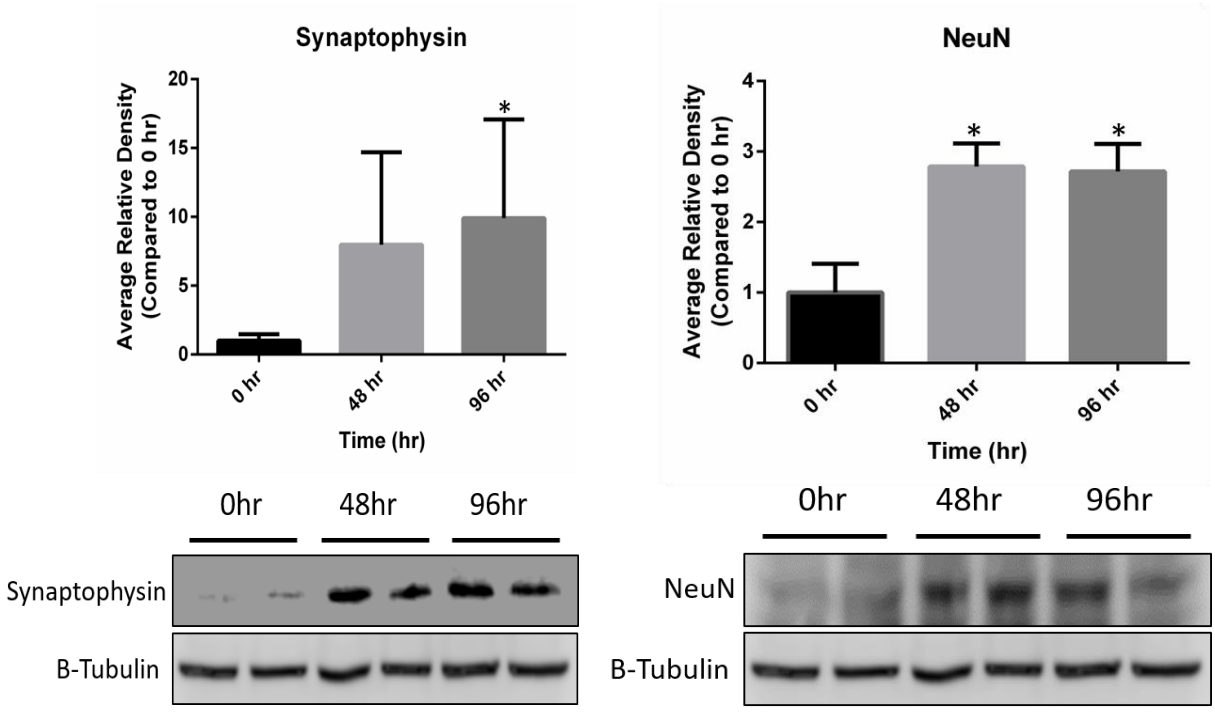
Synaptophysin
Average Relative Density (Compared to 0 hr)
20
15
10
5
0
*
0 hr
48 hr
96 hr
Time (hr)
NeuN
Average Relative Density (Compared to 0 hr)
4
3
2
1
0
*
*
0 hr
48 hr
96 hr
Time (hr)
0hr
48hr
96hr
Synaptophysin
B-Tubulin
0hr
48hr
96hr
NeuN
B-Tubulin

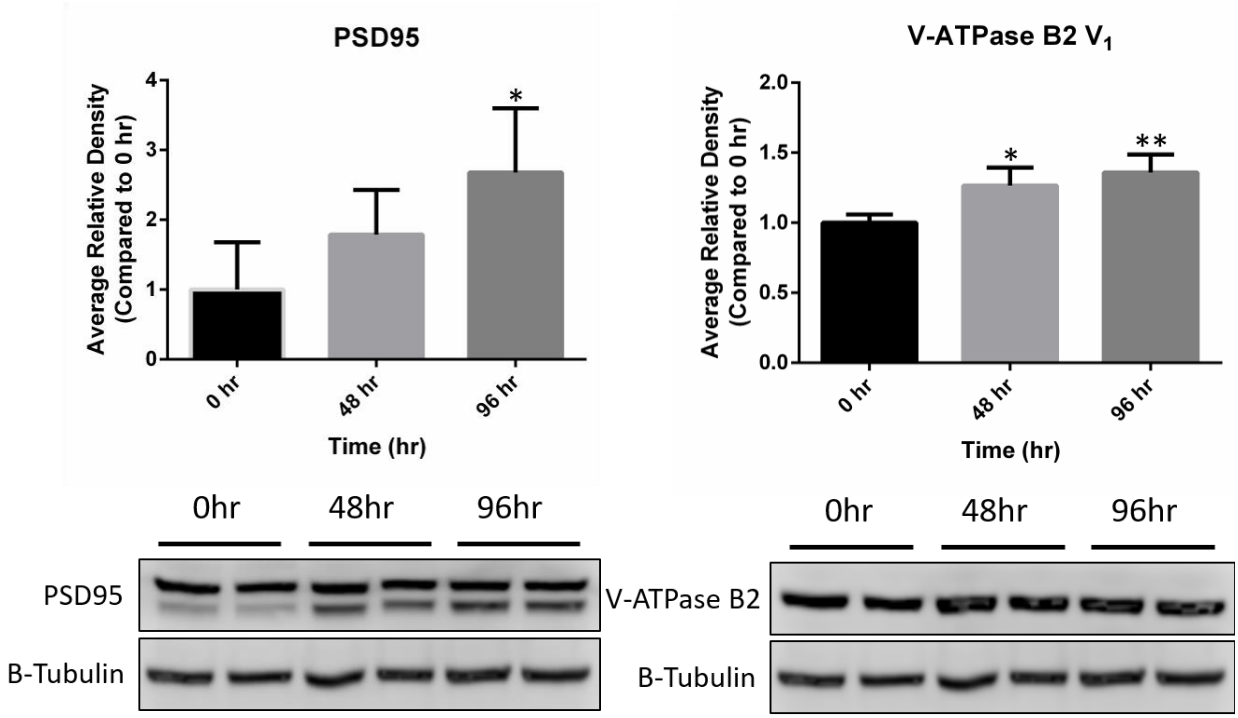

Figure 7. Morphological and Biochemical Characterization of Differentiated N2a cells. (a) Morphological phenotype validation of N2a cells differentiated by 20 µM RA and 2% FBS. The Zeiss inverted microscope with 20X magnification confirmed the progressive time-dependent increase in neuronal phenotype from 0 h, 48 h, to 96 h of differentiated N2a cells. The red scale bar represents a length of 50 µm. (b) Western blots of the neuronal markers NeuN, Synaptophysin, and PSD95 confirm the time-dependent increase in neuronal phenotype from 0h to 96 h. V-ATPase antibody for B2 (V_1) was also used to confirm the time-dependent increase in V-ATPase. Immunoblotting results were normalized to the undifferentiated 0 h condition and compared using a one-way ANOVA with Tukey's Post hoc Test. *$p<0.05$, **$p<0.01$. Data represent the group mean ± SD. N=2 for NeuN, N=3 for all other antibodies.

3. V_0/V_1 Protein Expression levels were not altered by glucose treatment

Since co-immunoprecipitation of the V-ATPase complex and immunoblotting will be used to determine V-ATPase assembly by calculating the V_0/V_1 ratio, the protein expression of

V_0V_1 was determined in treated cell lysate by measuring the average relative densities of the bands. First, 96 h dN2a were glucose-deprived overnight in glucose-free DMEM and 2% FBS. Control dN2a cells continued its maintenance in fresh medium composed of DMEM and 2% FBS. The next day, the glucose-stimulated condition was treated with 10mM or 25mM of D-Glucose or vehicle (ddH_2O) for 15-20 min before cell lysis. Next, equal amounts of treated cell lysate was used in immunoblotting. The membrane was probed with V-ATPase d1 (V_0) and then V-ATPase D (V_1) after stripping to measure the total protein expression of V_0 and V_1 in treated cell lysates. The results in **Fig 8** demonstrate there is no significant difference in the average relative density of V_0 or V_1 between treated cells – non-glucose-deprived (NGD), glucose-deprived (dep), and 10mM (G10) or 25mM (G25) glucose-stimulated cells. This result indicates that treatment with bioenergetic substrates does not lead to an alteration in protein expression. Therefore, any difference in measured V-ATPase Assembly V_0/V_1 through co-immunoprecipitation would be attributed to the substrate treatment and not due to the alteration of protein expression in stimulated cell lysate.

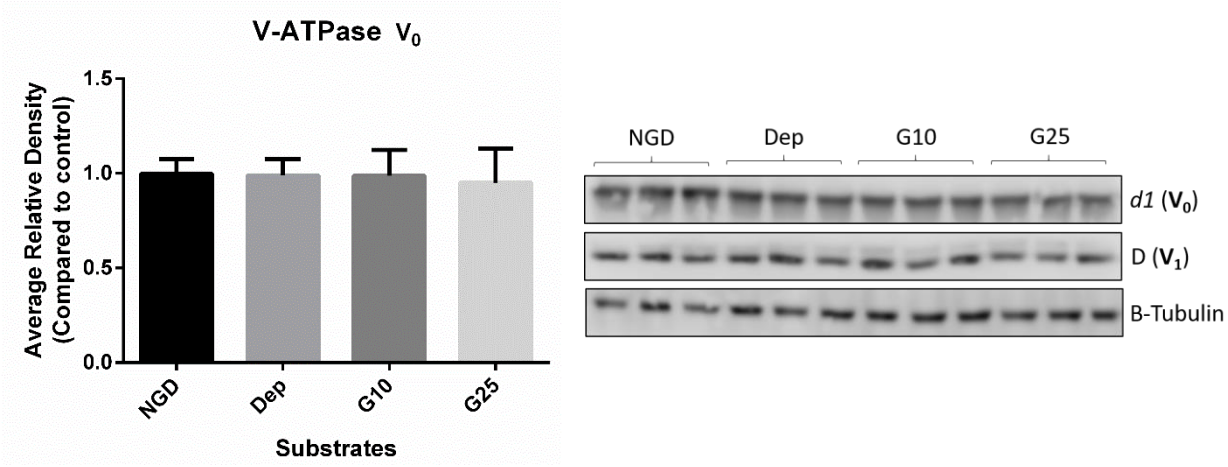

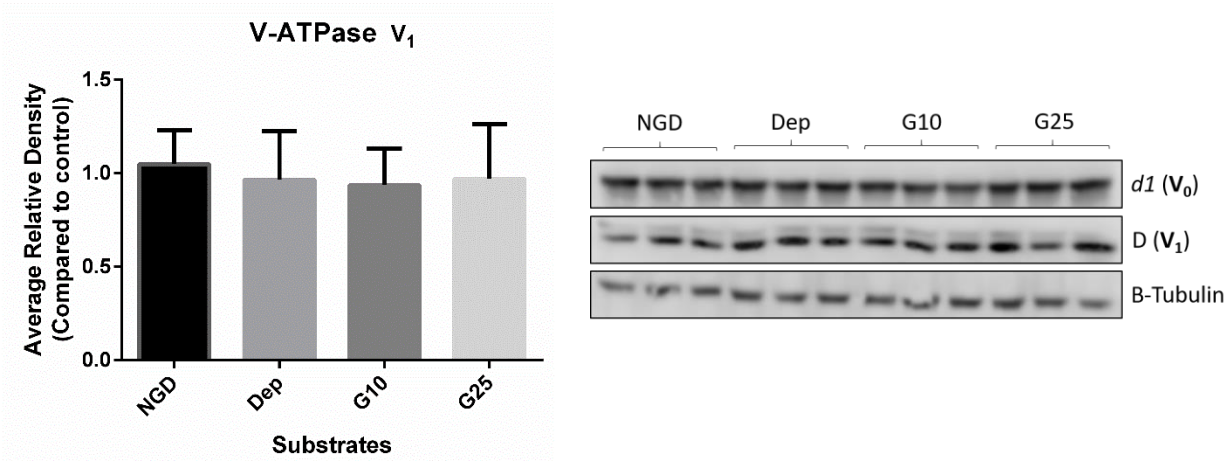

Fig 8. V_0V_1 protein expression levels in cell lysate were not altered by glucose treatment. Immunoblots of glucose-treated (non-glucose-deprived (NGD), glucose deprived (dep), 10mM glucose (G10), 25mM glucose (G25)) cell lysate was loaded in equal amounts and detected with V-ATPase d1 (V_0) and V-ATPase D (V_1) to measure the average relative density of V_0 and V_1. The total average relative densities of V_0 and V_1 were not significantly altered between the treated cell lysates, indicating treatment did not alter total protein expression. Therefore, differences in V_0/V_1 assembly levels between the treated groups from co-immunoprecipitation studies are attributed to the treatment and not an alteration in total protein expression. Immunoblotting results were normalized to the control NGD condition and compared using a one-way ANOVA with Tukey's hoc test. Data represent the group mean± SD. N=4 per group.

4. V-ATPase Assembly was not significantly altered by glucose stimulation

Glucose is a known regulator of V-ATPase V_0/V_1 assembly in yeast and mammalian cells (MP Collins et al., 2018; Chan et al., 2016). Glucose stimulation in these cells lead to an increase in V-ATPase V_0/V_1 assembly whereas deprivation leaves the V_0/V_1 disassembled. The mechanism of regulation for neuronal V-ATPase is unclear. To determine whether neuronal V-ATPase is regulated by glucose, the validated 96 h dN2a cells were used as model of investigation. The 96-hour differentiated N2a cells were deprived of glucose overnight in 2% of

FBS and glucose-free DMEM. The control dN2a cells continued its maintenance in fresh medium composed of DMEM and 2% FBS. The next day, the cells were stimulated with 10 mM of glucose or vehicle alone for 20 min before collection. Equal amounts of cell lysate were co-immunoprecipitated with V-ATPase B2 (V_1) antibody and assembled V-ATPase complexes and free V_1 were eluted. The eluate was diluted in Llaemmli sample buffer and equal volumes were loaded in a 10% SDS gel for western blotting. As shown in **Fig 9a**, glucose stimulation induced a significant increase in V_0/V_1 assembly compared with glucose deprived cells in preliminary studies. There was no significant difference between control non-glucose-deprived (NGD cells with either glucose stimulated or glucose-deprived cells. Further analysis with an increase in sample size and duplicates or triplicates in each treatment was conducted (**Fig 9b**). These results demonstrate there was no significant difference in V-ATPase assembly with glucose stimulation and glucose-deprivation across 5 different samples. One run (**Fig 9c**) out of the 5 samples indicated that stimulation with 10mM of glucose significantly induced V-ATPase disassembly as compared with the glucose-deprived cells and that stimulation with 25mM of glucose significantly increased and restored V-ATPase assembly.

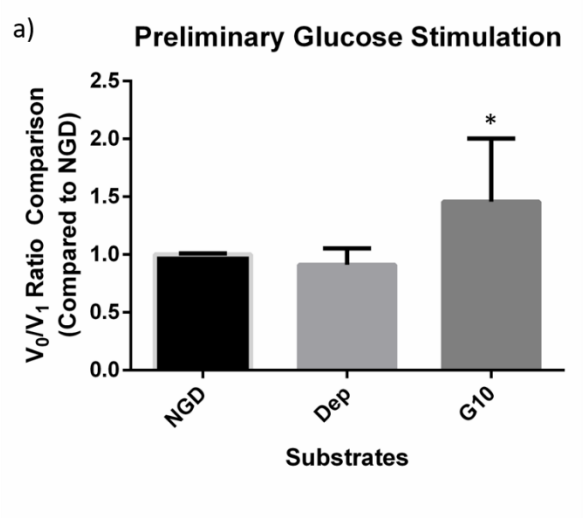

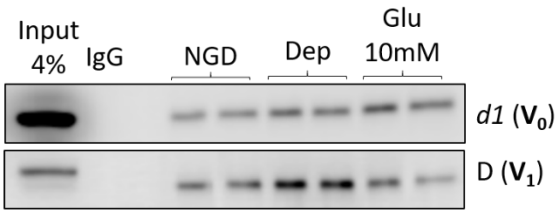

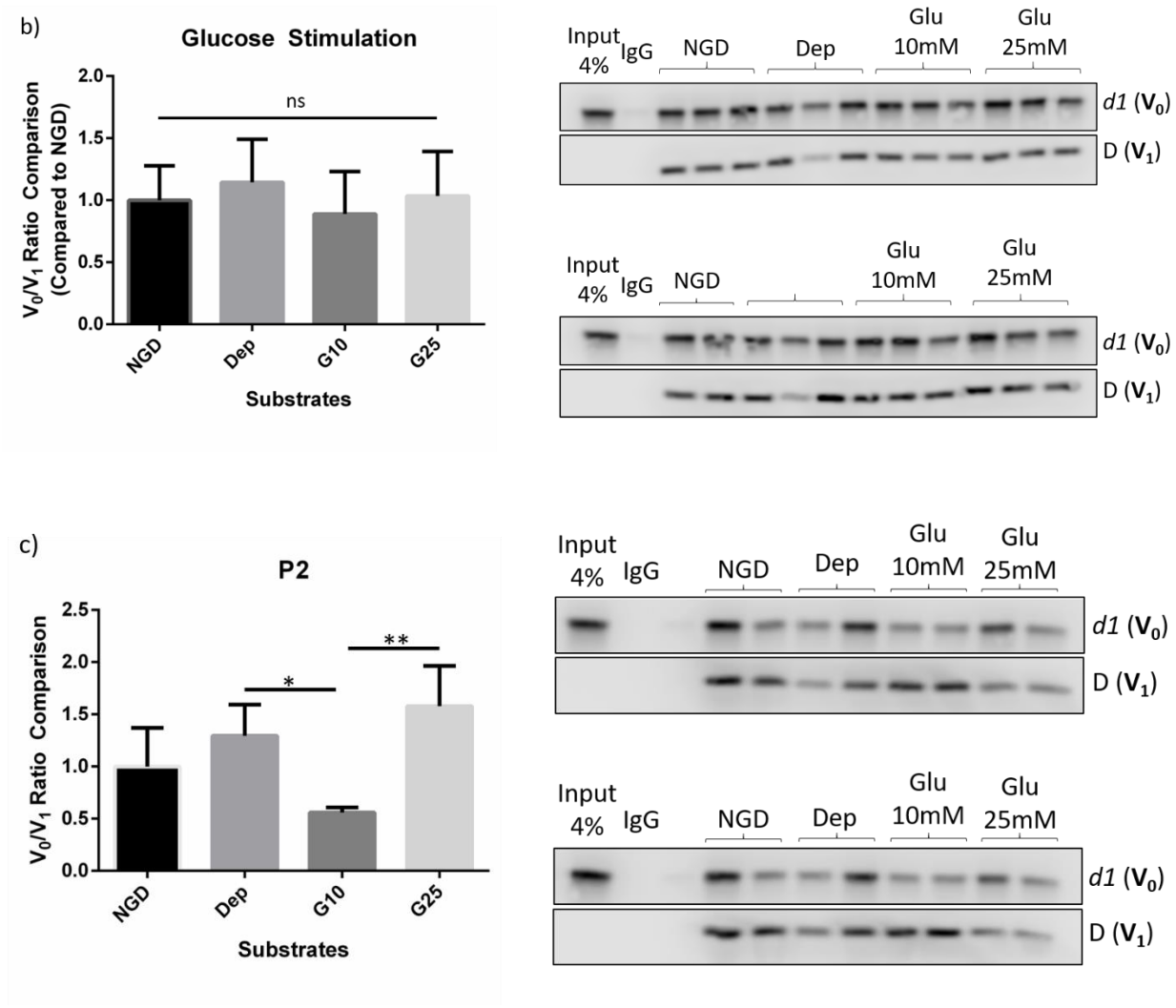

Fig 9. Neuronal V-ATPase regulation by glucose. 96h dN2a cells were glucose-deprived overnight before treatment with 10mM or 25mM of D-Glucose or vehicle alone for 20 min. Equal amounts of cell lysate were co-immunoprecipitated and protein expression was assessed using immunoblotting. V-ATPase d1 (V_0) and then V-ATPase D (V_1) antibody was detected. The density of the bands was quantified to calculate the V_0/ V_1 ratio to measure V-ATPase assembly. (a) Preliminary studies demonstrated Glucose-stimulated (G10) cells had significantly more assembled V-ATPase compared to glucose-deprived (Dep) cells, but there was no difference compared to control non-glucose-deprived (NGD) cells. Glucose-deprived cells were also not significantly different from control NGD cells. *p=0.0443, N=3 (b) Further investigation demonstrated there was no significant difference in V-ATPase assembly between the treatment groups. ns p=0.1253, N=5. (c) One experiment demonstrated a significant decrease in V-ATPase assembly from vehicle treated glucose-deprived cells and 10mM of glucose, as well as a significant increase from 10mM to 25mM of glucose treatment. **p=0.0034. Immunoblotting results were normalized to the control non-glucose-deprived (NGD) condition in each group and compared using one-way ANOVA with Tukey's Post hoc Test. *p<0.05, **p<0.01. Data represent the group mean± SD.

5. V-ATPase Assembly was not significantly altered by bioenergetic substrates

Next, various substrates were used to test the effects on V-ATPase assembly after the initial studies with glucose-stimulated and glucose-deprived cells. The substrates used were beta-hydroxybutyrate (βhb), pyruvate (pyr), creatine-phosphate (CrP), and creatine-monohydrate (CrMH). These substrates were used as they represent different entry points in energy metabolism. Previous research indicated yeast cells responded best to rapidly metabolizable substrates such as glucose, fructose, and mannose. The 96-h dN2a cells were deprived of glucose overnight in 2% FBS and glucose-free DMEM and regular DMEM for control cells. The next day, cells were stimulated with either 10 mM D-Glucose, βhb, sodium pyruvate, creatine-phosphate, creatine-monohydrate, or vehicle alone for 20 min before cell lysate collection. As shown in **Fig 10**, the bioenergetic substrates had no significant effect on V-ATPase assembly as compared with the vehicle treated glucose-deprived condition.

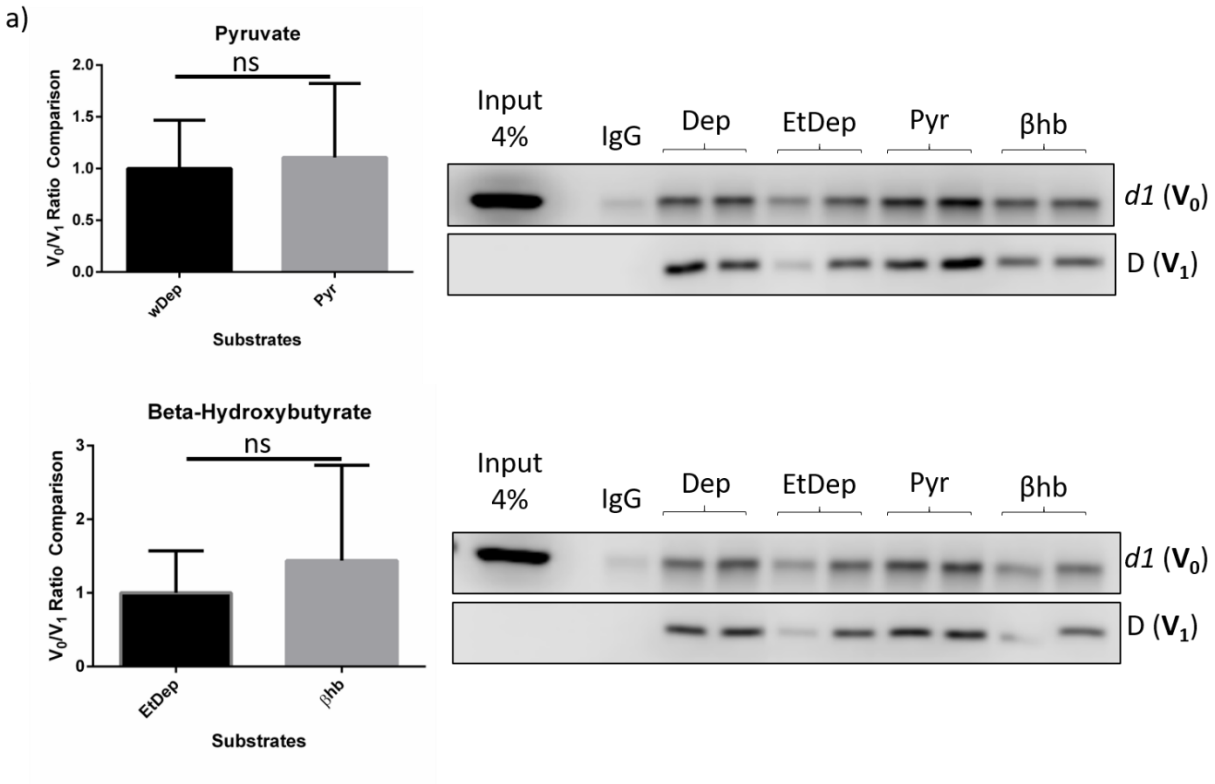

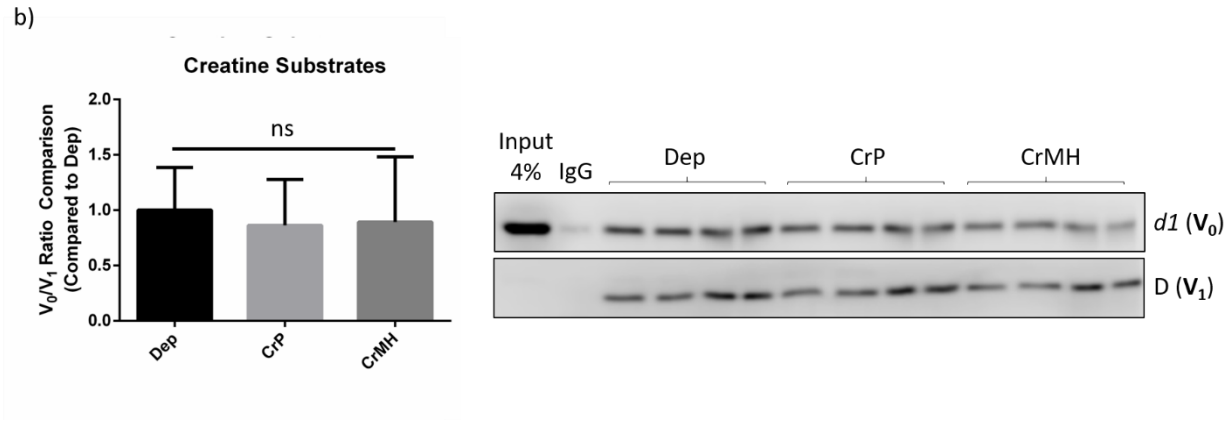

Fig 10. Neuronal V-ATPase regulation by other bioenergetic substrates. 96h dN2a cells were glucose-deprived overnight and then treated with 10 mM of each bioenergetic substrate or vehicle alone the next day for 20 min. Equal amounts of cell lysate were co-immunoprecipitated and equal volumes of the captured eluate was assessed for the protein expression of V-ATPase d1 (V_0) and then V-ATPase D (V_1) using immunoblotting. The density of the bands was quantified to calculate the V_0/ V_1 ratio to determine V-ATPase assembly. (a) Mitochondrial substrates, βhb and pyruvate, demonstrated no significant difference in V-ATPase assembly compared with their respective vehicle treated glucose-deprived cells. Dep vs Pyr, N=3. Dep vs βhb, N=4. (b) Creatine-phosphate and creatine-monohydrate also demonstrated no significant difference in V-ATPase assembly compared with the vehicle treated glucose-deprived cells. N=3. Immunoblotting results were normalized to the vehicle treated glucose-deprived condition in each group and compared using a one-way ANOVA with Tukey's Post hoc Test. *$p<0.05$, **$p<0.01$. A students T-test was used to compare βhb to the vehicle treated (ethanol) glucose-deprived condition and pyruvate to the vehicle treated (ddH_2O) glucose-deprived condition. Data represent the group mean± SD.

Chapter 4: Discussion

The purpose of this thesis was to determine whether neuronal V-ATPase is regulated by glucose and if so, to investigate the effect of other bioenergetic substrates on V-ATPase assembly. This discussion will address the results, potential pitfalls, and discrepancies compared with previous studies, and point to future directions.

Variance

Initial studies were conducted in N2a cells thawed at passage 7 or 8, whereas later studies were performed in N2a cells thawed at passage 5. Initial studies demonstrated that some bioenergetic substrates, such as glucose, significantly increased neuronal V-ATPase assembly, which contradicts later studies that showed no significant change in V-ATPase assembly. Several western blots from initial studies were repeated with more stringent conditions after later studies. There were a few repeated results that did not demonstrate the same significant results as previously. The cause of this discrepancy between initial and later studies is unknown. The variance between the bioenergetic substrates observed in initial data could be attributed to a low sample size and replicates, leading to low statistical power, or to cell health. The use of a higher number of samples, replicates, and lower passage of cells in later studies eliminated the variance observed in initial studies.

Antibody Validation

Neuronal and V-ATPase antibodies were validated to determine their specificity and sensitivity in dN2a cells. As expected, the antibodies were successfully detected in brain tissue. PANC-1 cells are a human pancreatic carcinoma cell line with neuroendocrine differentiation

that served as a positive control. The PANC-1 cells detected the neuronal and V-ATPase antibodies except for synaptophysin. This negative detection of synaptophysin is congruent with a previous study (Gradiz et al., 2016). Although, the negative detection of synaptophysin is likely due to the undifferentiated state of the PANC-1 cells. Synaptophysin detection was previously reported (Egawa, Maillet, VanDamme, De Greve, & Kloppel, 1996) to be enhanced in differentiated PANC-1 cells. In future experiments, synaptophysin could be characterized in differentiated PANC-1 cells to observe its expression. For the negative control, mouse latissimus dorsi muscle was used as a negative control for the neuronal antibodies and was unsuccessful for V-ATPase antibodies. V-ATPase is ubiquitous and present in most intracellular organelles such as lysosomes. Since the presence of lysosomes are controversial in skeletal muscle (Canonico & Bird, 1970), it was chosen as a negative control. As expected, neuronal antibodies were not detected in skeletal muscle tissue, but V-ATPase antibodies were detected. Although, the V-ATPase antibodies were detected with lower levels of sensitivity. Thus, skeletal muscle tissue was not the appropriate negative control for V-ATPase markers. The neuronal and V-ATPase antibodies were detected in dN2a cells, except NeuN expressed a lower sensitivity. The validation of the antibodies demonstrates the specificity of the neuronal antibodies and a varying level of specificity for the V-ATPase antibodies, which was expected due to the ubiquitous nature of V-ATPase.

Morphological and Biochemical Characterization of dN2a cells

Differentiated N2a (dN2a) cells were characterized morphologically and biochemically. In **Fig 7a**, microscopy images of N2a cells observed at 0 hr, 48 hr, and 96 hrs after differentiation demonstrate an increased growth in neural processes, indicating a neuronal phenotype. Next, the validated neuronal and V-ATPase antibodies were utilized to characterize

the differentiated N2a cells. In **Fig 7b**, the expression of the neuronal markers was shown to be significantly increased in a time-dependent manner in dN2a cells. The morphological images and significant time-dependent enhancement of validated neuronal markers confirms the neuronal phenotype of 96 h differentiated N2a cells.

Protein Expression levels of V_0V_1 in Cell Lysate

To ensure protein expression is not upregulated after treatment with bioenergetic substrates such as glucose, immunoblotting was performed to detect the average density of V-ATPase V_0 and V_1 antibodies on treated cell lysates. The results (**Fig 8**) demonstrated there was no significant difference in average relative density between the treatment groups for both the V-ATPase V_0 and V_1 antibodies. Beta-tubulin was used as a loading control. This result suggests any difference observed in further studies between the treatment groups is attributed to changes in V-ATPase assembly and not to changes in V_0 and V_1 expression.

Neuronal V-ATPase Regulation by Glucose after chronic glucose-deprivation

V-ATPase assembly in glucose-treated cells was measured through the co-immunoprecipitation of free V_1 and assembled V-ATPase complexes and immunoblotting of the captured eluate to calculate the ratio of the V_0 and V_1 antibodies. Excess V_1 is captured along with the V-ATPase complex with the use of a V_1 antibody. The low variability of the average density of total V_0 and V_1 in cell lysate and the fact that the V_0/V_1 ratio is used for the index of V-ATPase assembly corrects for the excess V_1.

The experimental design was modeled after a previous study conducted in mammalian cells (Sautin et al., 2005), specifically HK-2 (human proximal tubular cells) and LLC-PK (porcine renal epithelial cells). The renal epithelial cells were maintained in medium containing

10% FBS and 5.5mM of glucose, then chronically deprived of glucose in glucose-free DMEM overnight (16 h) and stimulated the next day with 10mM of glucose for 15 min. The V-ATPase complex was captured with a V_1 antibody in equal amounts of cell lysate and immunodetection with a V_0 and V_1 antibody was performed to calculate the ratio of V-ATPase assembly. This study reported overnight glucose-deprivation leads to significant V-ATPase disassembly compared with cells maintained in complete medium. Furthermore, cells stimulated with 10mM of glucose for 15 min rescued and increased V-ATPase assembly. The absence of a control condition with 5.5mM glucose to restore glucose levels after overnight deprivation makes it difficult to accurately compare whether the absence of glucose stimulation and 25mM glucose significantly impacted V-ATPase assembly. Due to these results, we expected to observe the disassembly of V-ATPase after chronic overnight glucose-deprivation and the restoration of V-ATPase assembly after acute glucose stimulation.

A more recent study investigating the effect of glucose on V-ATPase assembly in mammalian cells after acute glucose-deprivation demonstrated opposing results (McGuire & Forgac, 2018). In this study, HEK293T cells were maintained in serum-free DMEM with 5mM of glucose. The cells were then treated with fresh medium containing either glucose-free DMEM (10 min), 5mM glucose (1 h), 25mM glucose (1 h), or 0mM glucose (10 min) and then 5mM glucose (10 min). In contrast with the previous study, their results indicated acute glucose-deprivation (10 min) significantly increased V-ATPase assembly compared with cells maintained in physiological 5mM of glucose. In agreement with the previous study, cells stimulated with 25mM of glucose also had significantly increased V-ATPase assembly compared with the physiological condition. It is not clear why the cells were only deprived of glucose for 10 min when the other groups were treated for 1 h. Furthermore, the increase in V-ATPase assembly

observed after 10 min of glucose-deprivation may disappear or even decrease if lengthened to 1 h, possibly as a mechanism to preserve ATPs. Therefore, it is not known whether V-ATPase assembly was truly increased due to the lack of controls.

Consistent with literature, preliminary studies in passage 7 and 8 N2a cells indicated 10mM of glucose stimulation (G10) significantly increased neuronal V-ATPase assembly compared with glucose-deprived cells (Dep), although vehicle-treated non-glucose-deprived (NGD) cells were not significantly different compared with glucose-deprived cells (**Fig 9a**). The absence of change in V-ATPase assembly after chronic overnight glucose-deprivation suggests the activation of compensatory mechanisms that allow basal levels of V-ATPase assembly to maintain homeostatic conditions. Congruent with yeast and mammalian cells, the preliminary results suggest that V-ATPase assembly in neuronal cells respond to glucose fluctuations. This increase in V-ATPase assembly could be attributed to cytosolic alkalization and ATP production by glycolysis, rabconnectin binding, glycolytic enzymes, or a combination of these factors. This result indicates glucose plays a role in V-ATPase assembly and this regulatory mechanism is conserved in neuronal cells.

Further analysis of the effects of glucose on neuronal V-ATPase assembly was conducted under more stringent conditions, with an increased sample size and duplicates or triplicates of each treatment group included. Also, the experiments were performed in passage 5 N2a cells, a lower passage compared with preliminary studies. The overall results (**Fig 9b**) demonstrated there was no significant difference in V-ATPase assembly among the treatment groups. Three out of five experiments from different cell lysate samples demonstrated no significant changes in V-ATPase assembly among the treatment groups. One sample indicated significance, but the Tukey's post hoc test did not reveal which two groups were significantly different. Finally, one

sample (**Fig 9c**) demonstrated dN2a cells treated with 10mM of glucose significantly decreased V-ATPase assembly when compared with vehicle-treated glucose-deprived cells. Additionally, cells treated with 25mM of glucose significantly increased V-ATPase assembly compared with cells treated with 10mM of glucose. Congruent with preliminary results, the vehicle-treated non-glucose-deprived cells (maintained in medium containing 25mM of glucose) was not significantly different compared with glucose-deprived cells. This particular result demonstrated overnight glucose-deprivation does not lead to significant changes in V-ATPase assembly. Also, stimulation with 10mM of glucose induces V-ATPase disassembly and the addition of a higher concentration of glucose (25mM) reverses the disassembly and leads to an increase in V-ATPase assembly. The reason for the disassembly observed with the addition of 10mM of glucose compared with the glucose-deprived condition could be attributed to the cells being maintained and conditioned to 25mM of glucose prior to overnight deprivation. Thus, stimulation with a lower concentration of glucose may not allow V-ATPase assembly to be restored or exceed physiological levels. Compensatory mechanisms could be responsible, but more investigation is needed since the results were not reproducible.

Taken together, further analyses demonstrated glucose stimulation had no significant effect on neuronal V-ATPase assembly in chronically glucose-deprived cells and does not support preliminary results. This could be attributed to increased sample sizes and replications as well as a lower passage of N2a cells. The results also indicate neuronal dN2a cells may respond to glucose stimulation or chronic glucose-deprivation differently than mammalian and yeast cells and further investigation to optimize conditions for neuronal cells are needed.

Neuronal V-ATPase regulation by other bioenergetic substrates after chronic glucose-deprivation

Next, we tested the efficacy of other bioenergetic substrates on V-ATPase assembly. We sought to examine whether substrates that enter during later steps in cellular respiration could also influence neuronal V-ATPase assembly. The bioenergetic substrates tested were sodium pyruvate, beta-hydroxybutyrate (βhb), creatine-phosphate (CrP), and creatine-monohydrate (CrMH). Pyruvate, the end product of glycolysis, enters the mitochondrial matrix from the cytosol. There it is converted to acetyl-coA by pyruvate dehydrogenase (PDH) and enters the Citric Acid Cycle (TCA cycle). Beta-hydroxybutyrate (βhb), one of three ketone bodies, is a secondary source utilized by the body under low glucose conditions to maintain its' bioenergetic needs. Fatty acids are broken down by the liver during ketosis to produce D- βhb. It enters the mitochondria where it is converted into acetoacetate and then acetyl-coA, thereby entering the TCA cycle. Pyruvate and βhb are both involved in oxidative phosphorylation in the mitochondria and produce 38 ATP's (Gautheron, 1984), significantly more ATP's than glycolysis. Creatine is an amino acid that becomes phosphorylated by mitochondrial creatine kinase (CK) in the intermembrane of the mitochondria to become Cr-P, an energy storing compound. Cr-P shuttles into the cytosol where it can readily donate a high-energy phosphate by cytosolic CK to form ATP, then it reenters the mitochondria to become phosphorylated and the cycle continues. The rapid production of ATP makes creatine a common supplement for athletes that require short bursts of intense energy, with creatine-monohydrate (Cr-MH) as the most popular form. Cr-MH is indistinguishable from creatine and must enter the mitochondria to convert into the energy storing compound creatine phosphate.

Surprisingly, the results indicated the addition of 10mM of bioenergetic substrates did not significantly increase V-ATPase assembly compared with the chronically glucose-deprived condition. Therefore, bioenergetic substrates have no effect on neuronal V-ATPase assembly. The discrepancy compared with previous studies is unknown. We reason it could be attributed to nonoptimal conditions such as length of glucose-deprivation, substrate concentration, or incubation time of the substrate treatment.

Future Directions

To improve future experiments, potential pitfalls will be addressed in this section. The V-ATPase has been studied extensively in yeast and some mammalian cells, but there is a lack of research on neuronal V-ATPase. To properly investigate neuronal V-ATPase assembly, further experiments must be conducted to optimize experimental conditions and to determine the cellular response of neuronal V-ATPase.

In contrast to previous studies, the results of this study indicate glucose and other bioenergetic substrates do not induce a significant change in V-ATPase assembly. Studies investigating V-ATPase assembly in yeast cells typically deprived cells of glucose for 20-30 min; whereas mammalian cells were subjected to glucose-deprivation from acute deprivation for 10 min to overnight deprivation for up to 16 h. Future investigations could measure neuronal V-ATPase assembly at various time points after glucose deprivation to determine the optimal length of incubation. Another way to accomplish this would be to experimentally determine the length of time it takes for significant V-ATPase disassembly to occur by measuring V-ATPase activity levels. This would allow the optimization of incubation time for glucose-deprivation. Glucose and bioenergetic substrate concentrations exceeding the physiological level of 25mM could also be tested. A pitfall of the current study is the exclusion of a glucose stimulation group

with an elevated concentration relative to the physiological concentration of 25mM. This could also be corrected by conditioning dN2a cells to a lower concentration of glucose prior to bioenergetic substrate stimulation. Furthermore, the experiments could be replicated in other neuronal cells or primary neurons to validate the results.

Chapter 5: Conclusion

This study sought to investigate the effect of bioenergetic status on neuronal V-ATPase assembly. The results demonstrate bioenergetic substrates such as glucose, pyruvate, beta-hydroxybutyrate, creatine phosphate, and creatine monohydrate did not have a significant effect on neuronal V-ATPase assembly following chronic glucose-deprivation. This is not congruent with previous studies carried out in yeast and mammalian cells that provide overwhelming evidence supporting the regulation of V-ATPase assembly by glucose. Further investigations need to be conducted to optimize experimental conditions for neuronal V-ATPase studies. These findings, although negative, set a precedent for future studies on neuronal V-ATPase assembly.

Literature Cited

Alfarouk, K. O., Verduzco, D., Rauch, C., Muddathir, A. K., Adil, H. H., Elhassan, G. O., . . . Harguindey, S. (2014). Glycolysis, tumor metabolism, cancer growth and dissemination. A new pH-based etiopathogenic perspective and therapeutic approach to an old cancer question. *Oncoscience, 1*(12), 777-802. Retrieved from https://www.ncbi.nlm.nih.gov/pubmed/25621294. doi:10.18632/oncoscience.109

Bagh, M. B., Peng, S., Chandra, G., Zhang, Z., Singh, S. P., Pattabiraman, N., . . . Mukherjee, A. B. (2017). Misrouting of v-ATPase subunit V0a1 dysregulates lysosomal acidification in a neurodegenerative lysosomal storage disease model. *Nat Commun, 8*, 14612. Retrieved from https://www.ncbi.nlm.nih.gov/pubmed/28266544. doi:10.1038/ncomms14612

Beltran, C., & Nelson, N. (1992). The membrane sector of vacuolar H(+)-ATPase by itself is impermeable to protons. *Acta Physiol Scand Suppl, 607*, 41-47. Retrieved from https://www.ncbi.nlm.nih.gov/pubmed/1333159.

Benlekbir, S., Bueler, S. A., & Rubinstein, J. L. (2012). Structure of the vacuolar-type ATPase from Saccharomyces cerevisiae at 11-A resolution. *Nat Struct Mol Biol, 19*(12), 1356-1362. Retrieved from https://www.ncbi.nlm.nih.gov/pubmed/23142977. doi:10.1038/nsmb.2422

Boekema, E. J., Ubbink-Kok, T., Lolkema, J. S., Brisson, A., & Konings, W. N. (1997). Visualization of a peripheral stalk in V-type ATPase: evidence for the stator structure essential to rotational catalysis. *Proc Natl Acad Sci U S A, 94*(26), 14291-14293. Retrieved from https://www.ncbi.nlm.nih.gov/pubmed/9405605. doi:10.1073/pnas.94.26.14291

Bond, S., & Forgac, M. (2008). The Ras/cAMP/protein kinase A pathway regulates glucose-dependent assembly of the vacuolar (H+)-ATPase in yeast. *J Biol Chem, 283*(52), 36513-36521. Retrieved from https://www.ncbi.nlm.nih.gov/pubmed/18936098. doi:10.1074/jbc.M805232200

Boyle, W. J., Simonet, W. S., & Lacey, D. L. (2003). Osteoclast differentiation and activation. *Nature, 423*(6937), 337-342. Retrieved from https://www.ncbi.nlm.nih.gov/pubmed/12748652. doi:10.1038/nature01658

Colacurcio, D. J., & Nixon, R. A. (2016). Disorders of lysosomal acidification-The emerging role of v-ATPase in aging and neurodegenerative disease. *Ageing Res Rev, 32*, 75-88. Retrieved from https://www.ncbi.nlm.nih.gov/pubmed/27197071. doi:10.1016/j.arr.2016.05.004

Cooper, R., Naclerio, F., Allgrove, J., & Jimenez, A. (2012). Creatine supplementation with specific view to exercise/sports performance: an update. *J Int Soc Sports Nutr, 9*(1), 33. Retrieved from https://www.ncbi.nlm.nih.gov/pubmed/22817979. doi:10.1186/1550-2783-9-33

de Duve, C. (2005). The lysosome turns fifty. *Nat Cell Biol, 7*(9), 847-849. Retrieved from https://www.ncbi.nlm.nih.gov/pubmed/16136179. doi:10.1038/ncb0905-847

De Duve, C., & Wattiaux, R. (1966). Functions of lysosomes. *Annu Rev Physiol, 28*, 435-492. Retrieved from https://www.ncbi.nlm.nih.gov/pubmed/5322983. doi:10.1146/annurev.ph.28.030166.002251

Dechant, R., Binda, M., Lee, S. S., Pelet, S., Winderickx, J., & Peter, M. (2010). Cytosolic pH is a second messenger for glucose and regulates the PKA pathway through V-ATPase. *EMBO J, 29*(15), 2515-2526. Retrieved from https://www.ncbi.nlm.nih.gov/pubmed/20581803. doi:10.1038/emboj.2010.138

Dedkova, E. N., & Blatter, L. A. (2014). Role of beta-hydroxybutyrate, its polymer poly-beta-hydroxybutyrate and inorganic polyphosphate in mammalian health and disease. *Front Physiol, 5*, 260. Retrieved from https://www.ncbi.nlm.nih.gov/pubmed/25101001. doi:10.3389/fphys.2014.00260

Deprez, M. A., Eskes, E., Wilms, T., Ludovico, P., & Winderickx, J. (2018). pH homeostasis links the nutrient sensing PKA/TORC1/Sch9 menage-a-trois to stress tolerance and longevity. *Microb Cell,*

5(3), 119-136. Retrieved from https://www.ncbi.nlm.nih.gov/pubmed/29487859. doi:10.15698/mic2018.03.618

Diakov, T. T., & Kane, P. M. (2010). Regulation of vacuolar proton-translocating ATPase activity and assembly by extracellular pH. *J Biol Chem, 285*(31), 23771-23778. Retrieved from https://www.ncbi.nlm.nih.gov/pubmed/20511227. doi:10.1074/jbc.M110.110122

Erbsloh, F., Bernsmeier, A., & Hillesheim, H. (1958). [The glucose consumption of the brain & its dependence on the liver]. *Arch Psychiatr Nervenkr Z Gesamte Neurol Psychiatr, 196*(6), 611-626. Retrieved from https://www.ncbi.nlm.nih.gov/pubmed/13534602.

Forgac, M. (2007). Vacuolar ATPases: rotary proton pumps in physiology and pathophysiology. *Nat Rev Mol Cell Biol, 8*(11), 917-929. Retrieved from https://www.ncbi.nlm.nih.gov/pubmed/17912264. doi:10.1038/nrm2272

Frattini, A., Orchard, P. J., Sobacchi, C., Giliani, S., Abinun, M., Mattsson, J. P., . . . Villa, A. (2000). Defects in TCIRG1 subunit of the vacuolar proton pump are responsible for a subset of human autosomal recessive osteopetrosis. *Nat Genet, 25*(3), 343-346. Retrieved from https://www.ncbi.nlm.nih.gov/pubmed/10888887. doi:10.1038/77131

Fuller, M., Meikle, P. J., & Hopwood, J. J. (2006). Epidemiology of lysosomal storage diseases: an overview. In A. Mehta, M. Beck, & G. Sunder-Plassmann (Eds.), *Fabry Disease: Perspectives from 5 Years of FOS*. Oxford.

Futerman, A. H., & van Meer, G. (2004). The cell biology of lysosomal storage disorders. *Nat Rev Mol Cell Biol, 5*(7), 554-565. Retrieved from https://www.ncbi.nlm.nih.gov/pubmed/15232573. doi:10.1038/nrm1423

Gautheron, D. C. (1984). Mitochondrial oxidative phosphorylation and respiratory chain: review. *J Inherit Metab Dis, 7 Suppl 1*, 57-61. Retrieved from https://www.ncbi.nlm.nih.gov/pubmed/6153061.

Gluck, S., & Caldwell, J. (1987). Immunoaffinity purification and characterization of vacuolar H+ATPase from bovine kidney. *J Biol Chem, 262*(32), 15780-15789. Retrieved from https://www.ncbi.nlm.nih.gov/pubmed/2890634.

Graf, R., Harvey, W. R., & Wieczorek, H. (1996). Purification and properties of a cytosolic V1-ATPase. *J Biol Chem, 271*(34), 20908-20913. Retrieved from https://www.ncbi.nlm.nih.gov/pubmed/8702848. doi:10.1074/jbc.271.34.20908

Hanna-El-Daher, L., & Braissant, O. (2016). Creatine synthesis and exchanges between brain cells: What can be learned from human creatine deficiencies and various experimental models? *Amino Acids, 48*(8), 1877-1895. Retrieved from https://www.ncbi.nlm.nih.gov/pubmed/26861125. doi:10.1007/s00726-016-2189-0

Hayek, S. R., Rane, H. S., & Parra, K. J. (2019). Reciprocal Regulation of V-ATPase and Glycolytic Pathway Elements in Health and Disease. *Front Physiol, 10*, 127. Retrieved from https://www.ncbi.nlm.nih.gov/pubmed/30828305. doi:10.3389/fphys.2019.00127

Hinton, A., Sennoune, S. R., Bond, S., Fang, M., Reuveni, M., Sahagian, G. G., . . . Forgac, M. (2009). Function of a subunit isoforms of the V-ATPase in pH homeostasis and in vitro invasion of MDA-MB231 human breast cancer cells. *J Biol Chem, 284*(24), 16400-16408. Retrieved from https://www.ncbi.nlm.nih.gov/pubmed/19366680. doi:10.1074/jbc.M901201200

Imamura, H., Nakano, M., Noji, H., Muneyuki, E., Ohkuma, S., Yoshida, M., & Yokoyama, K. (2003). Evidence for rotation of V1-ATPase. *Proc Natl Acad Sci U S A, 100*(5), 2312-2315. Retrieved from https://www.ncbi.nlm.nih.gov/pubmed/12598655. doi:10.1073/pnas.0436796100

Jansen, E. J., van Bakel, N. H., Coenen, A. J., van Dooren, S. H., van Lith, H. A., & Martens, G. J. (2010). An isoform of the vacuolar (H(+))-ATPase accessory subunit Ac45. *Cell Mol Life Sci, 67*(4), 629-640. Retrieved from https://www.ncbi.nlm.nih.gov/pubmed/19946730. doi:10.1007/s00018-009-0200-6

Jefferies, K. C., & Forgac, M. (2008). Subunit H of the vacuolar (H+) ATPase inhibits ATP hydrolysis by the free V1 domain by interaction with the rotary subunit F. *J Biol Chem, 283*(8), 4512-4519. Retrieved from https://www.ncbi.nlm.nih.gov/pubmed/18156183. doi:10.1074/jbc.M707144200

Kane, P. M. (1995). Disassembly and reassembly of the yeast vacuolar H(+)-ATPase in vivo. *J Biol Chem, 270*(28), 17025-17032. Retrieved from https://www.ncbi.nlm.nih.gov/pubmed/7622524.

Katara, G. K., Kulshrestha, A., Jaiswal, M. K., Pamarthy, S., Gilman-Sachs, A., & Beaman, K. D. (2016). Inhibition of vacuolar ATPase subunit in tumor cells delays tumor growth by decreasing the essential macrophage population in the tumor microenvironment. *Oncogene, 35*(8), 1058-1065. Retrieved from https://www.ncbi.nlm.nih.gov/pubmed/25961933. doi:10.1038/onc.2015.159

Kawasaki-Nishi, S., Nishi, T., & Forgac, M. (2001a). Arg-735 of the 100-kDa subunit a of the yeast V-ATPase is essential for proton translocation. *Proc Natl Acad Sci U S A, 98*(22), 12397-12402. Retrieved from https://www.ncbi.nlm.nih.gov/pubmed/11592980. doi:10.1073/pnas.221291798

Kawasaki-Nishi, S., Nishi, T., & Forgac, M. (2001b). Yeast V-ATPase complexes containing different isoforms of the 100-kDa a-subunit differ in coupling efficiency and in vivo dissociation. *J Biol Chem, 276*(21), 17941-17948. Retrieved from https://www.ncbi.nlm.nih.gov/pubmed/11278748. doi:10.1074/jbc.M010790200

Lafourcade, C., Sobo, K., Kieffer-Jaquinod, S., Garin, J., & van der Goot, F. G. (2008). Regulation of the V-ATPase along the endocytic pathway occurs through reversible subunit association and membrane localization. *PLoS One, 3*(7), e2758. Retrieved from https://www.ncbi.nlm.nih.gov/pubmed/18648502. doi:10.1371/journal.pone.0002758

Liberti, M. V., & Locasale, J. W. (2016). The Warburg Effect: How Does it Benefit Cancer Cells? *Trends Biochem Sci, 41*(3), 211-218. Retrieved from https://www.ncbi.nlm.nih.gov/pubmed/26778478. doi:10.1016/j.tibs.2015.12.001

Liu, Y., Steinbusch, L. K. M., Nabben, M., Kapsokalyvas, D., van Zandvoort, M., Schonleitner, P., . . . Luiken, J. (2017). Palmitate-Induced Vacuolar-Type H(+)-ATPase Inhibition Feeds Forward Into Insulin Resistance and Contractile Dysfunction. *Diabetes, 66*(6), 1521-1534. Retrieved from https://www.ncbi.nlm.nih.gov/pubmed/28302654. doi:10.2337/db16-0727

Lu, M., Sautin, Y. Y., Holliday, L. S., & Gluck, S. L. (2004). The glycolytic enzyme aldolase mediates assembly, expression, and activity of vacuolar H+-ATPase. *J Biol Chem, 279*(10), 8732-8739. Retrieved from https://www.ncbi.nlm.nih.gov/pubmed/14672945. doi:10.1074/jbc.M303871200

MacLeod, K. J., Vasilyeva, E., Baleja, J. D., & Forgac, M. (1998). Mutational analysis of the nucleotide binding sites of the yeast vacuolar proton-translocating ATPase. *J Biol Chem, 273*(1), 150-156. Retrieved from https://www.ncbi.nlm.nih.gov/pubmed/9417059. doi:10.1074/jbc.273.1.150

Maher, M. J., Akimoto, S., Iwata, M., Nagata, K., Hori, Y., Yoshida, M., . . . Yokoyama, K. (2009). Crystal structure of A3B3 complex of V-ATPase from Thermus thermophilus. *EMBO J, 28*(23), 3771-3779. Retrieved from https://www.ncbi.nlm.nih.gov/pubmed/19893485. doi:10.1038/emboj.2009.310

McGuire, C. M., & Forgac, M. (2018). Glucose starvation increases V-ATPase assembly and activity in mammalian cells through AMP kinase and phosphatidylinositide 3-kinase/Akt signaling. *J Biol Chem, 293*(23), 9113-9123. Retrieved from https://www.ncbi.nlm.nih.gov/pubmed/29540478. doi:10.1074/jbc.RA117.001327

Meier, T., Polzer, P., Diederichs, K., Welte, W., & Dimroth, P. (2005). Structure of the rotor ring of F-Type Na+-ATPase from Ilyobacter tartaricus. *Science, 308*(5722), 659-662. Retrieved from https://www.ncbi.nlm.nih.gov/pubmed/15860619. doi:10.1126/science.1111199

Mellman, I., Fuchs, R., & Helenius, A. (1986). Acidification of the endocytic and exocytic pathways. *Annu Rev Biochem, 55*, 663-700. Retrieved from https://www.ncbi.nlm.nih.gov/pubmed/2874766. doi:10.1146/annurev.bi.55.070186.003311

Mergenthaler, P., Lindauer, U., Dienel, G. A., & Meisel, A. (2013). Sugar for the brain: the role of glucose in physiological and pathological brain function. *Trends Neurosci, 36*(10), 587-597. Retrieved from https://www.ncbi.nlm.nih.gov/pubmed/23968694. doi:10.1016/j.tins.2013.07.001

Moriyama, Y., Maeda, M., & Futai, M. (1992). The role of V-ATPase in neuronal and endocrine systems. *J Exp Biol, 172*, 171-178. Retrieved from https://www.ncbi.nlm.nih.gov/pubmed/1362770.

Muench, S. P., Huss, M., Song, C. F., Phillips, C., Wieczorek, H., Trinick, J., & Harrison, M. A. (2009). Cryo-electron microscopy of the vacuolar ATPase motor reveals its mechanical and regulatory complexity. *J Mol Biol, 386*(4), 989-999. Retrieved from https://www.ncbi.nlm.nih.gov/pubmed/19244615.

Muller, K. H., Kainov, D. E., El Bakkouri, K., Saelens, X., De Brabander, J. K., Kittel, C., . . . Muller, C. P. (2011). The proton translocation domain of cellular vacuolar ATPase provides a target for the treatment of influenza A virus infections. *Br J Pharmacol, 164*(2), 344-357. Retrieved from https://www.ncbi.nlm.nih.gov/pubmed/21418188. doi:10.1111/j.1476-5381.2011.01346.x

Muller, O., Neumann, H., Bayer, M. J., & Mayer, A. (2003). Role of the Vtc proteins in V-ATPase stability and membrane trafficking. *J Cell Sci, 116*(Pt 6), 1107-1115. Retrieved from https://www.ncbi.nlm.nih.gov/pubmed/12584253.

Murata, T., Yamato, I., Kakinuma, Y., Leslie, A. G., & Walker, J. E. (2005). Structure of the rotor of the V-Type Na+-ATPase from Enterococcus hirae. *Science, 308*(5722), 654-659. Retrieved from https://www.ncbi.nlm.nih.gov/pubmed/15802565. doi:10.1126/science.1110064

Newman, J. C., & Verdin, E. (2014). beta-hydroxybutyrate: much more than a metabolite. *Diabetes Res Clin Pract, 106*(2), 173-181. Retrieved from https://www.ncbi.nlm.nih.gov/pubmed/25193333. doi:10.1016/j.diabres.2014.08.009

Nishi, T., & Forgac, M. (2002). The vacuolar (H+)-ATPases--nature's most versatile proton pumps. *Nat Rev Mol Cell Biol, 3*(2), 94-103. Retrieved from https://www.ncbi.nlm.nih.gov/pubmed/11836511. doi:10.1038/nrm729

Nixon, R. A. (2013). The role of autophagy in neurodegenerative disease. *Nat Med, 19*(8), 983-997. Retrieved from https://www.ncbi.nlm.nih.gov/pubmed/23921753. doi:10.1038/nm.3232

Nouioua, S., Cheillan, D., Zaouidi, S., Salomons, G. S., Amedjout, N., Kessaci, F., . . . Tazir, M. (2013). Creatine deficiency syndrome. A treatable myopathy due to arginine-glycine amidinotransferase (AGAT) deficiency. *Neuromuscul Disord, 23*(8), 670-674. Retrieved from https://www.ncbi.nlm.nih.gov/pubmed/23770102. doi:10.1016/j.nmd.2013.04.011

Ochotny, N., Flenniken, A. M., Owen, C., Voronov, I., Zirngibl, R. A., Osborne, L. R., . . . Aubin, J. E. (2011). The V-ATPase a3 subunit mutation R740S is dominant negative and results in osteopetrosis in mice. *J Bone Miner Res, 26*(7), 1484-1493. Retrieved from https://www.ncbi.nlm.nih.gov/pubmed/21305608. doi:10.1002/jbmr.355

Parra, K. J., Chan, C. Y., & Chen, J. (2014). Saccharomyces cerevisiae vacuolar H+-ATPase regulation by disassembly and reassembly: one structure and multiple signals. *Eukaryot Cell, 13*(6), 706-714. Retrieved from https://www.ncbi.nlm.nih.gov/pubmed/24706019. doi:10.1128/EC.00050-14

Parra, K. J., & Kane, P. M. (1998). Reversible association between the V1 and V0 domains of yeast vacuolar H+-ATPase is an unconventional glucose-induced effect. *Mol Cell Biol, 18*(12), 7064-7074. Retrieved from https://www.ncbi.nlm.nih.gov/pubmed/9819393.

Parra, K. J., Keenan, K. L., & Kane, P. M. (2000). The H subunit (Vma13p) of the yeast V-ATPase inhibits the ATPase activity of cytosolic V1 complexes. *J Biol Chem, 275*(28), 21761-21767. Retrieved from https://www.ncbi.nlm.nih.gov/pubmed/10781598. doi:10.1074/jbc.M002305200

Parsons, S. M. (2000). Transport mechanisms in acetylcholine and monoamine storage. *FASEB J, 14*(15), 2423-2434. Retrieved from https://www.ncbi.nlm.nih.gov/pubmed/11099460. doi:10.1096/fj.00-0203rev

Pillay, C. S., Elliott, E., & Dennison, C. (2002). Endolysosomal proteolysis and its regulation. *Biochem J, 363*(Pt 3), 417-429. Retrieved from https://www.ncbi.nlm.nih.gov/pubmed/11964142. doi:10.1042/0264-6021:3630417

Rahman, N., Ramos-Espiritu, L., Milner, T. A., Buck, J., & Levin, L. R. (2016). Soluble adenylyl cyclase is essential for proper lysosomal acidification. *J Gen Physiol, 148*(4), 325-339. Retrieved from https://www.ncbi.nlm.nih.gov/pubmed/27670898. doi:10.1085/jgp.201611606

Rogatzki, M. J., Ferguson, B. S., Goodwin, M. L., & Gladden, L. B. (2015). Lactate is always the end product of glycolysis. *Front Neurosci, 9*, 22. Retrieved from https://www.ncbi.nlm.nih.gov/pubmed/25774123. doi:10.3389/fnins.2015.00022

Saftig, P., & Klumperman, J. (2009). Lysosome biogenesis and lysosomal membrane proteins: trafficking meets function. *Nat Rev Mol Cell Biol, 10*(9), 623-635. Retrieved from https://www.ncbi.nlm.nih.gov/pubmed/19672277. doi:10.1038/nrm2745

Sagermann, M., Stevens, T. H., & Matthews, B. W. (2001). Crystal structure of the regulatory subunit H of the V-type ATPase of Saccharomyces cerevisiae. *Proc Natl Acad Sci U S A, 98*(13), 7134-7139. Retrieved from https://www.ncbi.nlm.nih.gov/pubmed/11416198. doi:10.1073/pnas.131192798

Sagne, C., Agulhon, C., Ravassard, P., Darmon, M., Hamon, M., El Mestikawy, S., . . . Giros, B. (2001). Identification and characterization of a lysosomal transporter for small neutral amino acids. *Proc Natl Acad Sci U S A, 98*(13), 7206-7211. Retrieved from https://www.ncbi.nlm.nih.gov/pubmed/11390972. doi:10.1073/pnas.121183498

Sambongi, Y., Iko, Y., Tanabe, M., Omote, H., Iwamoto-Kihara, A., Ueda, I., . . . Futai, M. (1999). Mechanical rotation of the c subunit oligomer in ATP synthase (F0F1): direct observation. *Science, 286*(5445), 1722-1724. Retrieved from https://www.ncbi.nlm.nih.gov/pubmed/10576736.

Sautin, Y. Y., Lu, M., Gaugler, A., Zhang, L., & Gluck, S. L. (2005). Phosphatidylinositol 3-kinase-mediated effects of glucose on vacuolar H+-ATPase assembly, translocation, and acidification of intracellular compartments in renal epithelial cells. *Mol Cell Biol, 25*(2), 575-589. Retrieved from https://www.ncbi.nlm.nih.gov/pubmed/15632060. doi:10.1128/MCB.25.2.575-589.2005

Sennoune, S. R., Bakunts, K., Martinez, G. M., Chua-Tuan, J. L., Kebir, Y., Attaya, M. N., & Martinez-Zaguilan, R. (2004). Vacuolar H+-ATPase in human breast cancer cells with distinct metastatic potential: distribution and functional activity. *Am J Physiol Cell Physiol, 286*(6), C1443-1452. Retrieved from https://www.ncbi.nlm.nih.gov/pubmed/14761893. doi:10.1152/ajpcell.00407.2003

Sennoune, S. R., & Martinez-Zaguilan, R. (2007). Plasmalemmal vacuolar H+-ATPases in angiogenesis, diabetes and cancer. *J Bioenerg Biomembr, 39*(5-6), 427-433. Retrieved from https://www.ncbi.nlm.nih.gov/pubmed/18058006. doi:10.1007/s10863-007-9108-8

Seol, J. H., Shevchenko, A., Shevchenko, A., & Deshaies, R. J. (2001). Skp1 forms multiple protein complexes, including RAVE, a regulator of V-ATPase assembly. *Nat Cell Biol, 3*(4), 384-391. Retrieved from https://www.ncbi.nlm.nih.gov/pubmed/11283612. doi:10.1038/35070067

Smardon, A. M., Tarsio, M., & Kane, P. M. (2002). The RAVE complex is essential for stable assembly of the yeast V-ATPase. *J Biol Chem, 277*(16), 13831-13839. Retrieved from https://www.ncbi.nlm.nih.gov/pubmed/11844802. doi:10.1074/jbc.M200682200

Smith, R. N., Agharkar, A. S., & Gonzales, E. B. (2014). A review of creatine supplementation in age-related diseases: more than a supplement for athletes. *F1000Res, 3*, 222. Retrieved from https://www.ncbi.nlm.nih.gov/pubmed/25664170. doi:10.12688/f1000research.5218.1

Stevens, T. H., & Forgac, M. (1997). Structure, function and regulation of the vacuolar (H+)-ATPase. *Annu Rev Cell Dev Biol, 13*, 779-808. Retrieved from https://www.ncbi.nlm.nih.gov/pubmed/9442887. doi:10.1146/annurev.cellbio.13.1.779

Stransky, L. A., & Forgac, M. (2015). Amino Acid Availability Modulates Vacuolar H+-ATPase Assembly. *J Biol Chem, 290*(45), 27360-27369. Retrieved from https://www.ncbi.nlm.nih.gov/pubmed/26378229. doi:10.1074/jbc.M115.659128

Takamori, S., Holt, M., Stenius, K., Lemke, E. A., Gronborg, M., Riedel, D., . . . Jahn, R. (2006). Molecular anatomy of a trafficking organelle. *Cell, 127*(4), 831-846. Retrieved from https://www.ncbi.nlm.nih.gov/pubmed/17110340. doi:10.1016/j.cell.2006.10.030

Teitelbaum, S. L. (2000). Bone resorption by osteoclasts. *Science, 289*(5484), 1504-1508. Retrieved from https://www.ncbi.nlm.nih.gov/pubmed/10968780.

Teitelbaum, S. L. (2007). Osteoclasts: what do they do and how do they do it? *Am J Pathol, 170*(2), 427-435. Retrieved from https://www.ncbi.nlm.nih.gov/pubmed/17255310. doi:10.2353/ajpath.2007.060834

Tomashek, J. J., & Brusilow, W. S. (2000). Stoichiometry of energy coupling by proton-translocating ATPases: a history of variability. *J Bioenerg Biomembr, 32*(5), 493-500. Retrieved from https://www.ncbi.nlm.nih.gov/pubmed/15254384.

Torigoe, T., Izumi, H., Ise, T., Murakami, T., Uramoto, H., Ishiguchi, H., . . . Kohno, K. (2002). Vacuolar H(+)-ATPase: functional mechanisms and potential as a target for cancer chemotherapy. *Anticancer Drugs, 13*(3), 237-243. Retrieved from https://www.ncbi.nlm.nih.gov/pubmed/11984067.

Toyomura, T., Murata, Y., Yamamoto, A., Oka, T., Sun-Wada, G. H., Wada, Y., & Futai, M. (2003). From lysosomes to the plasma membrane: localization of vacuolar-type H+ -ATPase with the a3 isoform during osteoclast differentiation. *J Biol Chem, 278*(24), 22023-22030. Retrieved from https://www.ncbi.nlm.nih.gov/pubmed/12672822. doi:10.1074/jbc.M302436200

Wilkens, S., & Forgac, M. (2001). Three-dimensional structure of the vacuolar ATPase proton channel by electron microscopy. *J Biol Chem, 276*(47), 44064-44068. Retrieved from https://www.ncbi.nlm.nih.gov/pubmed/11533034. doi:10.1074/jbc.M106579200

Xu, T., & Forgac, M. (2001). Microtubules are involved in glucose-dependent dissociation of the yeast vacuolar [H+]-ATPase in vivo. *J Biol Chem, 276*(27), 24855-24861. Retrieved from https://www.ncbi.nlm.nih.gov/pubmed/11331282. doi:10.1074/jbc.M100637200

Yokoyama, K., & Imamura, H. (2005). Rotation, structure, and classification of prokaryotic V-ATPase. *J Bioenerg Biomembr, 37*(6), 405-410. Retrieved from https://www.ncbi.nlm.nih.gov/pubmed/16691473. doi:10.1007/s10863-005-9480-1

Zhang, C. S., Jiang, B., Li, M., Zhu, M., Peng, Y., Zhang, Y. L., . . . Lin, S. C. (2014). The lysosomal v-ATPase-Ragulator complex is a common activator for AMPK and mTORC1, acting as a switch between catabolism and anabolism. *Cell Metab, 20*(3), 526-540. Retrieved from https://www.ncbi.nlm.nih.gov/pubmed/25002183. doi:10.1016/j.cmet.2014.06.014

Zhang, L., Wang, X., Li, J., Zhu, X., Gao, F., & Zhou, G. (2017). Creatine Monohydrate Enhances Energy Status and Reduces Glycolysis via Inhibition of AMPK Pathway in Pectoralis Major Muscle of Transport-Stressed Broilers. *J Agric Food Chem, 65*(32), 6991-6999. Retrieved from https://www.ncbi.nlm.nih.gov/pubmed/28766947. doi:10.1021/acs.jafc.7b02740

Zhang, Z., Zheng, Y., Mazon, H., Milgrom, E., Kitagawa, N., Kish-Trier, E., . . . Wilkens, S. (2008). Structure of the yeast vacuolar ATPase. *J Biol Chem, 283*(51), 35983-35995. Retrieved from https://www.ncbi.nlm.nih.gov/pubmed/18955482. doi:10.1074/jbc.M805345200

Alfarouk, K. O., Verduzco, D., Rauch, C., Muddathir, A. K., Adil, H. H., Elhassan, G. O., . . . Harguindey, S. (2014). Glycolysis, tumor metabolism, cancer growth and dissemination. A new pH-based

etiopathogenic perspective and therapeutic approach to an old cancer question. *Oncoscience, 1*(12), 777-802. Retrieved from https://www.ncbi.nlm.nih.gov/pubmed/25621294. doi:10.18632/oncoscience.109

Bagh, M. B., Peng, S., Chandra, G., Zhang, Z., Singh, S. P., Pattabiraman, N., . . . Mukherjee, A. B. (2017). Misrouting of v-ATPase subunit V0a1 dysregulates lysosomal acidification in a neurodegenerative lysosomal storage disease model. *Nat Commun, 8*, 14612. Retrieved from https://www.ncbi.nlm.nih.gov/pubmed/28266544. doi:10.1038/ncomms14612

Beltran, C., & Nelson, N. (1992). The membrane sector of vacuolar H(+)-ATPase by itself is impermeable to protons. *Acta Physiol Scand Suppl, 607*, 41-47. Retrieved from https://www.ncbi.nlm.nih.gov/pubmed/1333159.

Benlekbir, S., Bueler, S. A., & Rubinstein, J. L. (2012). Structure of the vacuolar-type ATPase from Saccharomyces cerevisiae at 11-A resolution. *Nat Struct Mol Biol, 19*(12), 1356-1362. Retrieved from https://www.ncbi.nlm.nih.gov/pubmed/23142977. doi:10.1038/nsmb.2422

Boekema, E. J., Ubbink-Kok, T., Lolkema, J. S., Brisson, A., & Konings, W. N. (1997). Visualization of a peripheral stalk in V-type ATPase: evidence for the stator structure essential to rotational catalysis. *Proc Natl Acad Sci U S A, 94*(26), 14291-14293. Retrieved from https://www.ncbi.nlm.nih.gov/pubmed/9405605. doi:10.1073/pnas.94.26.14291

Bond, S., & Forgac, M. (2008). The Ras/cAMP/protein kinase A pathway regulates glucose-dependent assembly of the vacuolar (H+)-ATPase in yeast. *J Biol Chem, 283*(52), 36513-36521. Retrieved from https://www.ncbi.nlm.nih.gov/pubmed/18936098. doi:10.1074/jbc.M805232200

Boyle, W. J., Simonet, W. S., & Lacey, D. L. (2003). Osteoclast differentiation and activation. *Nature, 423*(6937), 337-342. Retrieved from https://www.ncbi.nlm.nih.gov/pubmed/12748652. doi:10.1038/nature01658

Colacurcio, D. J., & Nixon, R. A. (2016). Disorders of lysosomal acidification-The emerging role of v-ATPase in aging and neurodegenerative disease. *Ageing Res Rev, 32*, 75-88. Retrieved from https://www.ncbi.nlm.nih.gov/pubmed/27197071. doi:10.1016/j.arr.2016.05.004

Cooper, R., Naclerio, F., Allgrove, J., & Jimenez, A. (2012). Creatine supplementation with specific view to exercise/sports performance: an update. *J Int Soc Sports Nutr, 9*(1), 33. Retrieved from https://www.ncbi.nlm.nih.gov/pubmed/22817979. doi:10.1186/1550-2783-9-33

de Duve, C. (2005). The lysosome turns fifty. *Nat Cell Biol, 7*(9), 847-849. Retrieved from https://www.ncbi.nlm.nih.gov/pubmed/16136179. doi:10.1038/ncb0905-847

De Duve, C., & Wattiaux, R. (1966). Functions of lysosomes. *Annu Rev Physiol, 28*, 435-492. Retrieved from https://www.ncbi.nlm.nih.gov/pubmed/5322983. doi:10.1146/annurev.ph.28.030166.002251

Dechant, R., Binda, M., Lee, S. S., Pelet, S., Winderickx, J., & Peter, M. (2010). Cytosolic pH is a second messenger for glucose and regulates the PKA pathway through V-ATPase. *EMBO J, 29*(15), 2515-2526. Retrieved from https://www.ncbi.nlm.nih.gov/pubmed/20581803. doi:10.1038/emboj.2010.138

Dedkova, E. N., & Blatter, L. A. (2014). Role of beta-hydroxybutyrate, its polymer poly-beta-hydroxybutyrate and inorganic polyphosphate in mammalian health and disease. *Front Physiol, 5*, 260. Retrieved from https://www.ncbi.nlm.nih.gov/pubmed/25101001. doi:10.3389/fphys.2014.00260

Diakov, T. T., & Kane, P. M. (2010). Regulation of vacuolar proton-translocating ATPase activity and assembly by extracellular pH. *J Biol Chem, 285*(31), 23771-23778. Retrieved from https://www.ncbi.nlm.nih.gov/pubmed/20511227. doi:10.1074/jbc.M110.110122

Erbsloh, F., Bernsmeier, A., & Hillesheim, H. (1958). [The glucose consumption of the brain & its dependence on the liver]. *Arch Psychiatr Nervenkr Z Gesamte Neurol Psychiatr, 196*(6), 611-626. Retrieved from https://www.ncbi.nlm.nih.gov/pubmed/13534602.

Forgac, M. (2007). Vacuolar ATPases: rotary proton pumps in physiology and pathophysiology. *Nat Rev Mol Cell Biol, 8*(11), 917-929. Retrieved from https://www.ncbi.nlm.nih.gov/pubmed/17912264. doi:10.1038/nrm2272

Frattini, A., Orchard, P. J., Sobacchi, C., Giliani, S., Abinun, M., Mattsson, J. P., . . . Villa, A. (2000). Defects in TCIRG1 subunit of the vacuolar proton pump are responsible for a subset of human autosomal recessive osteopetrosis. *Nat Genet, 25*(3), 343-346. Retrieved from https://www.ncbi.nlm.nih.gov/pubmed/10888887. doi:10.1038/77131

Fuller, M., Meikle, P. J., & Hopwood, J. J. (2006). Epidemiology of lysosomal storage diseases: an overview. In A. Mehta, M. Beck, & G. Sunder-Plassmann (Eds.), *Fabry Disease: Perspectives from 5 Years of FOS*. Oxford.

Futerman, A. H., & van Meer, G. (2004). The cell biology of lysosomal storage disorders. *Nat Rev Mol Cell Biol, 5*(7), 554-565. Retrieved from https://www.ncbi.nlm.nih.gov/pubmed/15232573. doi:10.1038/nrm1423

Gluck, S., & Caldwell, J. (1987). Immunoaffinity purification and characterization of vacuolar H+ATPase from bovine kidney. *J Biol Chem, 262*(32), 15780-15789. Retrieved from https://www.ncbi.nlm.nih.gov/pubmed/2890634.

Graf, R., Harvey, W. R., & Wieczorek, H. (1996). Purification and properties of a cytosolic V1-ATPase. *J Biol Chem, 271*(34), 20908-20913. Retrieved from https://www.ncbi.nlm.nih.gov/pubmed/8702848. doi:10.1074/jbc.271.34.20908

Hanna-El-Daher, L., & Braissant, O. (2016). Creatine synthesis and exchanges between brain cells: What can be learned from human creatine deficiencies and various experimental models? *Amino Acids, 48*(8), 1877-1895. Retrieved from https://www.ncbi.nlm.nih.gov/pubmed/26861125. doi:10.1007/s00726-016-2189-0

Hinton, A., Sennoune, S. R., Bond, S., Fang, M., Reuveni, M., Sahagian, G. G., . . . Forgac, M. (2009). Function of a subunit isoforms of the V-ATPase in pH homeostasis and in vitro invasion of MDA-MB231 human breast cancer cells. *J Biol Chem, 284*(24), 16400-16408. Retrieved from https://www.ncbi.nlm.nih.gov/pubmed/19366680. doi:10.1074/jbc.M901201200

Imamura, H., Nakano, M., Noji, H., Muneyuki, E., Ohkuma, S., Yoshida, M., & Yokoyama, K. (2003). Evidence for rotation of V1-ATPase. *Proc Natl Acad Sci U S A, 100*(5), 2312-2315. Retrieved from https://www.ncbi.nlm.nih.gov/pubmed/12598655. doi:10.1073/pnas.0436796100

Jansen, E. J., van Bakel, N. H., Coenen, A. J., van Dooren, S. H., van Lith, H. A., & Martens, G. J. (2010). An isoform of the vacuolar (H(+))-ATPase accessory subunit Ac45. *Cell Mol Life Sci, 67*(4), 629-640. Retrieved from https://www.ncbi.nlm.nih.gov/pubmed/19946730. doi:10.1007/s00018-009-0200-6

Jefferies, K. C., & Forgac, M. (2008). Subunit H of the vacuolar (H+) ATPase inhibits ATP hydrolysis by the free V1 domain by interaction with the rotary subunit F. *J Biol Chem, 283*(8), 4512-4519. Retrieved from https://www.ncbi.nlm.nih.gov/pubmed/18156183. doi:10.1074/jbc.M707144200

Kane, P. M. (1995). Disassembly and reassembly of the yeast vacuolar H(+)-ATPase in vivo. *J Biol Chem, 270*(28), 17025-17032. Retrieved from https://www.ncbi.nlm.nih.gov/pubmed/7622524.

Katara, G. K., Kulshrestha, A., Jaiswal, M. K., Pamarthy, S., Gilman-Sachs, A., & Beaman, K. D. (2016). Inhibition of vacuolar ATPase subunit in tumor cells delays tumor growth by decreasing the essential macrophage population in the tumor microenvironment. *Oncogene, 35*(8), 1058-1065. Retrieved from https://www.ncbi.nlm.nih.gov/pubmed/25961933. doi:10.1038/onc.2015.159

Kawasaki-Nishi, S., Nishi, T., & Forgac, M. (2001a). Arg-735 of the 100-kDa subunit a of the yeast V-ATPase is essential for proton translocation. *Proc Natl Acad Sci U S A, 98*(22), 12397-12402. Retrieved from https://www.ncbi.nlm.nih.gov/pubmed/11592980. doi:10.1073/pnas.221291798

Kawasaki-Nishi, S., Nishi, T., & Forgac, M. (2001b). Yeast V-ATPase complexes containing different isoforms of the 100-kDa a-subunit differ in coupling efficiency and in vivo dissociation. *J Biol Chem, 276*(21), 17941-17948. Retrieved from https://www.ncbi.nlm.nih.gov/pubmed/11278748. doi:10.1074/jbc.M010790200

Lafourcade, C., Sobo, K., Kieffer-Jaquinod, S., Garin, J., & van der Goot, F. G. (2008). Regulation of the V-ATPase along the endocytic pathway occurs through reversible subunit association and membrane localization. *PLoS One, 3*(7), e2758. Retrieved from https://www.ncbi.nlm.nih.gov/pubmed/18648502. doi:10.1371/journal.pone.0002758

Liberti, M. V., & Locasale, J. W. (2016). The Warburg Effect: How Does it Benefit Cancer Cells? *Trends Biochem Sci, 41*(3), 211-218. Retrieved from https://www.ncbi.nlm.nih.gov/pubmed/26778478. doi:10.1016/j.tibs.2015.12.001

Liu, Y., Steinbusch, L. K. M., Nabben, M., Kapsokalyvas, D., van Zandvoort, M., Schonleitner, P., . . . Luiken, J. (2017). Palmitate-Induced Vacuolar-Type H(+)-ATPase Inhibition Feeds Forward Into Insulin Resistance and Contractile Dysfunction. *Diabetes, 66*(6), 1521-1534. Retrieved from https://www.ncbi.nlm.nih.gov/pubmed/28302654. doi:10.2337/db16-0727

Lu, M., Sautin, Y. Y., Holliday, L. S., & Gluck, S. L. (2004). The glycolytic enzyme aldolase mediates assembly, expression, and activity of vacuolar H+-ATPase. *J Biol Chem, 279*(10), 8732-8739. Retrieved from https://www.ncbi.nlm.nih.gov/pubmed/14672945. doi:10.1074/jbc.M303871200

MacLeod, K. J., Vasilyeva, E., Baleja, J. D., & Forgac, M. (1998). Mutational analysis of the nucleotide binding sites of the yeast vacuolar proton-translocating ATPase. *J Biol Chem, 273*(1), 150-156. Retrieved from https://www.ncbi.nlm.nih.gov/pubmed/9417059. doi:10.1074/jbc.273.1.150

Maher, M. J., Akimoto, S., Iwata, M., Nagata, K., Hori, Y., Yoshida, M., . . . Yokoyama, K. (2009). Crystal structure of A3B3 complex of V-ATPase from Thermus thermophilus. *EMBO J, 28*(23), 3771-3779. Retrieved from https://www.ncbi.nlm.nih.gov/pubmed/19893485. doi:10.1038/emboj.2009.310

McGuire, C. M., & Forgac, M. (2018). Glucose starvation increases V-ATPase assembly and activity in mammalian cells through AMP kinase and phosphatidylinositide 3-kinase/Akt signaling. *J Biol Chem, 293*(23), 9113-9123. Retrieved from https://www.ncbi.nlm.nih.gov/pubmed/29540478. doi:10.1074/jbc.RA117.001327

Meier, T., Polzer, P., Diederichs, K., Welte, W., & Dimroth, P. (2005). Structure of the rotor ring of F-Type Na+-ATPase from Ilyobacter tartaricus. *Science, 308*(5722), 659-662. Retrieved from https://www.ncbi.nlm.nih.gov/pubmed/15860619. doi:10.1126/science.1111199

Mellman, I., Fuchs, R., & Helenius, A. (1986). Acidification of the endocytic and exocytic pathways. *Annu Rev Biochem, 55*, 663-700. Retrieved from https://www.ncbi.nlm.nih.gov/pubmed/2874766. doi:10.1146/annurev.bi.55.070186.003311

Mergenthaler, P., Lindauer, U., Dienel, G. A., & Meisel, A. (2013). Sugar for the brain: the role of glucose in physiological and pathological brain function. *Trends Neurosci, 36*(10), 587-597. Retrieved from https://www.ncbi.nlm.nih.gov/pubmed/23968694. doi:10.1016/j.tins.2013.07.001

Moriyama, Y., Maeda, M., & Futai, M. (1992). The role of V-ATPase in neuronal and endocrine systems. *J Exp Biol, 172*, 171-178. Retrieved from https://www.ncbi.nlm.nih.gov/pubmed/1362770.

Muench, S. P., Huss, M., Song, C. F., Phillips, C., Wieczorek, H., Trinick, J., & Harrison, M. A. (2009). Cryo-electron microscopy of the vacuolar ATPase motor reveals its mechanical and regulatory complexity. *J Mol Biol, 386*(4), 989-999. Retrieved from https://www.ncbi.nlm.nih.gov/pubmed/19244615.

Muller, K. H., Kainov, D. E., El Bakkouri, K., Saelens, X., De Brabander, J. K., Kittel, C., . . . Muller, C. P. (2011). The proton translocation domain of cellular vacuolar ATPase provides a target for the

treatment of influenza A virus infections. *Br J Pharmacol, 164*(2), 344-357. Retrieved from https://www.ncbi.nlm.nih.gov/pubmed/21418188. doi:10.1111/j.1476-5381.2011.01346.x

Muller, O., Neumann, H., Bayer, M. J., & Mayer, A. (2003). Role of the Vtc proteins in V-ATPase stability and membrane trafficking. *J Cell Sci, 116*(Pt 6), 1107-1115. Retrieved from https://www.ncbi.nlm.nih.gov/pubmed/12584253.

Murata, T., Yamato, I., Kakinuma, Y., Leslie, A. G., & Walker, J. E. (2005). Structure of the rotor of the V-Type Na+-ATPase from Enterococcus hirae. *Science, 308*(5722), 654-659. Retrieved from https://www.ncbi.nlm.nih.gov/pubmed/15802565. doi:10.1126/science.1110064

Newman, J. C., & Verdin, E. (2014). beta-hydroxybutyrate: much more than a metabolite. *Diabetes Res Clin Pract, 106*(2), 173-181. Retrieved from https://www.ncbi.nlm.nih.gov/pubmed/25193333. doi:10.1016/j.diabres.2014.08.009

Nishi, T., & Forgac, M. (2002). The vacuolar (H+)-ATPases--nature's most versatile proton pumps. *Nat Rev Mol Cell Biol, 3*(2), 94-103. Retrieved from https://www.ncbi.nlm.nih.gov/pubmed/11836511. doi:10.1038/nrm729

Nixon, R. A. (2013). The role of autophagy in neurodegenerative disease. *Nat Med, 19*(8), 983-997. Retrieved from https://www.ncbi.nlm.nih.gov/pubmed/23921753. doi:10.1038/nm.3232

Nouioua, S., Cheillan, D., Zaouidi, S., Salomons, G. S., Amedjout, N., Kessaci, F., . . . Tazir, M. (2013). Creatine deficiency syndrome. A treatable myopathy due to arginine-glycine amidinotransferase (AGAT) deficiency. *Neuromuscul Disord, 23*(8), 670-674. Retrieved from https://www.ncbi.nlm.nih.gov/pubmed/23770102. doi:10.1016/j.nmd.2013.04.011

Ochotny, N., Flenniken, A. M., Owen, C., Voronov, I., Zirngibl, R. A., Osborne, L. R., . . . Aubin, J. E. (2011). The V-ATPase a3 subunit mutation R740S is dominant negative and results in osteopetrosis in mice. *J Bone Miner Res, 26*(7), 1484-1493. Retrieved from https://www.ncbi.nlm.nih.gov/pubmed/21305608. doi:10.1002/jbmr.355

Parra, K. J., Chan, C. Y., & Chen, J. (2014). Saccharomyces cerevisiae vacuolar H+-ATPase regulation by disassembly and reassembly: one structure and multiple signals. *Eukaryot Cell, 13*(6), 706-714. Retrieved from https://www.ncbi.nlm.nih.gov/pubmed/24706019. doi:10.1128/EC.00050-14

Parra, K. J., & Kane, P. M. (1998). Reversible association between the V1 and V0 domains of yeast vacuolar H+-ATPase is an unconventional glucose-induced effect. *Mol Cell Biol, 18*(12), 7064-7074. Retrieved from https://www.ncbi.nlm.nih.gov/pubmed/9819393.

Parra, K. J., Keenan, K. L., & Kane, P. M. (2000). The H subunit (Vma13p) of the yeast V-ATPase inhibits the ATPase activity of cytosolic V1 complexes. *J Biol Chem, 275*(28), 21761-21767. Retrieved from https://www.ncbi.nlm.nih.gov/pubmed/10781598. doi:10.1074/jbc.M002305200

Parsons, S. M. (2000). Transport mechanisms in acetylcholine and monoamine storage. *FASEB J, 14*(15), 2423-2434. Retrieved from https://www.ncbi.nlm.nih.gov/pubmed/11099460. doi:10.1096/fj.00-0203rev

Pillay, C. S., Elliott, E., & Dennison, C. (2002). Endolysosomal proteolysis and its regulation. *Biochem J, 363*(Pt 3), 417-429. Retrieved from https://www.ncbi.nlm.nih.gov/pubmed/11964142. doi:10.1042/0264-6021:3630417

Rahman, N., Ramos-Espiritu, L., Milner, T. A., Buck, J., & Levin, L. R. (2016). Soluble adenylyl cyclase is essential for proper lysosomal acidification. *J Gen Physiol, 148*(4), 325-339. Retrieved from https://www.ncbi.nlm.nih.gov/pubmed/27670898. doi:10.1085/jgp.201611606

Rogatzki, M. J., Ferguson, B. S., Goodwin, M. L., & Gladden, L. B. (2015). Lactate is always the end product of glycolysis. *Front Neurosci, 9*, 22. Retrieved from https://www.ncbi.nlm.nih.gov/pubmed/25774123. doi:10.3389/fnins.2015.00022

Saftig, P., & Klumperman, J. (2009). Lysosome biogenesis and lysosomal membrane proteins: trafficking meets function. *Nat Rev Mol Cell Biol, 10*(9), 623-635. Retrieved from https://www.ncbi.nlm.nih.gov/pubmed/19672277. doi:10.1038/nrm2745

Sagermann, M., Stevens, T. H., & Matthews, B. W. (2001). Crystal structure of the regulatory subunit H of the V-type ATPase of Saccharomyces cerevisiae. *Proc Natl Acad Sci U S A, 98*(13), 7134-7139. Retrieved from https://www.ncbi.nlm.nih.gov/pubmed/11416198. doi:10.1073/pnas.131192798

Sagne, C., Agulhon, C., Ravassard, P., Darmon, M., Hamon, M., El Mestikawy, S., . . . Giros, B. (2001). Identification and characterization of a lysosomal transporter for small neutral amino acids. *Proc Natl Acad Sci U S A, 98*(13), 7206-7211. Retrieved from https://www.ncbi.nlm.nih.gov/pubmed/11390972. doi:10.1073/pnas.121183498

Sambongi, Y., Iko, Y., Tanabe, M., Omote, H., Iwamoto-Kihara, A., Ueda, I., . . . Futai, M. (1999). Mechanical rotation of the c subunit oligomer in ATP synthase (F0F1): direct observation. *Science, 286*(5445), 1722-1724. Retrieved from https://www.ncbi.nlm.nih.gov/pubmed/10576736.

Sautin, Y. Y., Lu, M., Gaugler, A., Zhang, L., & Gluck, S. L. (2005). Phosphatidylinositol 3-kinase-mediated effects of glucose on vacuolar H+-ATPase assembly, translocation, and acidification of intracellular compartments in renal epithelial cells. *Mol Cell Biol, 25*(2), 575-589. Retrieved from https://www.ncbi.nlm.nih.gov/pubmed/15632060. doi:10.1128/MCB.25.2.575-589.2005

Sennoune, S. R., Bakunts, K., Martinez, G. M., Chua-Tuan, J. L., Kebir, Y., Attaya, M. N., & Martinez-Zaguilan, R. (2004). Vacuolar H+-ATPase in human breast cancer cells with distinct metastatic potential: distribution and functional activity. *Am J Physiol Cell Physiol, 286*(6), C1443-1452. Retrieved from https://www.ncbi.nlm.nih.gov/pubmed/14761893. doi:10.1152/ajpcell.00407.2003

Sennoune, S. R., & Martinez-Zaguilan, R. (2007). Plasmalemmal vacuolar H+-ATPases in angiogenesis, diabetes and cancer. *J Bioenerg Biomembr, 39*(5-6), 427-433. Retrieved from https://www.ncbi.nlm.nih.gov/pubmed/18058006. doi:10.1007/s10863-007-9108-8

Seol, J. H., Shevchenko, A., Shevchenko, A., & Deshaies, R. J. (2001). Skp1 forms multiple protein complexes, including RAVE, a regulator of V-ATPase assembly. *Nat Cell Biol, 3*(4), 384-391. Retrieved from https://www.ncbi.nlm.nih.gov/pubmed/11283612. doi:10.1038/35070067

Smardon, A. M., Tarsio, M., & Kane, P. M. (2002). The RAVE complex is essential for stable assembly of the yeast V-ATPase. *J Biol Chem, 277*(16), 13831-13839. Retrieved from https://www.ncbi.nlm.nih.gov/pubmed/11844802. doi:10.1074/jbc.M200682200

Stevens, T. H., & Forgac, M. (1997). Structure, function and regulation of the vacuolar (H+)-ATPase. *Annu Rev Cell Dev Biol, 13*, 779-808. Retrieved from https://www.ncbi.nlm.nih.gov/pubmed/9442887. doi:10.1146/annurev.cellbio.13.1.779

Stransky, L. A., & Forgac, M. (2015). Amino Acid Availability Modulates Vacuolar H+-ATPase Assembly. *J Biol Chem, 290*(45), 27360-27369. Retrieved from https://www.ncbi.nlm.nih.gov/pubmed/26378229. doi:10.1074/jbc.M115.659128

Takamori, S., Holt, M., Stenius, K., Lemke, E. A., Gronborg, M., Riedel, D., . . . Jahn, R. (2006). Molecular anatomy of a trafficking organelle. *Cell, 127*(4), 831-846. Retrieved from https://www.ncbi.nlm.nih.gov/pubmed/17110340. doi:10.1016/j.cell.2006.10.030

Teitelbaum, S. L. (2000). Bone resorption by osteoclasts. *Science, 289*(5484), 1504-1508. Retrieved from https://www.ncbi.nlm.nih.gov/pubmed/10968780.

Teitelbaum, S. L. (2007). Osteoclasts: what do they do and how do they do it? *Am J Pathol, 170*(2), 427-435. Retrieved from https://www.ncbi.nlm.nih.gov/pubmed/17255310. doi:10.2353/ajpath.2007.060834

Tomashek, J. J., & Brusilow, W. S. (2000). Stoichiometry of energy coupling by proton-translocating ATPases: a history of variability. *J Bioenerg Biomembr, 32*(5), 493-500. Retrieved from https://www.ncbi.nlm.nih.gov/pubmed/15254384.

Torigoe, T., Izumi, H., Ise, T., Murakami, T., Uramoto, H., Ishiguchi, H., . . . Kohno, K. (2002). Vacuolar H(+)-ATPase: functional mechanisms and potential as a target for cancer chemotherapy. *Anticancer Drugs, 13*(3), 237-243. Retrieved from https://www.ncbi.nlm.nih.gov/pubmed/11984067.

Toyomura, T., Murata, Y., Yamamoto, A., Oka, T., Sun-Wada, G. H., Wada, Y., & Futai, M. (2003). From lysosomes to the plasma membrane: localization of vacuolar-type H+ -ATPase with the a3 isoform during osteoclast differentiation. *J Biol Chem, 278*(24), 22023-22030. Retrieved from https://www.ncbi.nlm.nih.gov/pubmed/12672822. doi:10.1074/jbc.M302436200

Wilkens, S., & Forgac, M. (2001). Three-dimensional structure of the vacuolar ATPase proton channel by electron microscopy. *J Biol Chem, 276*(47), 44064-44068. Retrieved from https://www.ncbi.nlm.nih.gov/pubmed/11533034. doi:10.1074/jbc.M106579200

Xu, T., & Forgac, M. (2001). Microtubules are involved in glucose-dependent dissociation of the yeast vacuolar [H+]-ATPase in vivo. *J Biol Chem, 276*(27), 24855-24861. Retrieved from https://www.ncbi.nlm.nih.gov/pubmed/11331282. doi:10.1074/jbc.M100637200

Yokoyama, K., & Imamura, H. (2005). Rotation, structure, and classification of prokaryotic V-ATPase. *J Bioenerg Biomembr, 37*(6), 405-410. Retrieved from https://www.ncbi.nlm.nih.gov/pubmed/16691473. doi:10.1007/s10863-005-9480-1

Zhang, C. S., Jiang, B., Li, M., Zhu, M., Peng, Y., Zhang, Y. L., . . . Lin, S. C. (2014). The lysosomal v-ATPase-Ragulator complex is a common activator for AMPK and mTORC1, acting as a switch between catabolism and anabolism. *Cell Metab, 20*(3), 526-540. Retrieved from https://www.ncbi.nlm.nih.gov/pubmed/25002183. doi:10.1016/j.cmet.2014.06.014

Zhang, Z., Zheng, Y., Mazon, H., Milgrom, E., Kitagawa, N., Kish-Trier, E., . . . Wilkens, S. (2008). Structure of the yeast vacuolar ATPase. *J Biol Chem, 283*(51), 35983-35995. Retrieved from https://www.ncbi.nlm.nih.gov/pubmed/18955482. doi:10.1074/jbc.M805345200

Alfarouk, K. O., Verduzco, D., Rauch, C., Muddathir, A. K., Adil, H. H., Elhassan, G. O., . . . Harguindey, S. (2014). Glycolysis, tumor metabolism, cancer growth and dissemination. A new pH-based etiopathogenic perspective and therapeutic approach to an old cancer question. *Oncoscience, 1*(12), 777-802. Retrieved from https://www.ncbi.nlm.nih.gov/pubmed/25621294. doi:10.18632/oncoscience.109

Bagh, M. B., Peng, S., Chandra, G., Zhang, Z., Singh, S. P., Pattabiraman, N., . . . Mukherjee, A. B. (2017). Misrouting of v-ATPase subunit V0a1 dysregulates lysosomal acidification in a neurodegenerative lysosomal storage disease model. *Nat Commun, 8*, 14612. Retrieved from https://www.ncbi.nlm.nih.gov/pubmed/28266544. doi:10.1038/ncomms14612

Beltran, C., & Nelson, N. (1992). The membrane sector of vacuolar H(+)-ATPase by itself is impermeable to protons. *Acta Physiol Scand Suppl, 607*, 41-47. Retrieved from https://www.ncbi.nlm.nih.gov/pubmed/1333159.

Benlekbir, S., Bueler, S. A., & Rubinstein, J. L. (2012). Structure of the vacuolar-type ATPase from Saccharomyces cerevisiae at 11-A resolution. *Nat Struct Mol Biol, 19*(12), 1356-1362. Retrieved from https://www.ncbi.nlm.nih.gov/pubmed/23142977. doi:10.1038/nsmb.2422

Boekema, E. J., Ubbink-Kok, T., Lolkema, J. S., Brisson, A., & Konings, W. N. (1997). Visualization of a peripheral stalk in V-type ATPase: evidence for the stator structure essential to rotational catalysis. *Proc Natl Acad Sci U S A, 94*(26), 14291-14293. Retrieved from https://www.ncbi.nlm.nih.gov/pubmed/9405605. doi:10.1073/pnas.94.26.14291

Bond, S., & Forgac, M. (2008). The Ras/cAMP/protein kinase A pathway regulates glucose-dependent assembly of the vacuolar (H+)-ATPase in yeast. *J Biol Chem, 283*(52), 36513-36521. Retrieved from https://www.ncbi.nlm.nih.gov/pubmed/18936098. doi:10.1074/jbc.M805232200

Boyle, W. J., Simonet, W. S., & Lacey, D. L. (2003). Osteoclast differentiation and activation. *Nature, 423*(6937), 337-342. Retrieved from https://www.ncbi.nlm.nih.gov/pubmed/12748652. doi:10.1038/nature01658

Canonico, P. G., & Bird, J. W. (1970). Lysosomes in skeletal muscle tissue. Zonal centrifugation evidence for multiple cellular sources. *J Cell Biol, 45*(2), 321-333. Retrieved from https://www.ncbi.nlm.nih.gov/pubmed/4327573. doi:10.1083/jcb.45.2.321

Colacurcio, D. J., & Nixon, R. A. (2016). Disorders of lysosomal acidification-The emerging role of v-ATPase in aging and neurodegenerative disease. *Ageing Res Rev, 32*, 75-88. Retrieved from https://www.ncbi.nlm.nih.gov/pubmed/27197071. doi:10.1016/j.arr.2016.05.004

Cooper, R., Naclerio, F., Allgrove, J., & Jimenez, A. (2012). Creatine supplementation with specific view to exercise/sports performance: an update. *J Int Soc Sports Nutr, 9*(1), 33. Retrieved from https://www.ncbi.nlm.nih.gov/pubmed/22817979. doi:10.1186/1550-2783-9-33

de Duve, C. (2005). The lysosome turns fifty. *Nat Cell Biol, 7*(9), 847-849. Retrieved from https://www.ncbi.nlm.nih.gov/pubmed/16136179. doi:10.1038/ncb0905-847

De Duve, C., & Wattiaux, R. (1966). Functions of lysosomes. *Annu Rev Physiol, 28*, 435-492. Retrieved from https://www.ncbi.nlm.nih.gov/pubmed/5322983. doi:10.1146/annurev.ph.28.030166.002251

Dechant, R., Binda, M., Lee, S. S., Pelet, S., Winderickx, J., & Peter, M. (2010). Cytosolic pH is a second messenger for glucose and regulates the PKA pathway through V-ATPase. *EMBO J, 29*(15), 2515-2526. Retrieved from https://www.ncbi.nlm.nih.gov/pubmed/20581803. doi:10.1038/emboj.2010.138

Dedkova, E. N., & Blatter, L. A. (2014). Role of beta-hydroxybutyrate, its polymer poly-beta-hydroxybutyrate and inorganic polyphosphate in mammalian health and disease. *Front Physiol, 5*, 260. Retrieved from https://www.ncbi.nlm.nih.gov/pubmed/25101001. doi:10.3389/fphys.2014.00260

Deprez, M. A., Eskes, E., Wilms, T., Ludovico, P., & Winderickx, J. (2018). pH homeostasis links the nutrient sensing PKA/TORC1/Sch9 menage-a-trois to stress tolerance and longevity. *Microb Cell, 5*(3), 119-136. Retrieved from https://www.ncbi.nlm.nih.gov/pubmed/29487859. doi:10.15698/mic2018.03.618

Di Giovanni, J., Boudkkazi, S., Mochida, S., Bialowas, A., Samari, N., Leveque, C., . . . El Far, O. (2010). V-ATPase membrane sector associates with synaptobrevin to modulate neurotransmitter release. *Neuron, 67*(2), 268-279. Retrieved from https://www.ncbi.nlm.nih.gov/pubmed/20670834. doi:10.1016/j.neuron.2010.06.024

Diakov, T. T., & Kane, P. M. (2010). Regulation of vacuolar proton-translocating ATPase activity and assembly by extracellular pH. *J Biol Chem, 285*(31), 23771-23778. Retrieved from https://www.ncbi.nlm.nih.gov/pubmed/20511227. doi:10.1074/jbc.M110.110122

Doherty, P., & Walsh, F. S. (1996). CAM-FGF Receptor Interactions: A Model for Axonal Growth. *Mol Cell Neurosci, 8*(2/3), 99-111. Retrieved from https://www.ncbi.nlm.nih.gov/pubmed/8954625. doi:10.1006/mcne.1996.0049

Egawa, N., Maillet, B., VanDamme, B., De Greve, J., & Kloppel, G. (1996). Differentiation of pancreatic carcinoma induced by retinoic acid or sodium butyrate: a morphological and molecular analysis of four cell lines. *Virchows Arch, 429*(1), 59-68. Retrieved from https://www.ncbi.nlm.nih.gov/pubmed/8865855.

El Far, O., & Seagar, M. (2011). A role for V-ATPase subunits in synaptic vesicle fusion? *J Neurochem, 117*(4), 603-612. Retrieved from https://www.ncbi.nlm.nih.gov/pubmed/21375531. doi:10.1111/j.1471-4159.2011.07234.x

Erbsloh, F., Bernsmeier, A., & Hillesheim, H. (1958). [The glucose consumption of the brain & its dependence on the liver]. *Arch Psychiatr Nervenkr Z Gesamte Neurol Psychiatr, 196*(6), 611-626. Retrieved from https://www.ncbi.nlm.nih.gov/pubmed/13534602.

Forgac, M. (2007). Vacuolar ATPases: rotary proton pumps in physiology and pathophysiology. *Nat Rev Mol Cell Biol, 8*(11), 917-929. Retrieved from https://www.ncbi.nlm.nih.gov/pubmed/17912264. doi:10.1038/nrm2272

Frattini, A., Orchard, P. J., Sobacchi, C., Giliani, S., Abinun, M., Mattsson, J. P., . . . Villa, A. (2000). Defects in TCIRG1 subunit of the vacuolar proton pump are responsible for a subset of human autosomal recessive osteopetrosis. *Nat Genet, 25*(3), 343-346. Retrieved from https://www.ncbi.nlm.nih.gov/pubmed/10888887. doi:10.1038/77131

Fuller, M., Meikle, P. J., & Hopwood, J. J. (2006). Epidemiology of lysosomal storage diseases: an overview. In A. Mehta, M. Beck, & G. Sunder-Plassmann (Eds.), *Fabry Disease: Perspectives from 5 Years of FOS*. Oxford.

Futerman, A. H., & van Meer, G. (2004). The cell biology of lysosomal storage disorders. *Nat Rev Mol Cell Biol, 5*(7), 554-565. Retrieved from https://www.ncbi.nlm.nih.gov/pubmed/15232573. doi:10.1038/nrm1423

Gautheron, D. C. (1984). Mitochondrial oxidative phosphorylation and respiratory chain: review. *J Inherit Metab Dis, 7 Suppl 1*, 57-61. Retrieved from https://www.ncbi.nlm.nih.gov/pubmed/6153061.

Gluck, S., & Caldwell, J. (1987). Immunoaffinity purification and characterization of vacuolar H+ATPase from bovine kidney. *J Biol Chem, 262*(32), 15780-15789. Retrieved from https://www.ncbi.nlm.nih.gov/pubmed/2890634.

Gradiz, R., Silva, H. C., Carvalho, L., Botelho, M. F., & Mota-Pinto, A. (2016). MIA PaCa-2 and PANC-1 - pancreas ductal adenocarcinoma cell lines with neuroendocrine differentiation and somatostatin receptors. *Sci Rep, 6*, 21648. Retrieved from https://www.ncbi.nlm.nih.gov/pubmed/26884312. doi:10.1038/srep21648

Graf, R., Harvey, W. R., & Wieczorek, H. (1996). Purification and properties of a cytosolic V1-ATPase. *J Biol Chem, 271*(34), 20908-20913. Retrieved from https://www.ncbi.nlm.nih.gov/pubmed/8702848. doi:10.1074/jbc.271.34.20908

Hanna-El-Daher, L., & Braissant, O. (2016). Creatine synthesis and exchanges between brain cells: What can be learned from human creatine deficiencies and various experimental models? *Amino Acids, 48*(8), 1877-1895. Retrieved from https://www.ncbi.nlm.nih.gov/pubmed/26861125. doi:10.1007/s00726-016-2189-0

Hayek, S. R., Rane, H. S., & Parra, K. J. (2019). Reciprocal Regulation of V-ATPase and Glycolytic Pathway Elements in Health and Disease. *Front Physiol, 10*, 127. Retrieved from https://www.ncbi.nlm.nih.gov/pubmed/30828305. doi:10.3389/fphys.2019.00127

Hiesinger, P. R., Fayyazuddin, A., Mehta, S. Q., Rosenmund, T., Schulze, K. L., Zhai, R. G., . . . Bellen, H. J. (2005). The v-ATPase V0 subunit a1 is required for a late step in synaptic vesicle exocytosis in Drosophila. *Cell, 121*(4), 607-620. Retrieved from https://www.ncbi.nlm.nih.gov/pubmed/15907473. doi:10.1016/j.cell.2005.03.012

Hinton, A., Sennoune, S. R., Bond, S., Fang, M., Reuveni, M., Sahagian, G. G., . . . Forgac, M. (2009). Function of a subunit isoforms of the V-ATPase in pH homeostasis and in vitro invasion of MDA-MB231 human breast cancer cells. *J Biol Chem, 284*(24), 16400-16408. Retrieved from https://www.ncbi.nlm.nih.gov/pubmed/19366680. doi:10.1074/jbc.M901201200

Imamura, H., Nakano, M., Noji, H., Muneyuki, E., Ohkuma, S., Yoshida, M., & Yokoyama, K. (2003). Evidence for rotation of V1-ATPase. *Proc Natl Acad Sci U S A, 100*(5), 2312-2315. Retrieved from https://www.ncbi.nlm.nih.gov/pubmed/12598655. doi:10.1073/pnas.0436796100

Jain, I. H., Zazzeron, L., Goli, R., Alexa, K., Schatzman-Bone, S., Dhillon, H., . . . Mootha, V. K. (2016). Hypoxia as a therapy for mitochondrial disease. *Science, 352*(6281), 54-61. Retrieved from https://www.ncbi.nlm.nih.gov/pubmed/26917594. doi:10.1126/science.aad9642

Jansen, E. J., van Bakel, N. H., Coenen, A. J., van Dooren, S. H., van Lith, H. A., & Martens, G. J. (2010). An isoform of the vacuolar (H(+))-ATPase accessory subunit Ac45. *Cell Mol Life Sci, 67*(4), 629-640. Retrieved from https://www.ncbi.nlm.nih.gov/pubmed/19946730. doi:10.1007/s00018-009-0200-6

Jefferies, K. C., & Forgac, M. (2008). Subunit H of the vacuolar (H+) ATPase inhibits ATP hydrolysis by the free V1 domain by interaction with the rotary subunit F. *J Biol Chem, 283*(8), 4512-4519. Retrieved from https://www.ncbi.nlm.nih.gov/pubmed/18156183. doi:10.1074/jbc.M707144200

Kane, P. M. (1995). Disassembly and reassembly of the yeast vacuolar H(+)-ATPase in vivo. *J Biol Chem, 270*(28), 17025-17032. Retrieved from https://www.ncbi.nlm.nih.gov/pubmed/7622524.

Katara, G. K., Kulshrestha, A., Jaiswal, M. K., Pamarthy, S., Gilman-Sachs, A., & Beaman, K. D. (2016). Inhibition of vacuolar ATPase subunit in tumor cells delays tumor growth by decreasing the essential macrophage population in the tumor microenvironment. *Oncogene, 35*(8), 1058-1065. Retrieved from https://www.ncbi.nlm.nih.gov/pubmed/25961933. doi:10.1038/onc.2015.159

Kawasaki-Nishi, S., Nishi, T., & Forgac, M. (2001a). Arg-735 of the 100-kDa subunit a of the yeast V-ATPase is essential for proton translocation. *Proc Natl Acad Sci U S A, 98*(22), 12397-12402. Retrieved from https://www.ncbi.nlm.nih.gov/pubmed/11592980. doi:10.1073/pnas.221291798

Kawasaki-Nishi, S., Nishi, T., & Forgac, M. (2001b). Yeast V-ATPase complexes containing different isoforms of the 100-kDa a-subunit differ in coupling efficiency and in vivo dissociation. *J Biol Chem, 276*(21), 17941-17948. Retrieved from https://www.ncbi.nlm.nih.gov/pubmed/11278748. doi:10.1074/jbc.M010790200

Kolkova, K., Novitskaya, V., Pedersen, N., Berezin, V., & Bock, E. (2000). Neural cell adhesion molecule-stimulated neurite outgrowth depends on activation of protein kinase C and the Ras-mitogen-activated protein kinase pathway. *J Neurosci, 20*(6), 2238-2246. Retrieved from https://www.ncbi.nlm.nih.gov/pubmed/10704499.

Lafourcade, C., Sobo, K., Kieffer-Jaquinod, S., Garin, J., & van der Goot, F. G. (2008). Regulation of the V-ATPase along the endocytic pathway occurs through reversible subunit association and membrane localization. *PLoS One, 3*(7), e2758. Retrieved from https://www.ncbi.nlm.nih.gov/pubmed/18648502. doi:10.1371/journal.pone.0002758

Li, H., Thali, R. F., Smolak, C., Gong, F., Alzamora, R., Wallimann, T., . . . Hallows, K. R. (2010). Regulation of the creatine transporter by AMP-activated protein kinase in kidney epithelial cells. *Am J Physiol Renal Physiol, 299*(1), F167-177. Retrieved from https://www.ncbi.nlm.nih.gov/pubmed/20462973. doi:10.1152/ajprenal.00162.2010

Liberti, M. V., & Locasale, J. W. (2016). The Warburg Effect: How Does it Benefit Cancer Cells? *Trends Biochem Sci, 41*(3), 211-218. Retrieved from https://www.ncbi.nlm.nih.gov/pubmed/26778478. doi:10.1016/j.tibs.2015.12.001

Liu, Y., Steinbusch, L. K. M., Nabben, M., Kapsokalyvas, D., van Zandvoort, M., Schonleitner, P., . . . Luiken, J. (2017). Palmitate-Induced Vacuolar-Type H(+)-ATPase Inhibition Feeds Forward Into Insulin Resistance and Contractile Dysfunction. *Diabetes, 66*(6), 1521-1534. Retrieved from https://www.ncbi.nlm.nih.gov/pubmed/28302654. doi:10.2337/db16-0727

Lu, M., Sautin, Y. Y., Holliday, L. S., & Gluck, S. L. (2004). The glycolytic enzyme aldolase mediates assembly, expression, and activity of vacuolar H+-ATPase. *J Biol Chem, 279*(10), 8732-8739. Retrieved from https://www.ncbi.nlm.nih.gov/pubmed/14672945. doi:10.1074/jbc.M303871200

MacLeod, K. J., Vasilyeva, E., Baleja, J. D., & Forgac, M. (1998). Mutational analysis of the nucleotide binding sites of the yeast vacuolar proton-translocating ATPase. *J Biol Chem, 273*(1), 150-156. Retrieved from https://www.ncbi.nlm.nih.gov/pubmed/9417059. doi:10.1074/jbc.273.1.150

Maher, M. J., Akimoto, S., Iwata, M., Nagata, K., Hori, Y., Yoshida, M., . . . Yokoyama, K. (2009). Crystal structure of A3B3 complex of V-ATPase from Thermus thermophilus. *EMBO J, 28*(23), 3771-3779. Retrieved from https://www.ncbi.nlm.nih.gov/pubmed/19893485. doi:10.1038/emboj.2009.310

McGuire, C. M., & Forgac, M. (2018). Glucose starvation increases V-ATPase assembly and activity in mammalian cells through AMP kinase and phosphatidylinositide 3-kinase/Akt signaling. *J Biol Chem, 293*(23), 9113-9123. Retrieved from https://www.ncbi.nlm.nih.gov/pubmed/29540478. doi:10.1074/jbc.RA117.001327

Meier, T., Polzer, P., Diederichs, K., Welte, W., & Dimroth, P. (2005). Structure of the rotor ring of F-Type Na+-ATPase from Ilyobacter tartaricus. *Science, 308*(5722), 659-662. Retrieved from https://www.ncbi.nlm.nih.gov/pubmed/15860619. doi:10.1126/science.1111199

Mellman, I., Fuchs, R., & Helenius, A. (1986). Acidification of the endocytic and exocytic pathways. *Annu Rev Biochem, 55*, 663-700. Retrieved from https://www.ncbi.nlm.nih.gov/pubmed/2874766. doi:10.1146/annurev.bi.55.070186.003311

Mergenthaler, P., Lindauer, U., Dienel, G. A., & Meisel, A. (2013). Sugar for the brain: the role of glucose in physiological and pathological brain function. *Trends Neurosci, 36*(10), 587-597. Retrieved from https://www.ncbi.nlm.nih.gov/pubmed/23968694. doi:10.1016/j.tins.2013.07.001

Mookerjee, S. A., Gerencser, A. A., Nicholls, D. G., & Brand, M. D. (2017). Quantifying intracellular rates of glycolytic and oxidative ATP production and consumption using extracellular flux measurements. *J Biol Chem, 292*(17), 7189-7207. Retrieved from https://www.ncbi.nlm.nih.gov/pubmed/28270511. doi:10.1074/jbc.M116.774471

Morel, N., Dedieu, J. C., & Philippe, J. M. (2003). Specific sorting of the a1 isoform of the V-H+ATPase a subunit to nerve terminals where it associates with both synaptic vesicles and the presynaptic plasma membrane. *J Cell Sci, 116*(Pt 23), 4751-4762. Retrieved from https://www.ncbi.nlm.nih.gov/pubmed/14600261. doi:10.1242/jcs.00791

Morel, N., Dunant, Y., & Israel, M. (2001). Neurotransmitter release through the V0 sector of V-ATPase. *J Neurochem, 79*(3), 485-488. Retrieved from https://www.ncbi.nlm.nih.gov/pubmed/11701751.

Moriyama, Y., Maeda, M., & Futai, M. (1992). The role of V-ATPase in neuronal and endocrine systems. *J Exp Biol, 172*, 171-178. Retrieved from https://www.ncbi.nlm.nih.gov/pubmed/1362770.

Muench, S. P., Huss, M., Song, C. F., Phillips, C., Wieczorek, H., Trinick, J., & Harrison, M. A. (2009). Cryo-electron microscopy of the vacuolar ATPase motor reveals its mechanical and regulatory complexity. *J Mol Biol, 386*(4), 989-999. Retrieved from https://www.ncbi.nlm.nih.gov/pubmed/19244615.

Muller, K. H., Kainov, D. E., El Bakkouri, K., Saelens, X., De Brabander, J. K., Kittel, C., . . . Muller, C. P. (2011). The proton translocation domain of cellular vacuolar ATPase provides a target for the treatment of influenza A virus infections. *Br J Pharmacol, 164*(2), 344-357. Retrieved from https://www.ncbi.nlm.nih.gov/pubmed/21418188. doi:10.1111/j.1476-5381.2011.01346.x

Muller, O., Neumann, H., Bayer, M. J., & Mayer, A. (2003). Role of the Vtc proteins in V-ATPase stability and membrane trafficking. *J Cell Sci, 116*(Pt 6), 1107-1115. Retrieved from https://www.ncbi.nlm.nih.gov/pubmed/12584253.

Murata, T., Yamato, I., Kakinuma, Y., Leslie, A. G., & Walker, J. E. (2005). Structure of the rotor of the V-Type Na+-ATPase from Enterococcus hirae. *Science, 308*(5722), 654-659. Retrieved from https://www.ncbi.nlm.nih.gov/pubmed/15802565. doi:10.1126/science.1110064

Newman, J. C., & Verdin, E. (2014). beta-hydroxybutyrate: much more than a metabolite. *Diabetes Res Clin Pract, 106*(2), 173-181. Retrieved from https://www.ncbi.nlm.nih.gov/pubmed/25193333. doi:10.1016/j.diabres.2014.08.009

Nishi, T., & Forgac, M. (2002). The vacuolar (H+)-ATPases--nature's most versatile proton pumps. *Nat Rev Mol Cell Biol, 3*(2), 94-103. Retrieved from https://www.ncbi.nlm.nih.gov/pubmed/11836511. doi:10.1038/nrm729

Nixon, R. A. (2013). The role of autophagy in neurodegenerative disease. *Nat Med, 19*(8), 983-997. Retrieved from https://www.ncbi.nlm.nih.gov/pubmed/23921753. doi:10.1038/nm.3232

Nouioua, S., Cheillan, D., Zaouidi, S., Salomons, G. S., Amedjout, N., Kessaci, F., . . . Tazir, M. (2013). Creatine deficiency syndrome. A treatable myopathy due to arginine-glycine amidinotransferase (AGAT) deficiency. *Neuromuscul Disord, 23*(8), 670-674. Retrieved from https://www.ncbi.nlm.nih.gov/pubmed/23770102. doi:10.1016/j.nmd.2013.04.011

Ochotny, N., Flenniken, A. M., Owen, C., Voronov, I., Zirngibl, R. A., Osborne, L. R., . . . Aubin, J. E. (2011). The V-ATPase a3 subunit mutation R740S is dominant negative and results in osteopetrosis in mice. *J Bone Miner Res, 26*(7), 1484-1493. Retrieved from https://www.ncbi.nlm.nih.gov/pubmed/21305608. doi:10.1002/jbmr.355

Parra, K. J., Chan, C. Y., & Chen, J. (2014). Saccharomyces cerevisiae vacuolar H+-ATPase regulation by disassembly and reassembly: one structure and multiple signals. *Eukaryot Cell, 13*(6), 706-714. Retrieved from https://www.ncbi.nlm.nih.gov/pubmed/24706019. doi:10.1128/EC.00050-14

Parra, K. J., & Kane, P. M. (1998). Reversible association between the V1 and V0 domains of yeast vacuolar H+-ATPase is an unconventional glucose-induced effect. *Mol Cell Biol, 18*(12), 7064-7074. Retrieved from https://www.ncbi.nlm.nih.gov/pubmed/9819393.

Parra, K. J., Keenan, K. L., & Kane, P. M. (2000). The H subunit (Vma13p) of the yeast V-ATPase inhibits the ATPase activity of cytosolic V1 complexes. *J Biol Chem, 275*(28), 21761-21767. Retrieved from https://www.ncbi.nlm.nih.gov/pubmed/10781598. doi:10.1074/jbc.M002305200

Parsons, S. M. (2000). Transport mechanisms in acetylcholine and monoamine storage. *FASEB J, 14*(15), 2423-2434. Retrieved from https://www.ncbi.nlm.nih.gov/pubmed/11099460. doi:10.1096/fj.00-0203rev

Pillay, C. S., Elliott, E., & Dennison, C. (2002). Endolysosomal proteolysis and its regulation. *Biochem J, 363*(Pt 3), 417-429. Retrieved from https://www.ncbi.nlm.nih.gov/pubmed/11964142. doi:10.1042/0264-6021:3630417

Rahman, N., Ramos-Espiritu, L., Milner, T. A., Buck, J., & Levin, L. R. (2016). Soluble adenylyl cyclase is essential for proper lysosomal acidification. *J Gen Physiol, 148*(4), 325-339. Retrieved from https://www.ncbi.nlm.nih.gov/pubmed/27670898. doi:10.1085/jgp.201611606

Ramirez Rios, S., Lamarche, F., Cottet-Rousselle, C., Klaus, A., Tuerk, R., Thali, R., . . . Schlattner, U. (2014). Regulation of brain-type creatine kinase by AMP-activated protein kinase: interaction, phosphorylation and ER localization. *Biochim Biophys Acta, 1837*(8), 1271-1283. Retrieved from https://www.ncbi.nlm.nih.gov/pubmed/24727412. doi:10.1016/j.bbabio.2014.03.020

Rogatzki, M. J., Ferguson, B. S., Goodwin, M. L., & Gladden, L. B. (2015). Lactate is always the end product of glycolysis. *Front Neurosci, 9*, 22. Retrieved from https://www.ncbi.nlm.nih.gov/pubmed/25774123. doi:10.3389/fnins.2015.00022

Saftig, P., & Klumperman, J. (2009). Lysosome biogenesis and lysosomal membrane proteins: trafficking meets function. *Nat Rev Mol Cell Biol, 10*(9), 623-635. Retrieved from https://www.ncbi.nlm.nih.gov/pubmed/19672277. doi:10.1038/nrm2745

Sagermann, M., Stevens, T. H., & Matthews, B. W. (2001). Crystal structure of the regulatory subunit H of the V-type ATPase of Saccharomyces cerevisiae. *Proc Natl Acad Sci U S A, 98*(13), 7134-7139. Retrieved from https://www.ncbi.nlm.nih.gov/pubmed/11416198. doi:10.1073/pnas.131192798

Sagne, C., Agulhon, C., Ravassard, P., Darmon, M., Hamon, M., El Mestikawy, S., . . . Giros, B. (2001). Identification and characterization of a lysosomal transporter for small neutral amino acids. *Proc Natl Acad Sci U S A, 98*(13), 7206-7211. Retrieved from https://www.ncbi.nlm.nih.gov/pubmed/11390972. doi:10.1073/pnas.121183498

Sambongi, Y., Iko, Y., Tanabe, M., Omote, H., Iwamoto-Kihara, A., Ueda, I., . . . Futai, M. (1999). Mechanical rotation of the c subunit oligomer in ATP synthase (F0F1): direct observation. *Science, 286*(5445), 1722-1724. Retrieved from https://www.ncbi.nlm.nih.gov/pubmed/10576736.

Sautin, Y. Y., Lu, M., Gaugler, A., Zhang, L., & Gluck, S. L. (2005). Phosphatidylinositol 3-kinase-mediated effects of glucose on vacuolar H+-ATPase assembly, translocation, and acidification of intracellular compartments in renal epithelial cells. *Mol Cell Biol, 25*(2), 575-589. Retrieved from https://www.ncbi.nlm.nih.gov/pubmed/15632060. doi:10.1128/MCB.25.2.575-589.2005

Sennoune, S. R., Bakunts, K., Martinez, G. M., Chua-Tuan, J. L., Kebir, Y., Attaya, M. N., & Martinez-Zaguilan, R. (2004). Vacuolar H+-ATPase in human breast cancer cells with distinct metastatic potential: distribution and functional activity. *Am J Physiol Cell Physiol, 286*(6), C1443-1452. Retrieved from https://www.ncbi.nlm.nih.gov/pubmed/14761893. doi:10.1152/ajpcell.00407.2003

Sennoune, S. R., & Martinez-Zaguilan, R. (2007). Plasmalemmal vacuolar H+-ATPases in angiogenesis, diabetes and cancer. *J Bioenerg Biomembr, 39*(5-6), 427-433. Retrieved from https://www.ncbi.nlm.nih.gov/pubmed/18058006. doi:10.1007/s10863-007-9108-8

Seol, J. H., Shevchenko, A., Shevchenko, A., & Deshaies, R. J. (2001). Skp1 forms multiple protein complexes, including RAVE, a regulator of V-ATPase assembly. *Nat Cell Biol, 3*(4), 384-391. Retrieved from https://www.ncbi.nlm.nih.gov/pubmed/11283612. doi:10.1038/35070067

Shaw, R. J., Bardeesy, N., Manning, B. D., Lopez, L., Kosmatka, M., DePinho, R. A., & Cantley, L. C. (2004). The LKB1 tumor suppressor negatively regulates mTOR signaling. *Cancer Cell, 6*(1), 91-99. Retrieved from https://www.ncbi.nlm.nih.gov/pubmed/15261145. doi:10.1016/j.ccr.2004.06.007

Shojaiefard, M., Christie, D. L., & Lang, F. (2006). Stimulation of the creatine transporter SLC6A8 by the protein kinase mTOR. *Biochem Biophys Res Commun, 341*(4), 945-949. Retrieved from https://www.ncbi.nlm.nih.gov/pubmed/16466692. doi:10.1016/j.bbrc.2006.01.055

Smardon, A. M., Tarsio, M., & Kane, P. M. (2002). The RAVE complex is essential for stable assembly of the yeast V-ATPase. *J Biol Chem, 277*(16), 13831-13839. Retrieved from https://www.ncbi.nlm.nih.gov/pubmed/11844802. doi:10.1074/jbc.M200682200

Stevens, T. H., & Forgac, M. (1997). Structure, function and regulation of the vacuolar (H+)-ATPase. *Annu Rev Cell Dev Biol, 13*, 779-808. Retrieved from https://www.ncbi.nlm.nih.gov/pubmed/9442887. doi:10.1146/annurev.cellbio.13.1.779

Stransky, L. A., & Forgac, M. (2015). Amino Acid Availability Modulates Vacuolar H+-ATPase Assembly. *J Biol Chem, 290*(45), 27360-27369. Retrieved from https://www.ncbi.nlm.nih.gov/pubmed/26378229. doi:10.1074/jbc.M115.659128

Sun-Wada, G. H., & Wada, Y. (2015). Role of vacuolar-type proton ATPase in signal transduction. *Biochim Biophys Acta, 1847*(10), 1166-1172. Retrieved from https://www.ncbi.nlm.nih.gov/pubmed/26072192. doi:10.1016/j.bbabio.2015.06.010

Takamori, S., Holt, M., Stenius, K., Lemke, E. A., Gronborg, M., Riedel, D., . . . Jahn, R. (2006). Molecular anatomy of a trafficking organelle. *Cell, 127*(4), 831-846. Retrieved from https://www.ncbi.nlm.nih.gov/pubmed/17110340. doi:10.1016/j.cell.2006.10.030

Teitelbaum, S. L. (2000). Bone resorption by osteoclasts. *Science, 289*(5484), 1504-1508. Retrieved from https://www.ncbi.nlm.nih.gov/pubmed/10968780.

Teitelbaum, S. L. (2007). Osteoclasts: what do they do and how do they do it? *Am J Pathol, 170*(2), 427-435. Retrieved from https://www.ncbi.nlm.nih.gov/pubmed/17255310. doi:10.2353/ajpath.2007.060834

Theurl, M., Schgoer, W., Albrecht, K., Jeschke, J., Egger, M., Beer, A. G., . . . Kirchmair, R. (2010). The neuropeptide catestatin acts as a novel angiogenic cytokine via a basic fibroblast growth factor-dependent mechanism. *Circ Res, 107*(11), 1326-1335. Retrieved from https://www.ncbi.nlm.nih.gov/pubmed/20930149. doi:10.1161/CIRCRESAHA.110.219493

Toei, M., Saum, R., & Forgac, M. (2010). Regulation and isoform function of the V-ATPases. *Biochemistry, 49*(23), 4715-4723. Retrieved from https://www.ncbi.nlm.nih.gov/pubmed/20450191. doi:10.1021/bi100397s

Tomashek, J. J., & Brusilow, W. S. (2000). Stoichiometry of energy coupling by proton-translocating ATPases: a history of variability. *J Bioenerg Biomembr, 32*(5), 493-500. Retrieved from https://www.ncbi.nlm.nih.gov/pubmed/15254384.

Torigoe, T., Izumi, H., Ise, T., Murakami, T., Uramoto, H., Ishiguchi, H., . . . Kohno, K. (2002). Vacuolar H(+)-ATPase: functional mechanisms and potential as a target for cancer chemotherapy. *Anticancer Drugs, 13*(3), 237-243. Retrieved from https://www.ncbi.nlm.nih.gov/pubmed/11984067.

Toyomura, T., Murata, Y., Yamamoto, A., Oka, T., Sun-Wada, G. H., Wada, Y., & Futai, M. (2003). From lysosomes to the plasma membrane: localization of vacuolar-type H+ -ATPase with the a3 isoform during osteoclast differentiation. *J Biol Chem, 278*(24), 22023-22030. Retrieved from https://www.ncbi.nlm.nih.gov/pubmed/12672822. doi:10.1074/jbc.M302436200

Wilkens, S., & Forgac, M. (2001). Three-dimensional structure of the vacuolar ATPase proton channel by electron microscopy. *J Biol Chem, 276*(47), 44064-44068. Retrieved from https://www.ncbi.nlm.nih.gov/pubmed/11533034. doi:10.1074/jbc.M106579200

Xu, T., & Forgac, M. (2001). Microtubules are involved in glucose-dependent dissociation of the yeast vacuolar [H+]-ATPase in vivo. *J Biol Chem, 276*(27), 24855-24861. Retrieved from https://www.ncbi.nlm.nih.gov/pubmed/11331282. doi:10.1074/jbc.M100637200

Yokoyama, K., & Imamura, H. (2005). Rotation, structure, and classification of prokaryotic V-ATPase. *J Bioenerg Biomembr, 37*(6), 405-410. Retrieved from https://www.ncbi.nlm.nih.gov/pubmed/16691473. doi:10.1007/s10863-005-9480-1

Zhang, C. S., Jiang, B., Li, M., Zhu, M., Peng, Y., Zhang, Y. L., . . . Lin, S. C. (2014). The lysosomal v-ATPase-Ragulator complex is a common activator for AMPK and mTORC1, acting as a switch between catabolism and anabolism. *Cell Metab, 20*(3), 526-540. Retrieved from https://www.ncbi.nlm.nih.gov/pubmed/25002183. doi:10.1016/j.cmet.2014.06.014

Zhang, Z., Zheng, Y., Mazon, H., Milgrom, E., Kitagawa, N., Kish-Trier, E., . . . Wilkens, S. (2008). Structure of the yeast vacuolar ATPase. *J Biol Chem, 283*(51), 35983-35995. Retrieved from https://www.ncbi.nlm.nih.gov/pubmed/18955482. doi:10.1074/jbc.M805345200

Appendix
Supplementary Figures

SFigure 1. Biochemical Validation of Neuronal and V-ATPase Antibodies in Differentiated Neuro2a cells

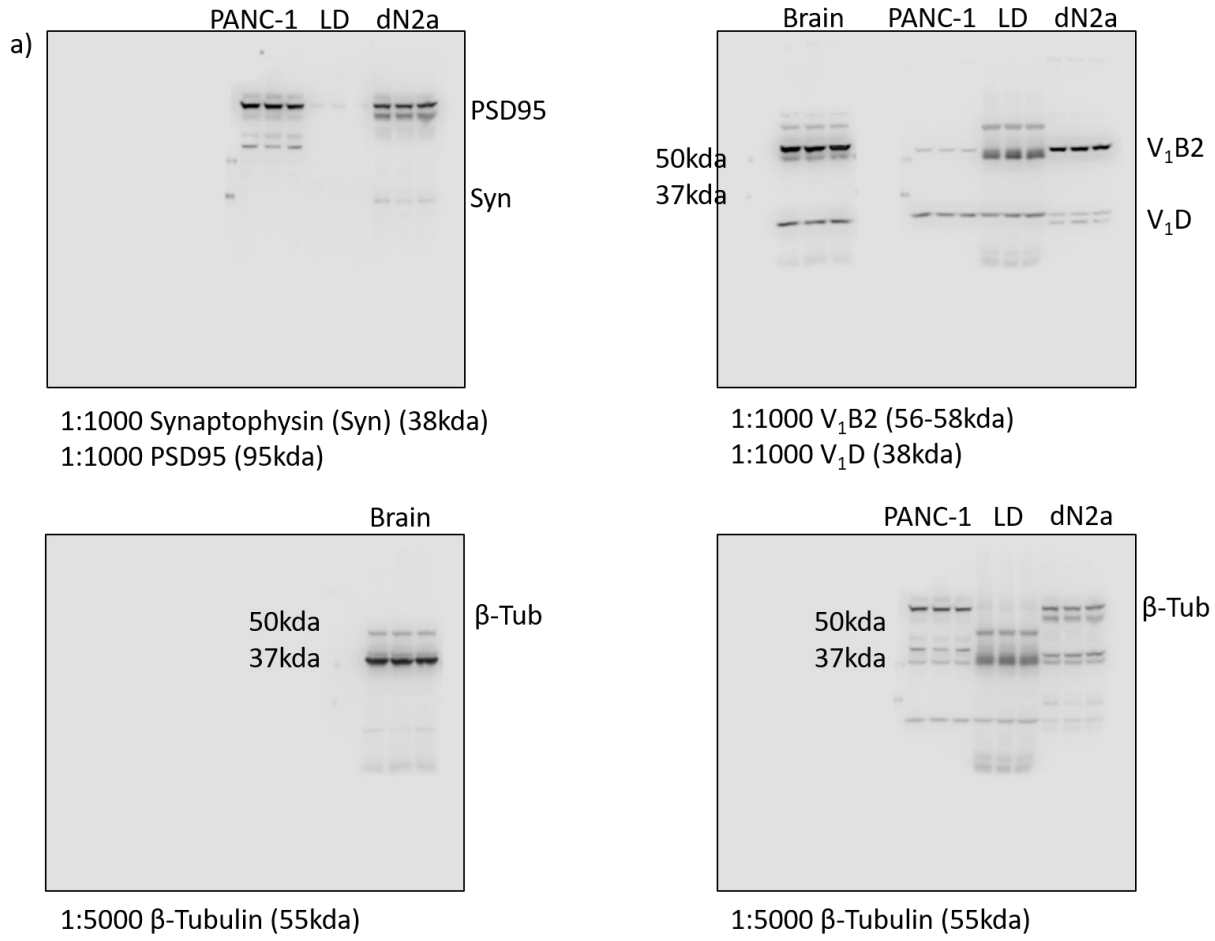

b)

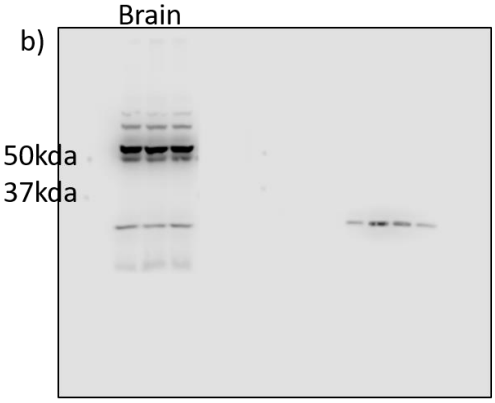

1:1000 V_1B2 (56-58kda)
1:1000 V_1D (38kda)

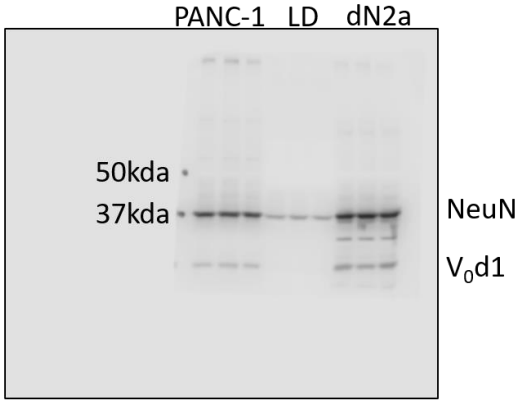

1:1000 NeuN (48-50kda)
1:2000 V_0d1 (40kda)

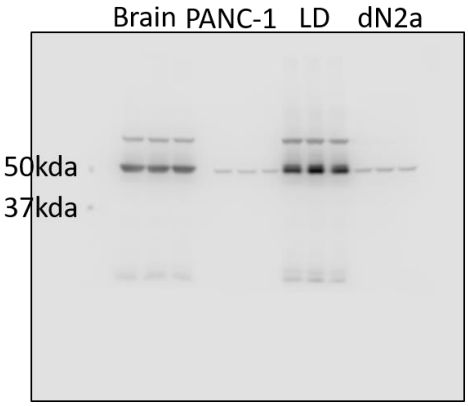

1:5000 β-Tubulin (55kda)

SFigure 2. Morphological and Biochemical Characterization of Neuronal Phenotype of RA-differentiated N2a cells

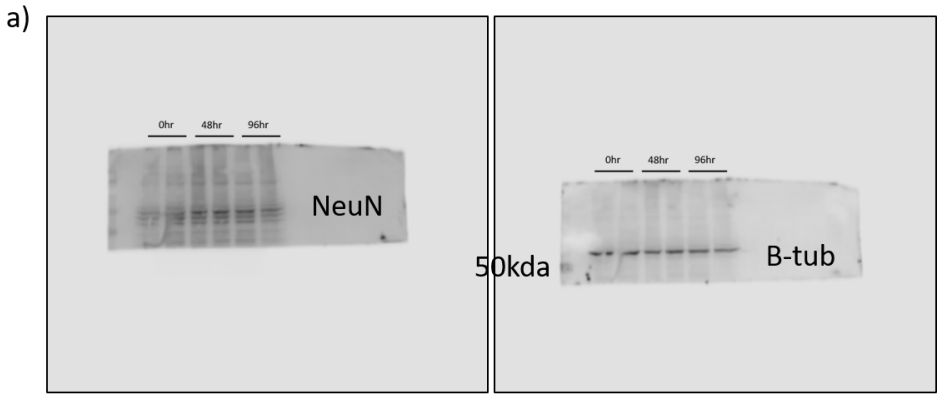

1:5000 NeuN (55kda) 1:5000 β-Tubulin (55kda)

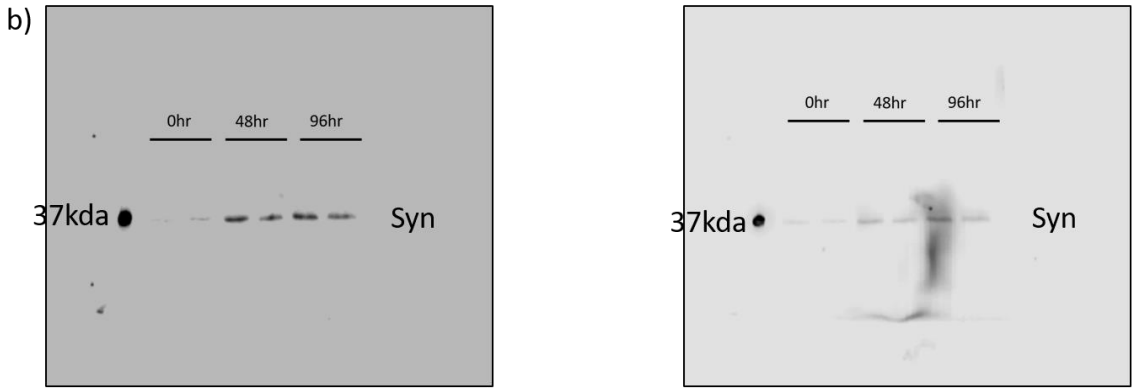

1:1000 Synaptophysin (38kda) 1:1000 Synaptophysin (38kda)

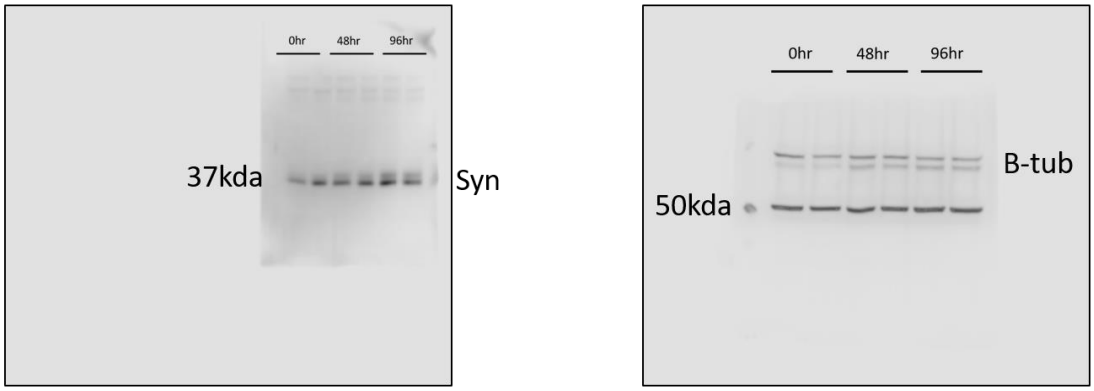

1:1000 Synaptophysin (38kda) 1:5000 β-Tubulin (55kda)

c)

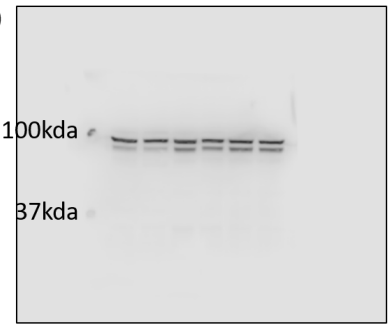

1:1000 PSD95 (95kda)

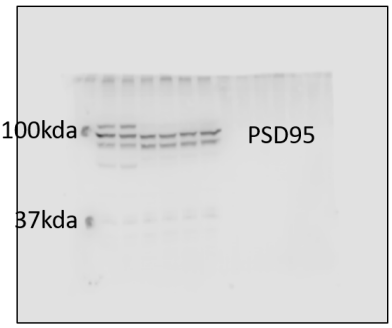

1:1000 PSD95 (95kda)

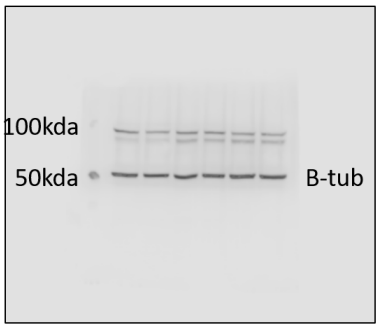

1:5000 β-Tubulin (55kda)

d)

1:1000 V_1B2 (56-58kda)

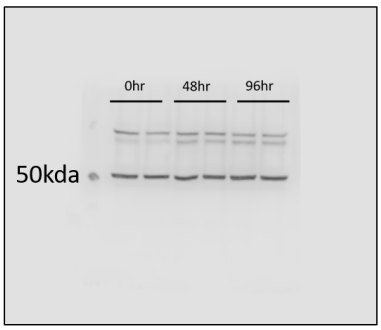

1:5000 β-Tubulin (55kda)

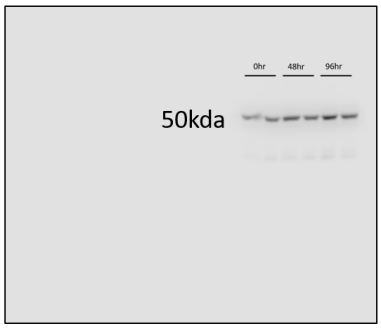

1:1000 V_1B2 (56-58kda)

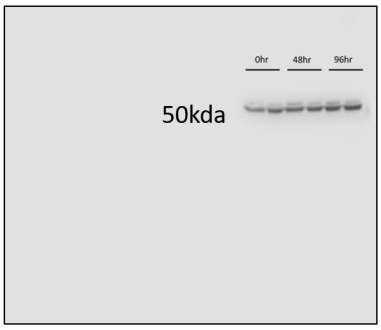

1:5000 β-Tubulin (55kda)

SFigure 3. V_0V_1 Protein Expression levels were not altered by glucose treatment

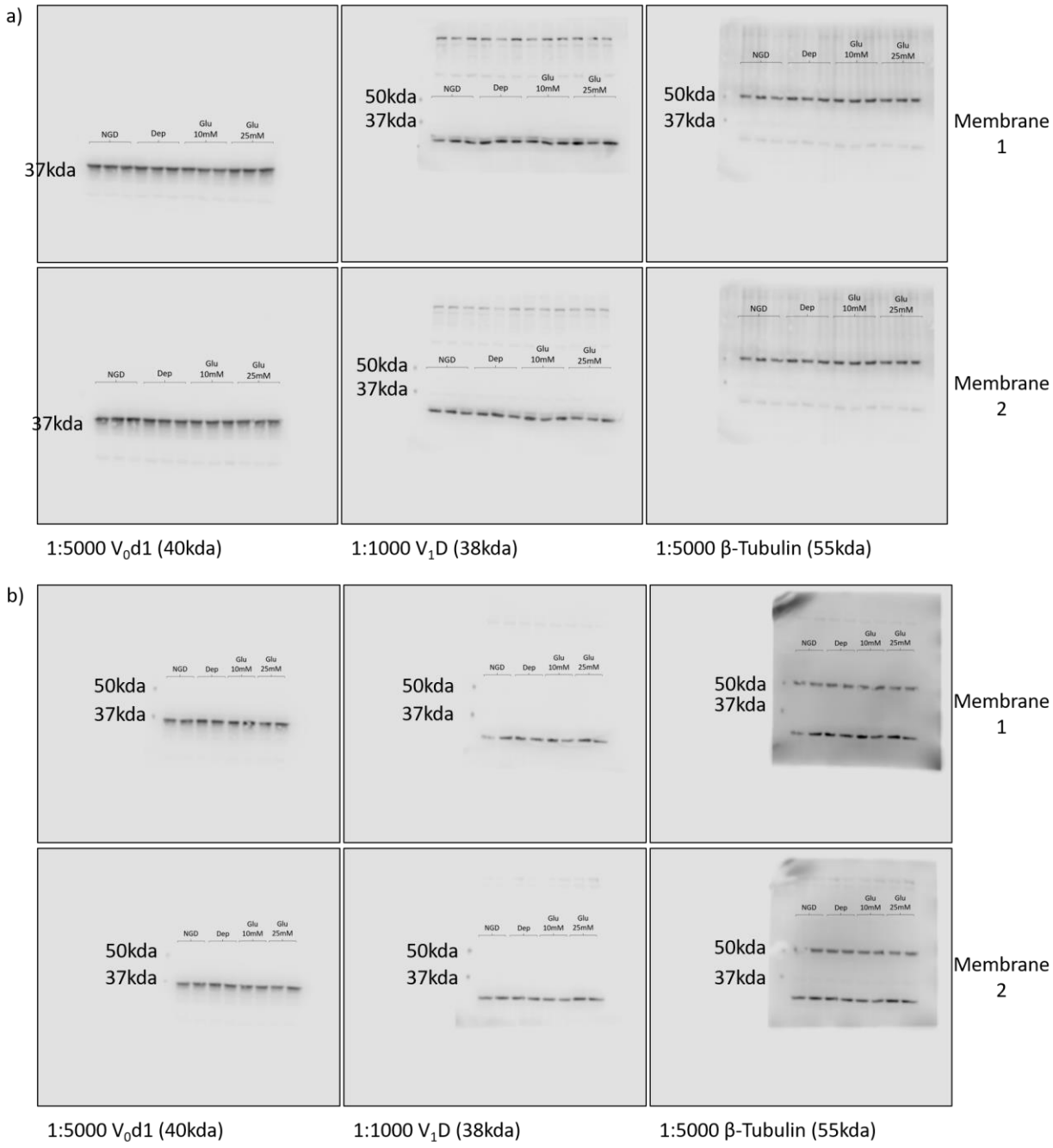

c)

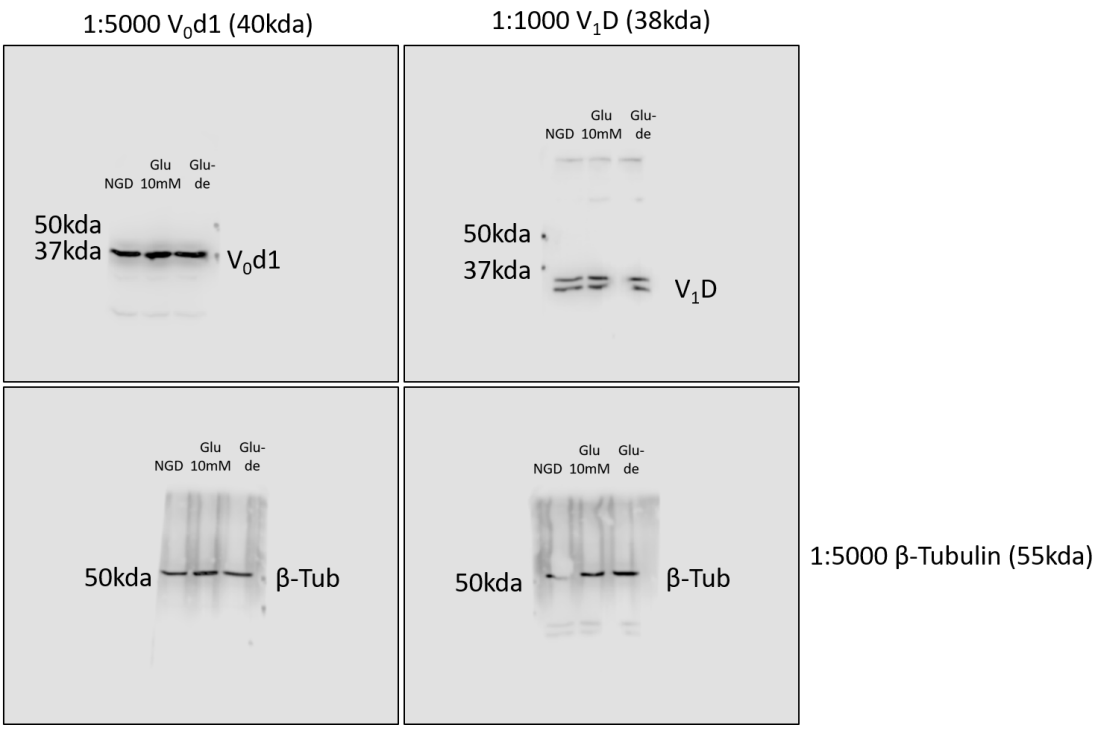
1:5000 V0d1 (40kda)
1:1000 V1D (38kda)
Glu
NGD 10mM
Glu-
de
50kda
37kda
V0d1
V1D
β-Tub
1:5000 β-Tubulin (55kda)

d)

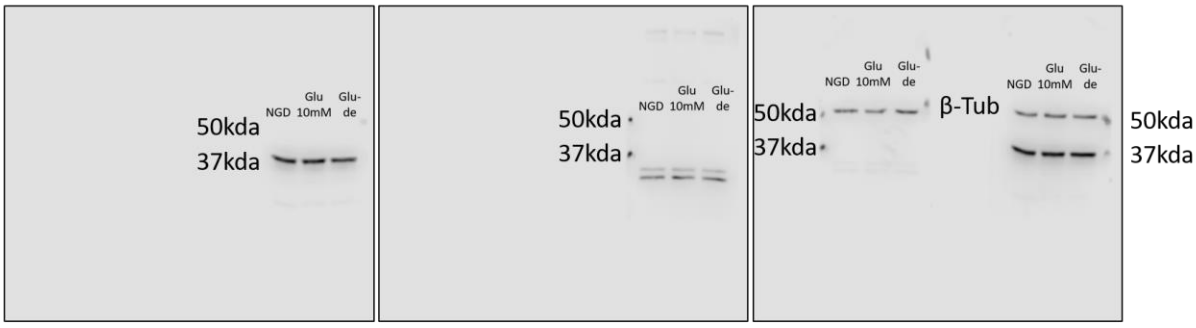
Glu
NGD 10mM
Glu-
de
50kda
37kda
β-Tub
1:5000 V0d1 (40kda)
1:1000 V1D (38kda)
1:5000 β-Tubulin (55kda)

SFigure 4. V-ATPase Assembly was not significantly altered by glucose stimulation

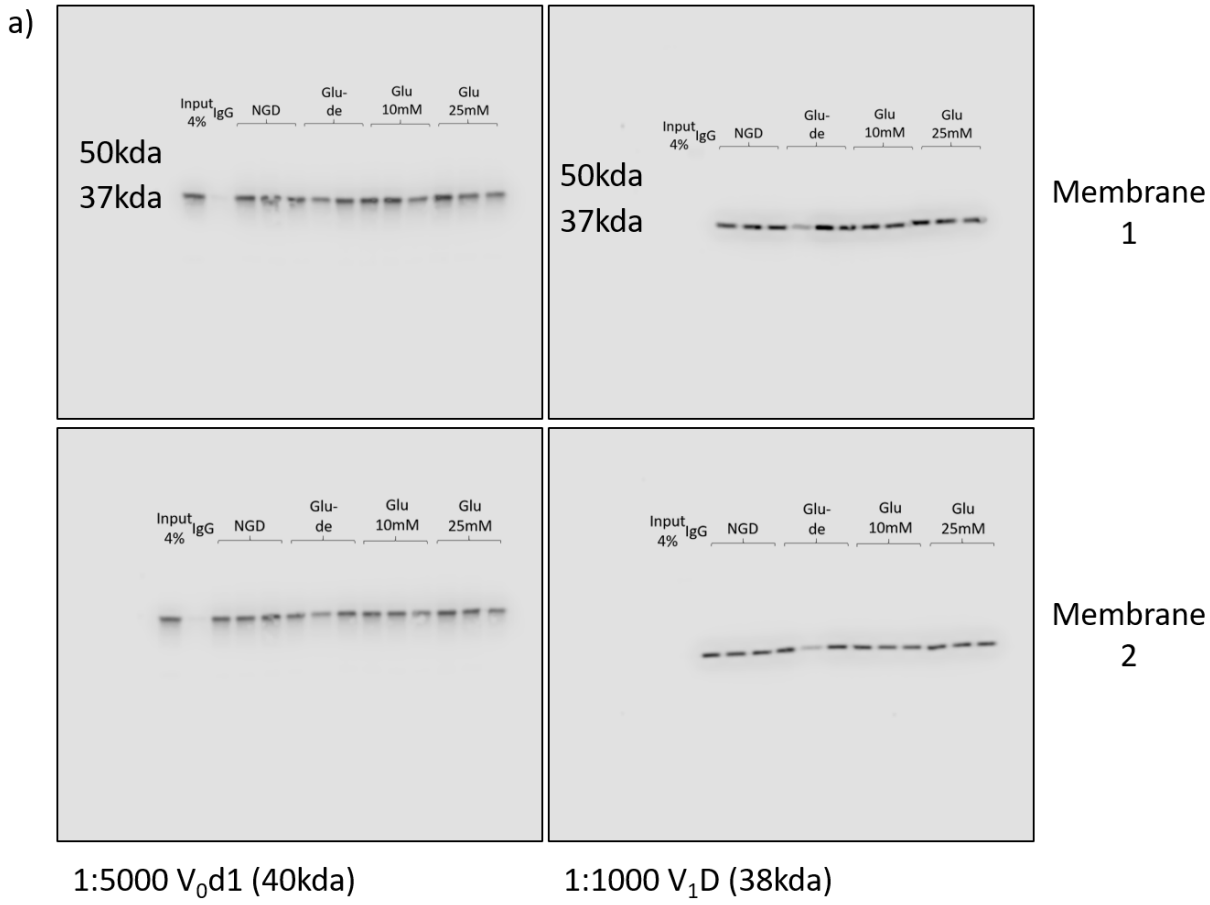

b)

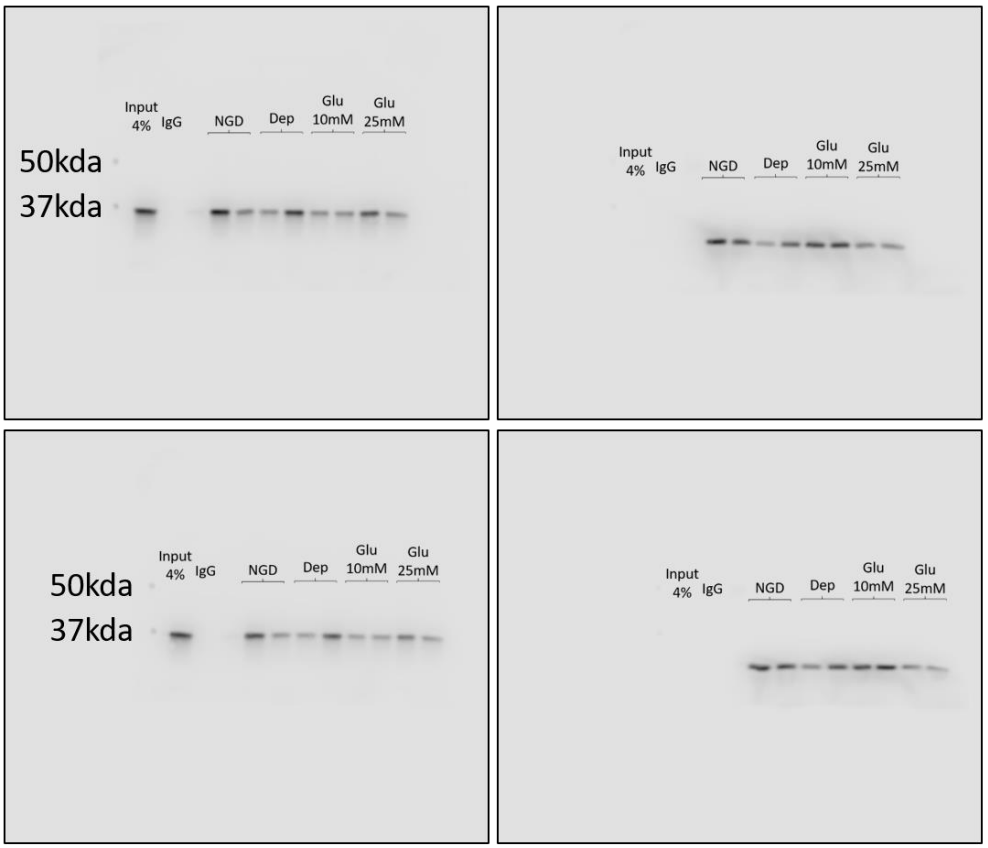
Input 4%
IgG
NGD
Dep
Glu 10mM
Glu 25mM
50kda
37kda
Membrane 1
Membrane 2
1:5000 V0d1 (40kda)
1:1000 V1D (38kda)

c)

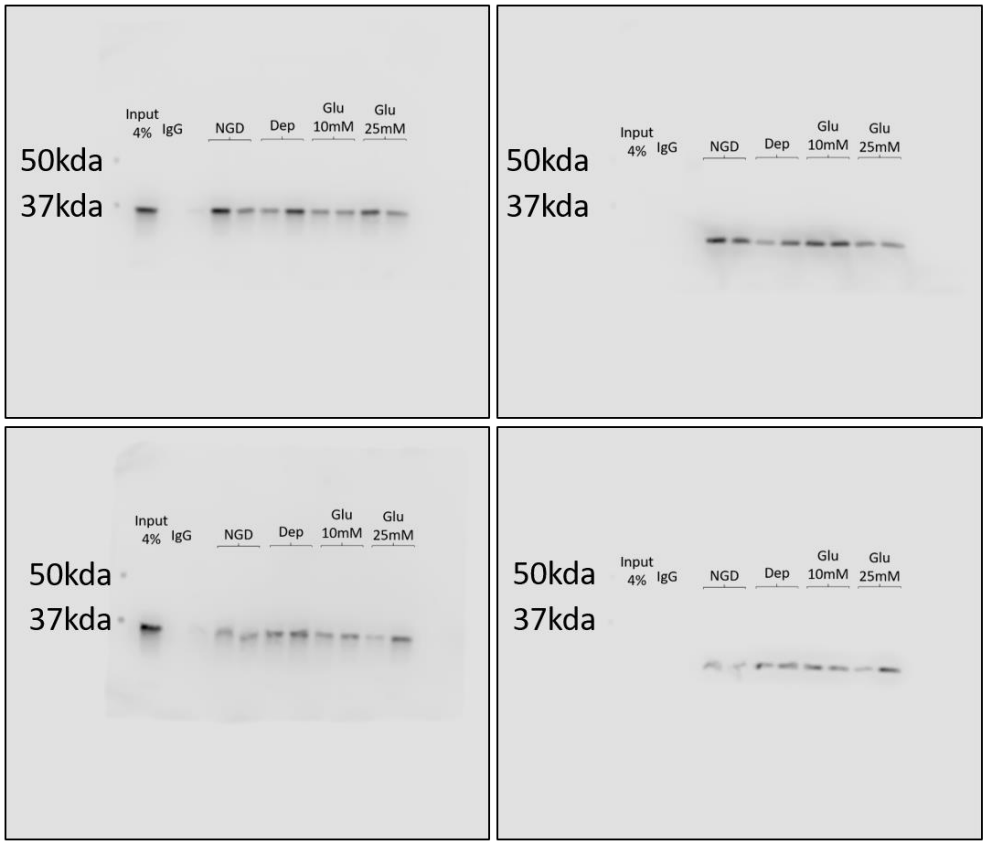
Input 4%
IgG
NGD
Dep
Glu 10mM
Glu 25mM
50kda
37kda
Membrane 1
Membrane 2
1:5000 V0d1 (40kda)
1:1000 V1D (38kda)

d)

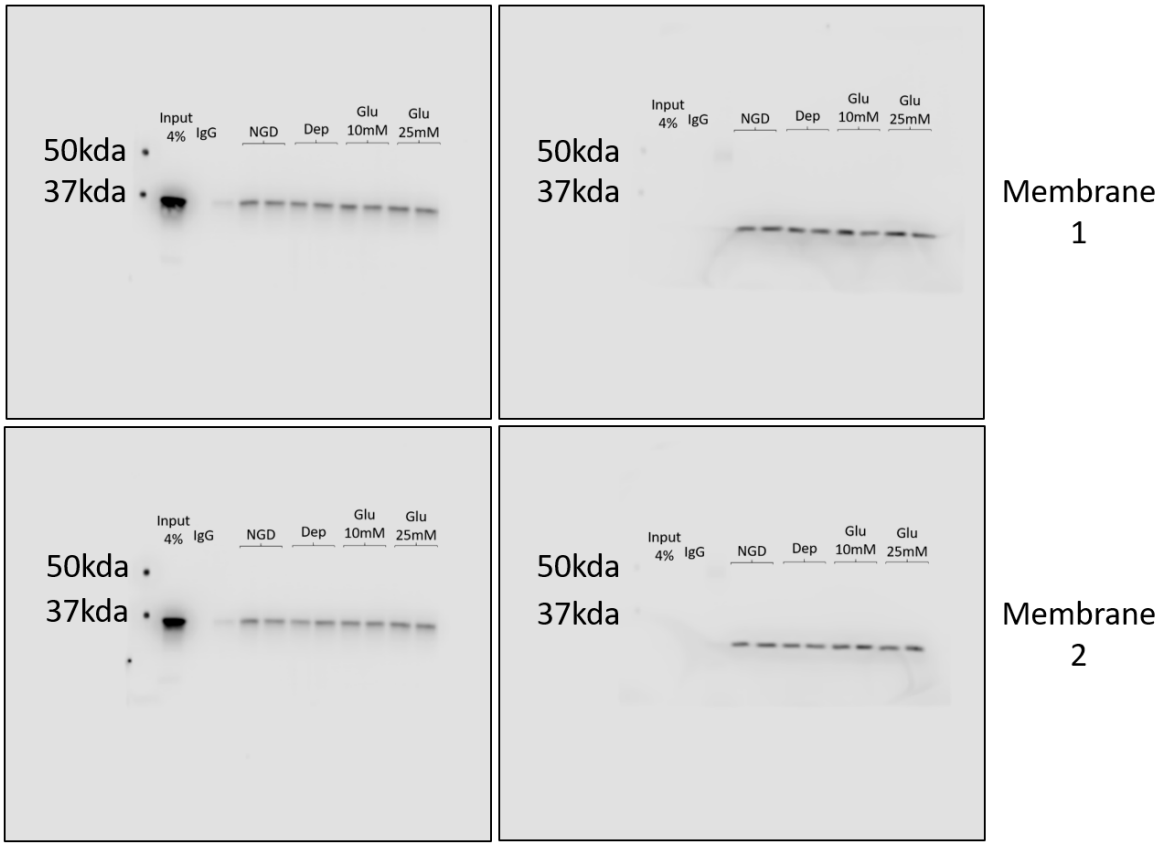

1:5000 V_0d1 (40kda)

1:1000 V_1D (38kda)

e)

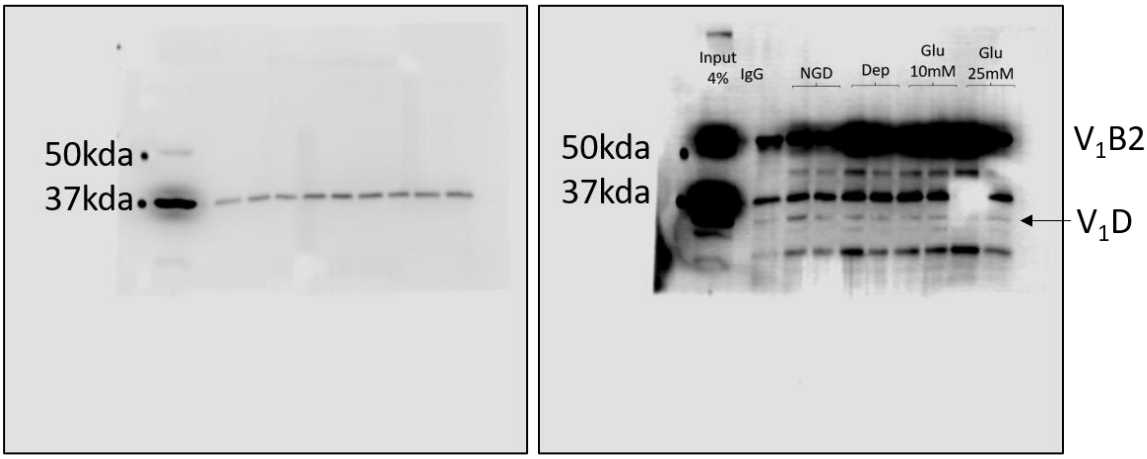

1:5000 V_0d1 (40kda)

1:1000 V_1D (38kda)
1:1000 V_1B2 (56-58kda)

SFigure 5. V-ATPase Assembly was not significantly altered by mitochondrial substrates

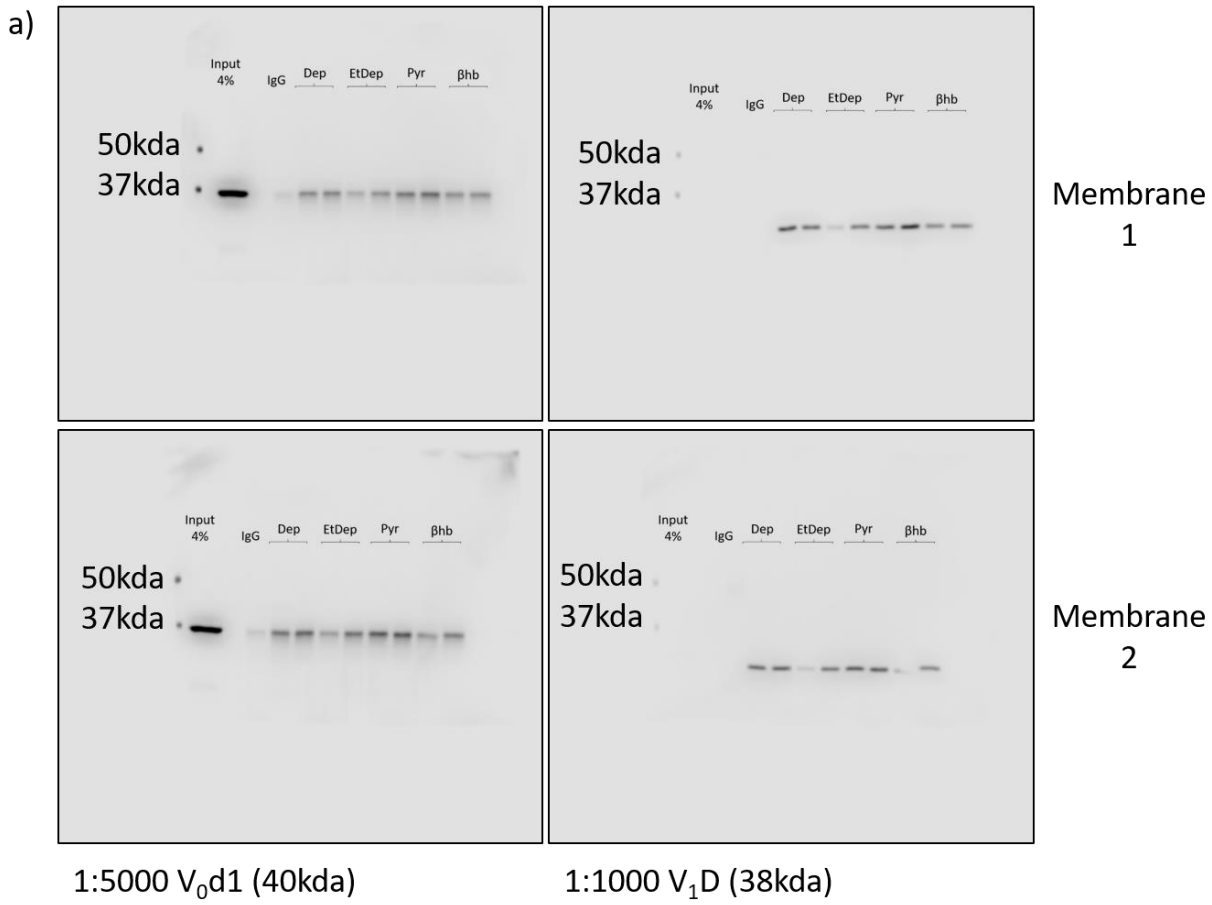

b)

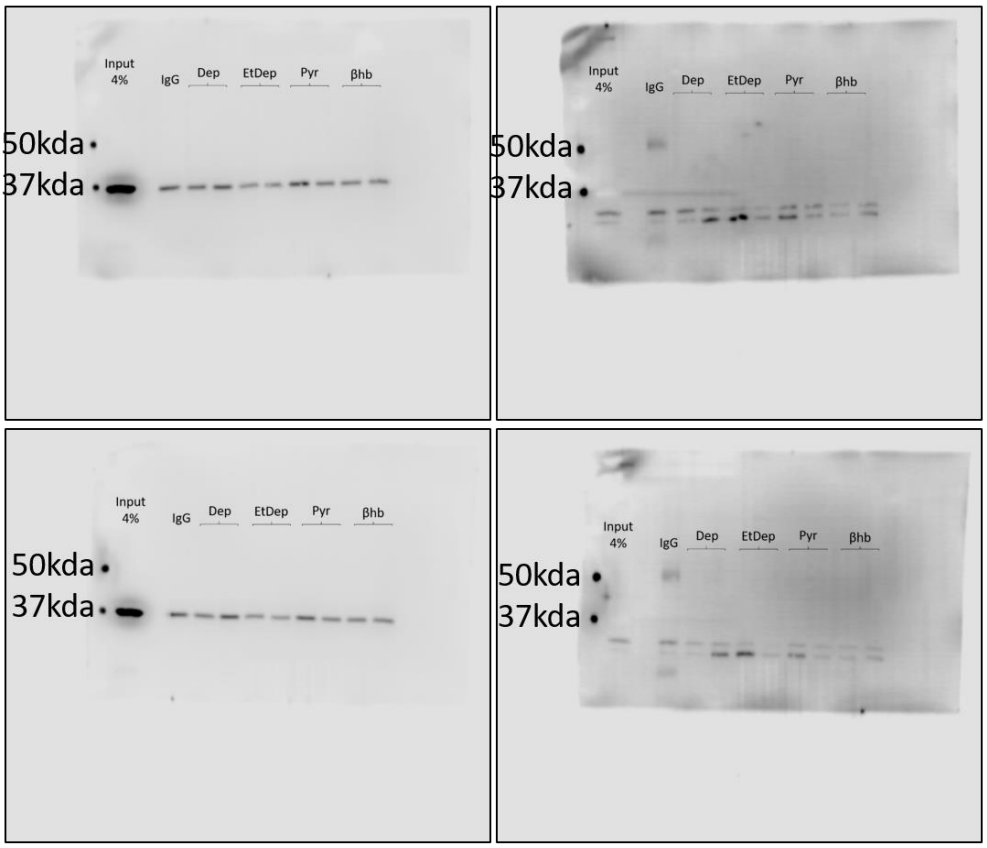

1:5000 V_0d1 (40kda) 1:1000 V_1D (38kda)

c)

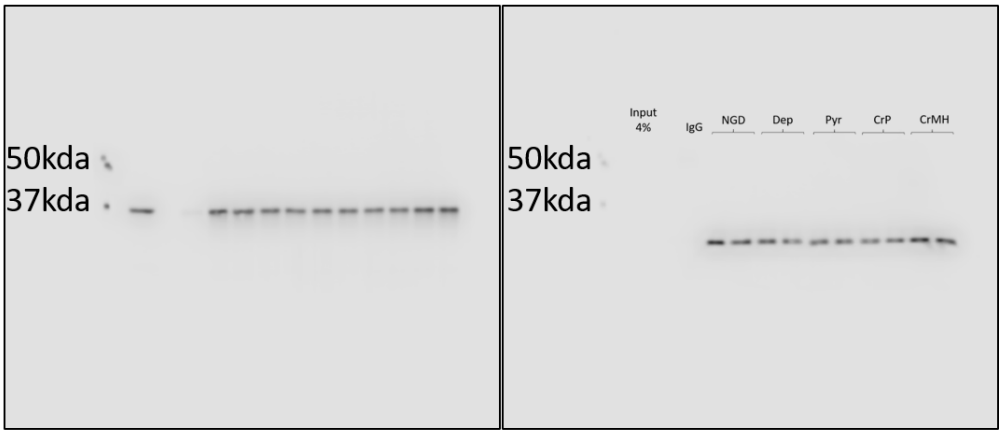

1:5000 V_0d1 (40kda) 1:1000 V_1D (38kda)

d)

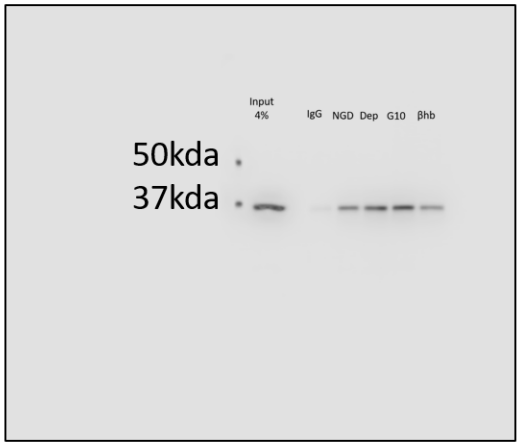

1:5000 V_0d1 (40kda)

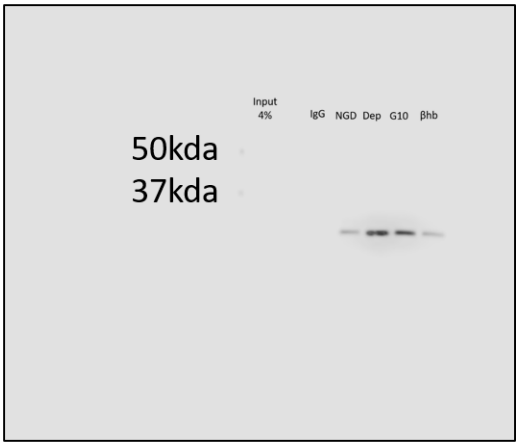

1:1000 V_1D (38kda)

e)

1:5000 V_0d1 (40kda)

1:1000 V_1D (38kda)

SFigure 6

V-ATPase was not significantly altered by creatine substrates

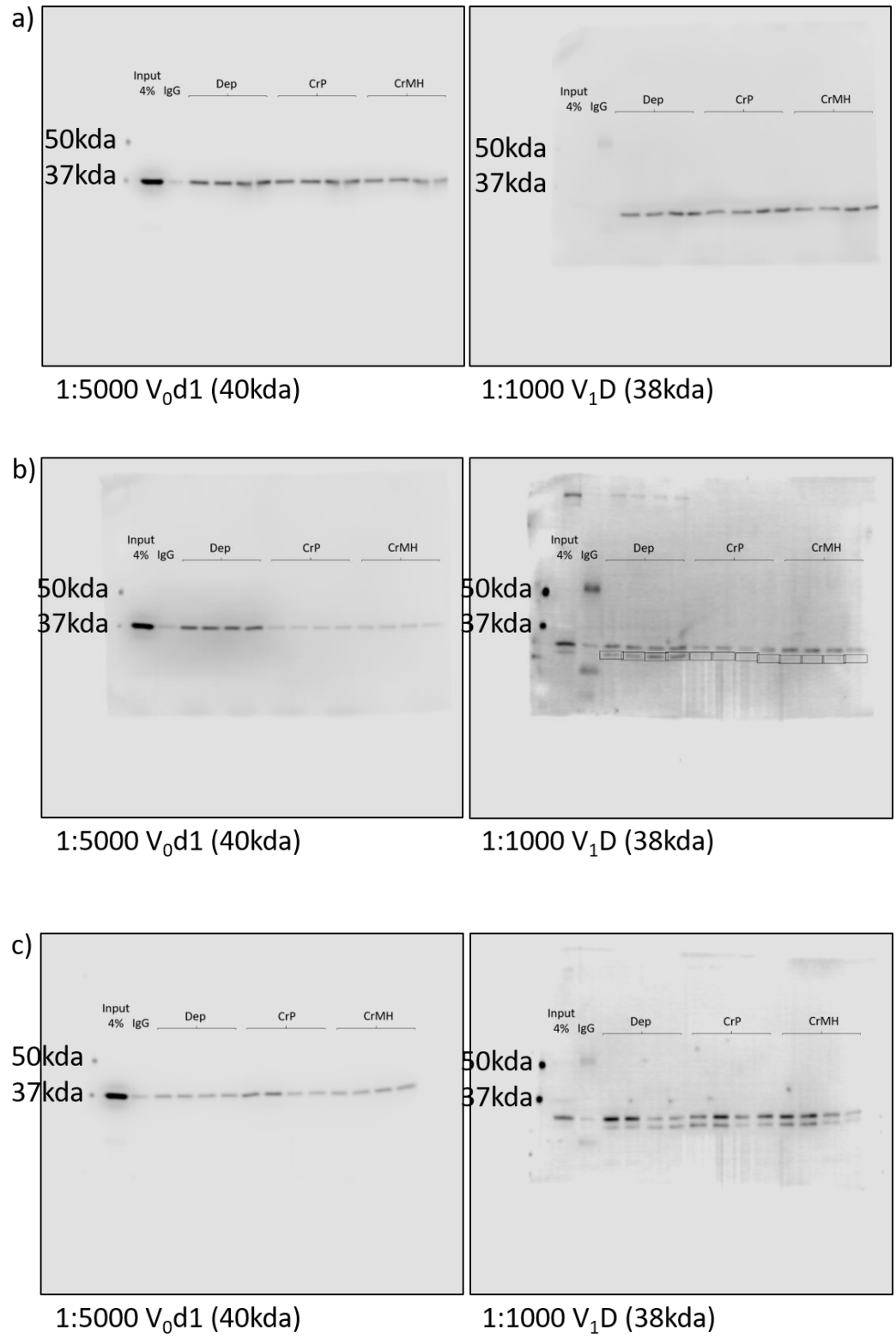

SFigure 7

N2a Cell Authentication

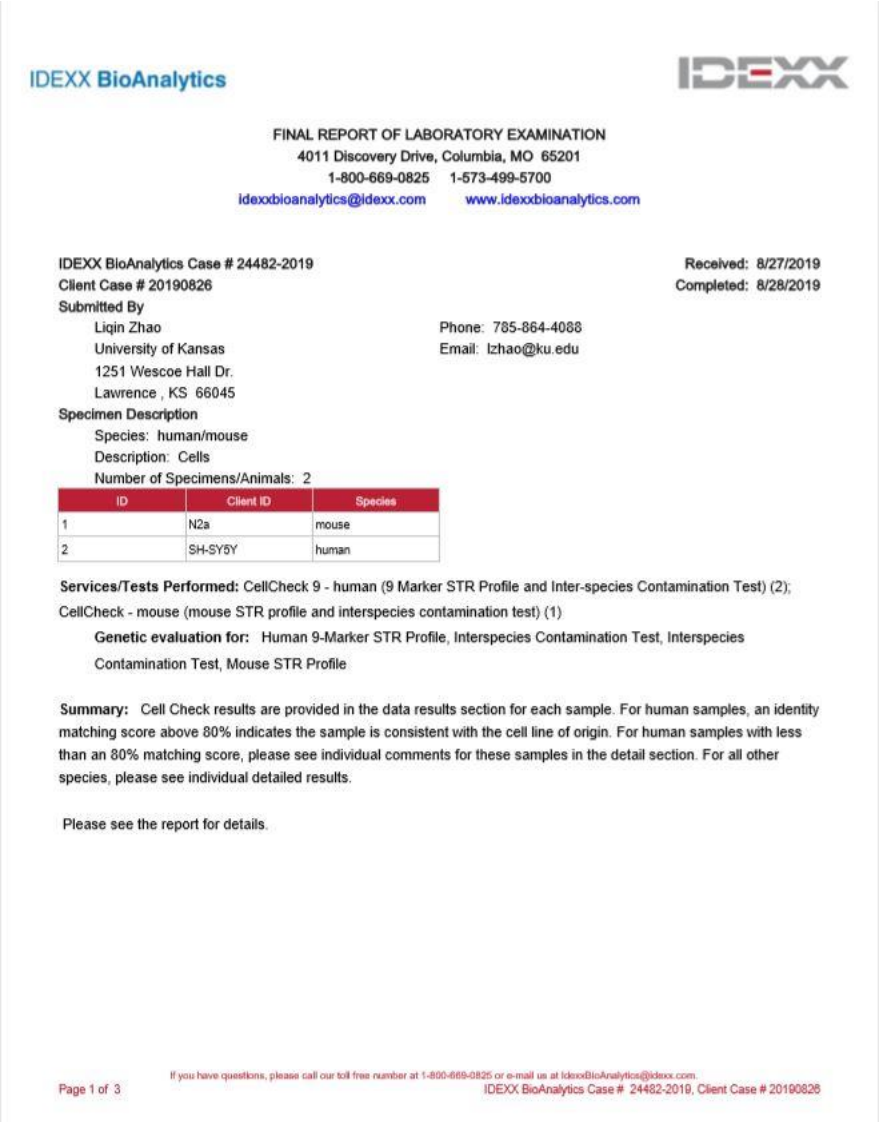

IDEXX BioAnalytics

IDEXX

FINAL REPORT OF LABORATORY EXAMINATION
4011 Discovery Drive, Columbia, MO 65201
1-800-669-0825 1-573-499-5700
idexxbioanalytics@idexx.com www.idexxbioanalytics.com

IDEXX BioAnalytics Case # 24482-2019 **Received: 8/27/2019**
Client Case # 20190826 **Completed: 8/28/2019**
Submitted By
Liqin Zhao Phone: 785-864-4088
University of Kansas Email: lzhao@ku.edu
1251 Wescoe Hall Dr.
Lawrence , KS 66045
Specimen Description
Species: human/mouse
Description: Cells
Number of Specimens/Animals: 2

ID	Client ID	Species
1	N2a	mouse
2	SH-SY5Y	human

Services/Tests Performed: CellCheck 9 - human (9 Marker STR Profile and Inter-species Contamination Test) (2); CellCheck - mouse (mouse STR profile and interspecies contamination test) (1)

Genetic evaluation for: Human 9-Marker STR Profile, Interspecies Contamination Test, Interspecies Contamination Test, Mouse STR Profile

Summary: Cell Check results are provided in the data results section for each sample. For human samples, an identity matching score above 80% indicates the sample is consistent with the cell line of origin. For human samples with less than an 80% matching score, please see individual comments for these samples in the detail section. For all other species, please see individual detailed results.

Please see the report for details.

If you have questions, please call our toll free number at 1-800-669-0825 or e-mail us at IdexxBioAnalytics@idexx.com.
Page 1 of 3 IDEXX BioAnalytics Case # 24482-2019, Client Case # 20190826

CELL CHECK

Species-specific PCR Evaluation

Species	1
mouse	+
rat	-
human	-
Chinese hamster	-
African green monkey	-

Marker Analysis

Marker Name	1	
	Sample Results	Neuro 2A (IBA Profile)
MCA-4-2	21.3, 22.3	21.3, 22.3
MCA-5-5	15, 17	15, 17
MCA-6-4	18, 20	18, 20
MCA-6-7	12	12
MCA-9-2	15, 16	15, 16
MCA-12-1	16	16
MCA-15-3	21.3, 22.3, 23.3	21.3, 22.3, 23.3
MCA-18-3	22	22
MCA-X-1	26, 27	26, 27

Sample ID	Remarks
1	The sample was confirmed to be of mouse origin and no mammalian interspecies contamination was detected. A genetic profile was generated for the sample by using a panel of STR markers for genotyping. The sample profile matches identically to the genetic profile established for this cell line.

Species-specific PCR Evaluation

Species	2
mouse	-
rat	-
human	+
Chinese hamster	-
African green monkey	-

Marker Analysis

Marker Name	2	
	Sample Results	SH-SY5Y (ATCC# CRL-2266)
AMEL	X	X
CSF1PO	11	11
D13S317	11	11
D16S539	8, 13	8, 13
D5S818	12	12
D7S820	7, 10	7, 10
TH01	7, 10	7, 10
TPOX	8, 11	8, 11
vWA	14, 18	14, 18
Identity Match	100%	